

UNIVERSITÀ DEGLI STUDI DI PADOVA

DIPARTIMENTO DI INGEGNERIA INDUSTRIALE

CORSO DI LAUREA MAGISTRALE IN INGEGNERIA CHIMICA E DEI PROCESSI INDUSTRIALI

**Tesi di Laurea Magistrale in
Ingegneria Chimica e dei Processi Industriali**

**ARTIFICIAL BIOMINERALISATION OF FLAX FIBRES IN THE
PRESENCE OF AMINO ACIDS FOR USE IN NATURAL FIBRE
REINFORCED COMPOSITES**

Relatore: Prof. Manuele Dabalà

Correlatore: Prof.(adj.) Parvez Alam, Åbo Akademi University (FIN)

Laureando: ANDREA CALZAVARA

ANNO ACCADEMICO 2013 – 2014

Riassunto

Negli ultimi anni la comunità scientifica si è focalizzata sullo sviluppo di criteri per la salvaguardia ambientale che accompagnino la progettazione di un determinato bene. Questa tendenza si traduce anche in innovazione nella scienza e nella tecnologia con l'obiettivo di ridurre le emissioni di gas ad effetto serra e le quantità di sostanze che sono difficilmente riciclabili alla fine del loro ciclo di vita; il tutto, senza però rinunciare alle prestazioni del prodotto.

Nel campo dei materiali compositi, i rinforzi fibrosi naturali e le matrici biopolimeriche diventano un logico approccio verso uno sviluppo sostenibile, ma l'elevato costo dei biopolimeri non consente loro un ampio utilizzo. La via più praticabile verso materiali compositi eco-compatibili risulta quindi, per ora, l'utilizzo, ove possibile, di fibre naturali nei materiali compositi rinforzati a fibre. Il riciclo, la biodegradabilità e la combustibilità non sono le uniche ragioni che promuovono lo sviluppo di tecniche innovative riguardanti le fibre rinnovabili. Altri vantaggi significativi derivano dalle loro elevate proprietà meccaniche specifiche ed il loro basso costo. Dall'altra parte, le ragioni principali che ostacolano una loro ampia diffusione sono: la bassa resistenza ad agenti esterni ed agli attacchi microbici, la sensibilità all'umidità, la bassa resistenza termica, la natura idrofila (la quale comporta una scarsa aderenza superficiale con la matrice polimerica idrofobica) e la mancanza di ripetibilità delle proprietà (essendo queste strettamente legate al luogo ed alle condizioni di coltura).

Molti settori dell'industria, tra cui quello automobilistico, fanno ampio uso di materiali compositi rinforzati con fibra naturale, ma per applicazioni che non richiedono particolari requisiti di tipo meccanico. La tecnica utilizzata per aumentare le proprietà meccaniche delle fibre impiegate nel materiale composito abbraccia il campo della biomimetica, ovvero, lo studio dei processi biologici e biomeccanici della natura come fonte di ispirazione per il miglioramento delle attività e delle tecnologie umane.

Il lavoro di tesi, è stato condotto presso il laboratorio di ricerca "Paper Coating and Converting" dell'Åbo Akademi University della città di Turku in Finlandia. Il gruppo di ricerca sta valutando l'ipotesi di migliorare le proprietà meccaniche dei rinforzi fibrosi naturali per materiali compositi fibro-rinforzati mediante un trattamento di biomineralizzazione artificiale. La biomineralizzazione è un processo estremamente complesso, attraverso il quale, gli organismi marini formano minerali; tale processo prevede la conversione di ioni in soluzione in solidi mineralizzati attraverso attività cellulari. In altre parole, la biomineralizzazione è un processo che prevede l'interazione tra le regioni organiche di questi organismi ed i componenti inorganici o ioni presenti in soluzione consentendo la formazione di strutture specifiche ad elevate capacità meccaniche. La componente organica

(proteine, polisaccaridi e/o lipidi) di cui sono costituiti tali organismi è in grado di controllare la fase, la morfologia e la dinamica di crescita della frazione inorganica. Il biominerale formato presenterà una struttura complessa su micro e nanoscala con un'eccellente combinazione di tenacità, elevato modulo elastico e forza, mentre i compositi sintetici tradizionali tendono a diminuire in tenacità con l'aumentare del modulo elastico. In questo lavoro di tesi, l'obiettivo è stato l'ottenimento di un rivestimento di carbonato di calcio (composto prevalente nei biominerali) biomineralizzato artificialmente sulla superficie di fibre di lino. Tre amminoacidi (Glicina, Beta-Alanina e Licina) a tre concentrazioni differenti per ognuno ($30 \cdot 10^{-3}$ M, $50 \cdot 10^{-3}$ M, $100 \cdot 10^{-3}$ M) sono stati presi in considerazione per il controllo del processo di precipitazione del carbonato di calcio sulla superficie delle fibre naturali; tali fibre sono state poi inserite come rinforzo fibroso unidirezionale in una matrice copolimerica di stirene-butadiene. L'utilizzo di questi composti organici deriva da un precedente studio effettuato nello stesso laboratorio di ricerca, nel quale si dimostra come la presenza di amminoacidi diversi influenzi la morfologia cristallina del carbonato di calcio e di conseguenza comporti una diversa rugosità superficiale della fibra di lino modificandone l'adesione con la matrice polimerica e quindi le proprietà a sforzo dell'intero composito.

Le analisi delle fibre di lino effettuate con il microscopio elettronico a scansione hanno permesso di valutare le diverse configurazioni nella morfologia cristallina del carbonato di calcio indotta dalle molecole organiche.

I campioni di matrice polimerica rinforzata con fibre di lino biomineralizzate sono stati sottoposti a prova di trazione per la valutazione dei parametri meccanici ottenibili dalla curva sforzo-deformazione. Inoltre, le simulazioni di dinamica molecolare applicate ai sistemi carbonato di calcio in presenza dei diversi amminoacidi alle tre concentrazioni considerate, ha permesso la valutazione delle energie intermolecolari.

Tra gli amminoacidi utilizzati, la Licina è stata riscontrata come il composto organico che consente le più elevate energie molecolari all'interno del sistema carbonato di calcio creando compositi con i più elevati valori di resistenza e rigidità.

Abstract

Biom mineralisation is gaining increasing interest as a potential technology for coating fibres for use in high-performance composites. The application of molecular biology and protein chemistry into material engineering creates an important interface between traditional methods in materials design and structural biology. Artificially controlling the process of biom mineralisation *in-vitro*, to create a product similar to biom minerals found in nature (*in-vivo*), would allow for the development of lightweight products with excellent mechanical properties for a variety of applications.

In this thesis, three amino acids were taken into account (Glycine, β -alanine and L-lysine) and three different concentrations for each amino acid ($30 \cdot 10^{-3}$ M, $50 \cdot 10^{-3}$ M, $100 \cdot 10^{-3}$ M) were used to artificially biom mineralise natural fibres for use in natural fibres reinforced composite. Of the three amino acids, higher concentrations of L-lysine were found to have (a) the highest intermolecular energies and (b) create composites with the highest values of strength and stiffness.

Table of contents

INTRODUCTION	1
CHAPTER 1 - Composite materials and composites reinforced with natural fibres	5
1.1 Composites: matrices and reinforcements.....	5
1.2 Renewable plant fibres.....	9
1.3 Applications of natural fibres.....	12
1.4 Flax fibres.....	16
CHAPTER 2 – Surface treatments and biomineralisation	19
2.1 Reinforcement-matrix interface in composites based on natural fibres and characterisation methods	19
2.2 Biomimetics	32
2.3 Biomineralisation	34
2.4 Crystal engineering	39
2.5 Calcium carbonate.....	43
CHAPTER 3 - Experimental work	44
3.1 Background on previous work	44
3.2 Molecular modelling: molecular dynamic simulations.....	47
3.3 Manufacture of natural fibre reinforced composites and SEM (Scanning Electron Microscope).....	504
3.4 Tensile testing	58
3.5 Nano-indentation testing	64
CONCLUSIONS	69
APPENDIX	71
REFERENCES	77

Introduction

A composite is a material of two or more components possessing characteristics of the individual components combined. Typical engineered composite materials include; building materials, metal matrix composites, ceramic composites and reinforced plastics, such as fibre-reinforced plastics (FRP). FRP are often manufactured to meet demands for low weight and high mechanical properties.

In recent years, the scientific community has focused on developing engineering criteria for environmental protection. There is growing interest from industry for innovation in science and technology where environmental protection plays a key role in material design. Many companies, for example, are increasingly beginning to adopt environmental management systems as a tool for the analysis of the environmental performance of their activities and their services. This also helps economically because it allows for process optimisation, a reduction in the amount of waste and it creates a clean image for the company. Companies and governmental bodies in high income countries aim for a rapid transition of the world economy towards “green growth”. This consists of a production mode based on clean techniques which are able to significantly reduce emissions of carbon dioxide and other greenhouse gases. New priorities promoted by scientific and technological innovation are based on general principles aimed at eliminating, or at least reducing, the use of processes and substances harmful to both humans and the environment.

Figure “a” shows the production of plastic material in various continents amongst the world's largest suppliers over recent decades. The use of plastics in every sector of production involves a huge amount of waste that needs to be disposed (Cristaldi *et al.*, 2010). Problems due to waste disposal combined with new regulations to protect the environment emphasise the importance of eco-composites containing a biopolymer matrix and/or natural fibres. Therefore, natural fibres and biopolymer matrices are a logical approach towards sustainable development. They are moreover a viable alternative to glass fibre composites (Mohanty *et al.*, 2005). The high price of biopolymers disallows their wide use, and hence the most viable route towards eco-friendly composites is in the use of natural fibres in fibre reinforced composites (Cristaldi *et al.*, 2010).

Data on the global and European markets demonstrate a growing interest in biopolymers and reinforcements obtained by sustainable means. The average annual growth rate of bio-plastics from 2003 to 2007 was 38% globally and 48% in Europe. It is predicted that the worldwide capacity of bio-based composites will increase from 0,36 of 2007 to 2,33 million metric tons in 2013 and to 3,45 million metric tons in 2020 (Faruk *et al.*, 2012).

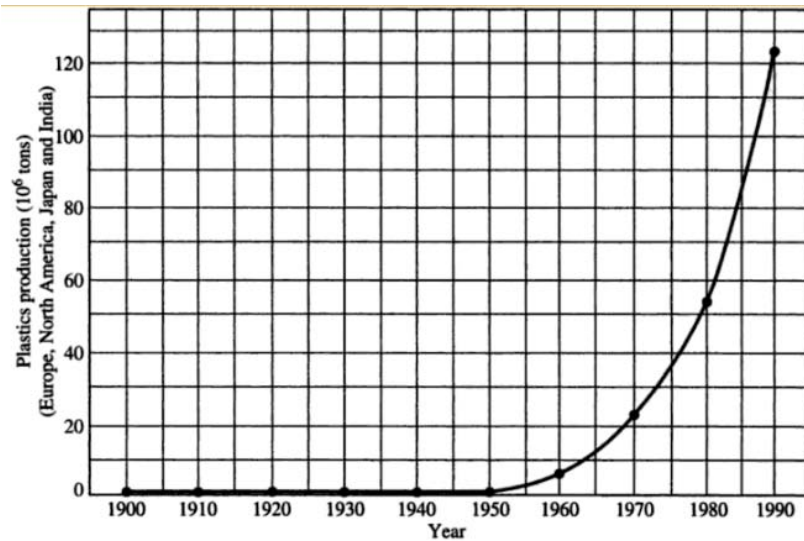


Figure a Plastics production (Griskey , 1995)

Engineering challenges related to the utility of natural fibres include; low resistance to chemical and to microbial attacks, moisture sensitivity, low thermal resistance, hydrophilic nature leading to poor surface adhesion with the polymer matrix, and the lack of repeatability of the properties of natural fibres. As a consequence, industry still prefers synthetic fibres for use in composites (carbon, glass, boron etc). Nevertheless, the production of such high performance synthetic fibres requires a high amount of energy expenditure and consequently large volumes of greenhouse gases are emitted into the atmosphere. As can be seen in Figure “b”, the energy required for the production of one ton of any natural fibre is negligible when compared with the energy required for the production of the same amount by weight of carbon fibre.

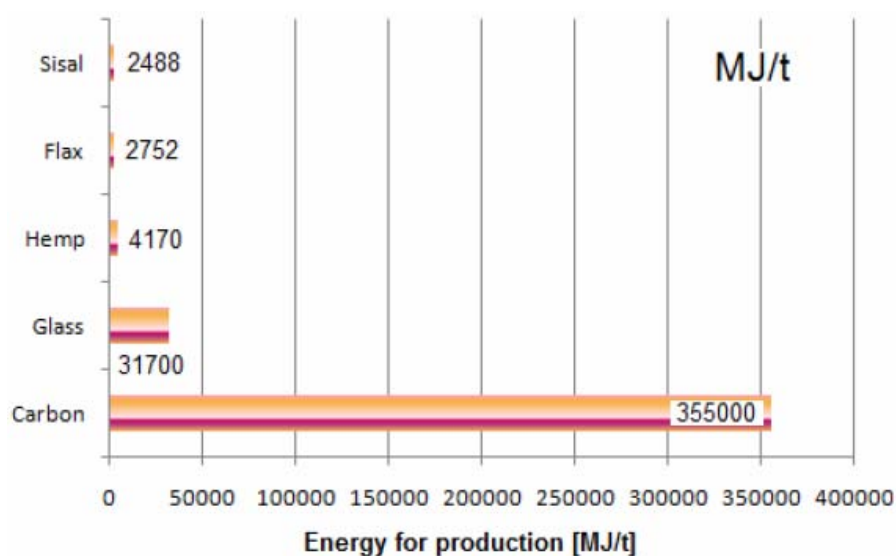


Figure b Amount of energy required to produce a ton of fibre (Cristaldi et al., 2010)

It is necessary to introduce the concept of embodied energy which is a methodology for assessing and quantifying the total energy required for the realisation of a product – from raw materials extraction to disposal. Embodied energy describes the entire life cycle in environmental management systems to compare competitive products (Cabeza *et al.*, 2013). A study of the Advanced Composites Manufacturing Centre (ACMC) of the University of Plymouth revealed that the energy required for the production of flax fibres can be, under certain conditions, higher than the energy required for glass fibres. In this study, it has been found that for the production of flax fibres, only mat fabrics (a randomly oriented reinforcement where there is not any preferential stress direction) are greener; 54 GJ/ton against 54.7 GJ/ton for glass fibres. Flax yarns have a higher embodied energy with respect to glass fibre in continuous filament production; 80GJ/ton against 31.7 GJ/ton respectively. Therefore, when selecting reinforcements for a given composite, it is important to evaluate the costs and the alternatives associated with a specific application.

In general, environmental concerns are not the only reasons why researchers now focus on developing renewable fibre technology. Other significant benefits can exist such as; low density, low cost (wide availability), biodegradability (synthetic fibres require more energy for disposal), recycling and combustibility. Moreover, natural fibres pose no real hazard to human health. They also exhibit excellent thermal insulation, acoustic and electrical properties. In Table “c”, the costs of certain fibres are reported (in US Dollar/Kg). Dittenber and Gangarao (2012) evaluated also the relative cost to mechanical performance; in particular the cost is expressed per unit length capable of resisting 100KN (in US Dollar/m for amount of fibres able to resist tensile load of 100KN).

Table c Costs: a comparison between natural fibres and synthetic fibres (Yan *et al.*, 2014, Dittenber *et al.*, 2012, Joshi *et al.*, 2004)

Fiber	US Dollar/Kg	US Dollar/m
Cotton	1.55 - 2.20	0.3 – 1.25
Flax	0.3 - 1.55	0.03 – 0.65
	0.22 - 1.10	
Hemp	0.3 - 1.65	0.05 – 0.93
Glass	1.6 - 3.25	0.12 – 0.42
	1.3 - 2	

For the reasons above, the market for natural fibres is growing and there are many industrial sectors that make great use of them. Examples include the automotive industry, the agricultural sectors, the construction industry and consumer product industries. In the field of materials science, natural fibres are one of the more utilised reinforcements for thermoplastics (Mohanty *et al.*, 2005).

Synthetic fibres still have superior properties to natural fibres. Biomimetics is the study of biological processes and systems as inspiration for human applications in order to integrate determined properties into synthetic materials (Weiner and Dove, 2003). Many organic biological materials, such as corals and sponges, have very high strength and stiffness, even though like natural fibres, their core is organic material. This is because they biomineralise and create hardened mineralised exoskeletons on their surfaces reinforcing the softer and weaker organic material. In this thesis, the aim is to mimic the mineralised calcium carbonate skeletons of corals as a coating exoskeleton to natural (flax) fibres. The hypothesis is that by doing so, it will be possible to match the effects of high performance synthetic fibres (such as glass fibre). In marine structures, the process of biomineralisation is controlled by amino acids and proteins. These organic “glues” essentially control the crystal growth mechanism, which in turn affects the morphology, properties of adhesion and interlocking of the calcium carbonate.

Chapter 1 provides a general overview about composite materials, paying particular attention to composite materials based on natural fibres. A description of the various types of renewable plant fibres and of their application in the engineering field is also explained. The end of the chapter is focused on the flax fibre, since it is used in this thesis work.

Chapter 2 describes surface treatments commonly applied to natural fibres to promote adhesion to hydrophobic polymeric matrices and to prevent damage caused by the moisture, since natural fibres are hydrophilic in nature. The base concepts of biomimetics and biomineralisation are also introduced for a better understanding of the manufacture of natural fibres composites, which is described in the following chapter. Moreover, a brief description of the crystallisation process, considering the nucleation and growth stages, is presented.

Chapter 3 provides a description on the equipments, materials and procedures used to carry out the experimental work. The results obtained and a discussion are shown at the end of each corresponding paragraph.

Finally, conclusions, limitations and future prospects of work are expounded.

Chapter 1

Composite materials and composites reinforced with natural fibres

This chapter gives a brief introduction about composite materials and their fundamental constituents, paying particular attention to natural fiber reinforced composites materials. Following this is a general overview of natural fibers used in engineering and their applications. At the end of the chapter, the properties of flax fiber are highlighted.

1.1 Composites: matrices and reinforcements.

In recent years, there has been a significant increase in the demand for the design of advanced new materials, as traditional ones are no longer deemed able to meet the challenges of technological development. Material science is geared to the design of new materials that contain all the desirable features for specific use. High strength and stiffness, coupled to low weight and high impact tolerance are just a few examples.

Composite materials comprise two or more constituents (phases) which are separated by an interface. In general, these constituents are divided into a continuous phase (matrix) and a dispersed phase (reinforcement). Composite materials are essentially multiphase structures and can exhibit a wide range of different physical and chemical properties at the macroscopic level. Each constituent has to be present in an amount of at least of 5% in engineered structures (Matthews and Rawlings, 2000).

The matrix has the function of binding together reinforcements and transferring external loads to them. The reinforcements are responsible for the improvement of the mechanical properties of the matrix and the interface allows the transfer of mechanical stress from the matrix to the reinforcement. The binding qualities of this interface are therefore very important in composites design.

There are essentially two classes of composite material. The first class is related to the type of reinforcement and may include; fibre reinforced composite materials, composite materials with particulate filler and structural composites. The second class is based on the constitution of the matrix phase. The main composites types in this class may be based on a polymer matrix (Polymer-Matrix Composite), a metal matrix (Metal-Matrix Composite) or a ceramic matrix (Ceramic-Matrix Composite).

Often, a primary motivation for choosing the matrix lies in the operating temperature. The matrix must be able to maintain the solid state and not become viscous, such that the external loads can be transferred in an appropriate manner to the reinforcement phase (Cristaldi, 2011). Table 1.1 shows the operating temperatures of some matrices.

Table 1.1: Operating temperatures of the main matrices for composite materials (Cristaldi, 2011)

Matrices	Operating Temperature [°C]
Polymer matrix	< 250
Metal matrix	< 1000
Ceramic matrix	> 1000

Rises in temperature can change the mechanical, electrical and optical responses of composites up to an order of magnitude, and up to three orders of magnitude for the diffusion of humidity (Mahieux, 2005).

Ceramic matrix composites produce materials with characteristics of high temperature resistance and high tolerance to damage caused by thermal shock (Chawla, 1993). Reinforcements for this type of refractory and chemically inert (strong covalent atomic bonds) matrix are usually used to increase the fracture toughness (Boccaccini *et al.*, 2001). Given the high elastic modulus of the matrix, the fibres are able to effectively dissipate fracture energy. Metal matrix composites ensure high thermal conductivity and a high coefficient of thermal expansion. This allows for the reduction of thermal stresses (Xuan-Hui *et al.*, 2011). In certain applications, the coefficient of thermal expansion may be too high and the addition of reinforcement allows this to be controlled.

Polymeric matrices may be thermoplastic or thermoset. Thermoplastic matrices are formed by linear polymeric chains, or linear with little side branching. Importantly, they are not cross-linked and for this reason, these products are meltable and therefore suitable for use in common composite manufacturing technologies such as; extrusion, blow moulding and injection molding. By applying heat, it is possible to model the shape of thermoplastic material, which is advantageous for recycling. However, depending on the type of polymer there are a finite number of heating-cooling cycles beyond which it is possible to see the effects of degradation. Thermoplastic polymers can be further divided into amorphous and semi-crystalline polymers. Amorphous polymers are characterised by tangled chains and they have a glass transition temperature which separates the glassy (below the T_g) and rubbery (above the T_g) phases. Amorphous polymers do not have a true melting temperature, hence they do not melt, but rather they soften within a given temperature range. Semi-crystalline polymers exhibit both an amorphous fraction and a crystalline fraction. The amorphous region behaves exactly as amorphous polymers and therefore it is characterised by a glass transition

temperature, while the crystalline region, in which the chains are ordered, has a true melting temperature (Brazel and Rosen, 2012). For these polymers, it is possible to calculate the degree of crystallinity by thermal measurements or by measuring density. From the point of view of mechanical properties, crystallinity generally makes the material stiffer, but a polymer with a high degree of crystallinity is also very brittle. The amorphous regions, in fact, increase toughness, that is, the ability to deform without breaking.

Thermosetting matrices consist of cross-linked chains. Strong intermolecular bonds prevent softening and the application of sufficient heat leads to the chemical degradation, or charring, of the polymer. In contrast to thermoplastic polymers, in most of the thermosetting polymers, hardening takes place by means of the heat application or through a chemically catalysed reaction (Modesti, 2012).

In terms of environmentally responsible engineering, biodegradable polymers are gaining importance in the market as potential substitutes for current synthetic polymers. Biodegradable polymers can be obtained from renewable sources, such as biomass, and from non-renewable sources, such as those derived petrochemically. High cost and poor mechanical properties are the greatest disadvantages of biodegradable polymers. For the moment, the advantages of biopolymers cover only the environmental aspect.

Polymeric matrices have the following properties; low density, high corrosion resistance, high thermal insulation and high dielectric/dimagnetic properties. Reinforcements in polymers are primarily used to increase the tensile, the flexural and the impact properties (Fancey, 2010).

The most common polymers used in natural fibres reinforced composites are polyesters, epoxy resins and phenolic resins (thermosets), and polyethylene, polystyrene and polypropylene (thermoplastics) (Mohanty *et al.*, 2005).

In most cases, the reinforcing phase of a composite is harder, stronger and stiffer than the matrix, whether it be particulate or fibre. The particle reinforcements often have an aspect ratio (defined as the ratio of the fibre length to the diameter) close to unity and hence are able to yield the characteristics of isotropy in the composite. The physical and chemical properties of a composite loaded with particles depend strongly on the quality of the material they are made from. This may include the shape (spherical, cubic, or irregular), the size and their volume fraction within the matrix. Often they perform the role of fillers, occupying a certain volume fraction of the matrix. This is essentially to reduce the cost of the matrix and increase its dimensional stability. Despite the reinforcing effect of the particles, they generally do not contribute a great deal to the mechanical properties of the material when used as a filler (Chawla, 2012). For high strength/weight ratio (specific resistance) and the high elastic modulus/weight ratio (specific modulus), long fibres are superior reinforcements. The fibres may be continuous (long), with an aspect ratio greater than 1000, or they may be discontinuous (short) aligned/randomly arranged, with an aspect ratio between 10 and 1000 (Lee, 1992). It is clear that given the high length/diameter ratio, the final product will have

distinctly anisotropic features, but this is not a disadvantage as it is also possible to align the fibres in the direction of loading via simple manufacturing routes. From the point of view of the quality of the material, a distinction can be made between synthetic fibres and natural fibres. Until a few years ago, synthetic fibres were the only alternative on the market for composite materials. From amongst them, glass fibre is the most commonly used due to its high strength/weight ratio, its low density and mostly importantly, its relatively low cost. Carbon fibres have excellent mechanical properties due to the particular structure of the graphite together with an extremely low density, however these fibres are considerably more expensive to fabricate than glass fibres. Another type of fibre is the aramid fibre, which is primarily known for its high resistance to traction. At present, these fibres are at the top of the range on the market, however, given the general high costs involved, they are usually utilised in niche areas. Natural fibres are those originating in plants and animals. For engineering applications, such as for use in composites, plant fibres are the most common and suitable (Cristaldi, 2011).

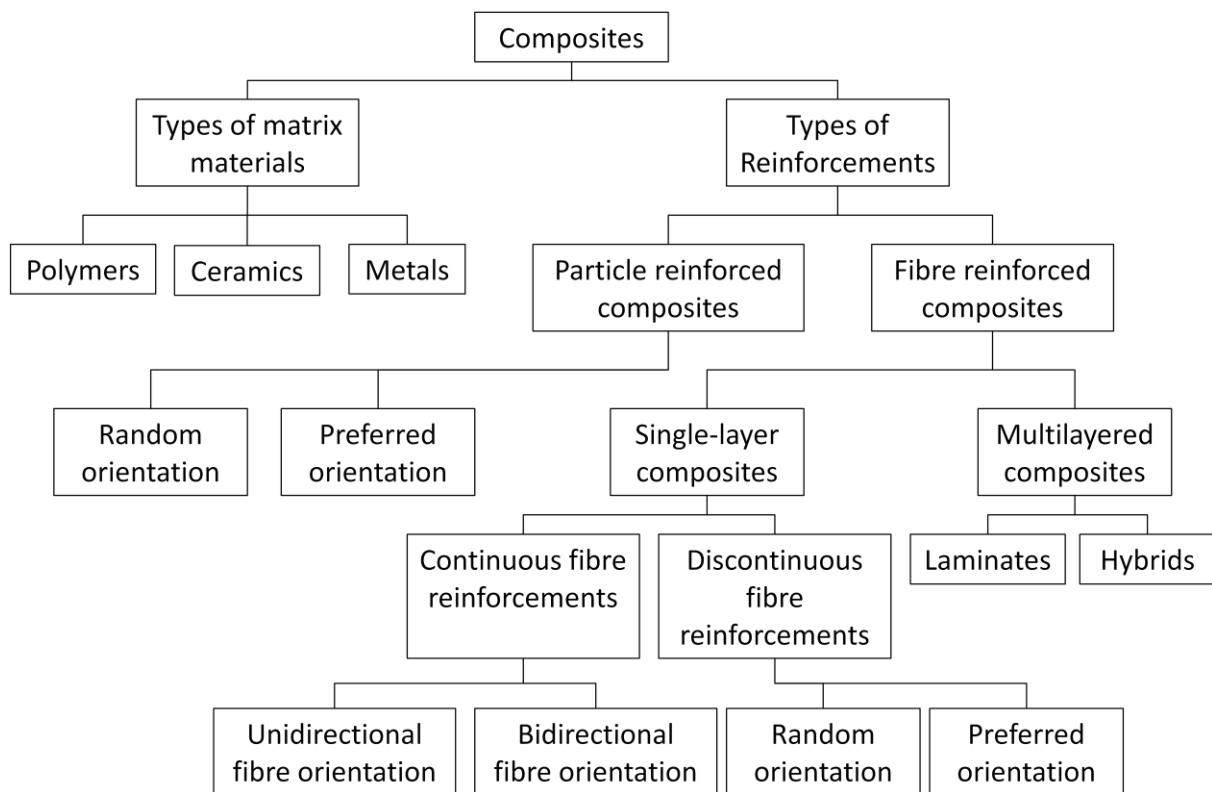


Figure 1.1 Summary diagram of composite materials

In addition to the major constituents, coupling agents can be added to composites. These work at the matrix-reinforcement interface and they are often used when there are problems of wettability between the matrix and the reinforcement. In the cases where the matrix is hydrophobic and the reinforcement is hydrophilic, it can be necessary to add a coupling agent

to improve the wettability and/or to promote the formation of bonds at the interface. In this way the materials will transmit external stresses more effectively. Other functions of coupling agents may include protection of the fibre surface and the reduction of static electricity (Kim and Mai, 1999, National Research Council of the National Academies, 2005). Figure 1.1 summarises the main classifications of composites materials.

1.2 Renewable plant fibres

Natural fibres have become popular as reinforcement in composite materials (Müssig, 2010). New regulations for environmental protection and the life cycle of the product have changed the criteria that must be taken into account in materials selection and design.

The variety of natural fibres in nature is enormous. From plants, flax, hemp, jute, and sisal are amongst the most commonly used in engineering composites. Figure 1.2 provides an overview of organic plant natural fibres.

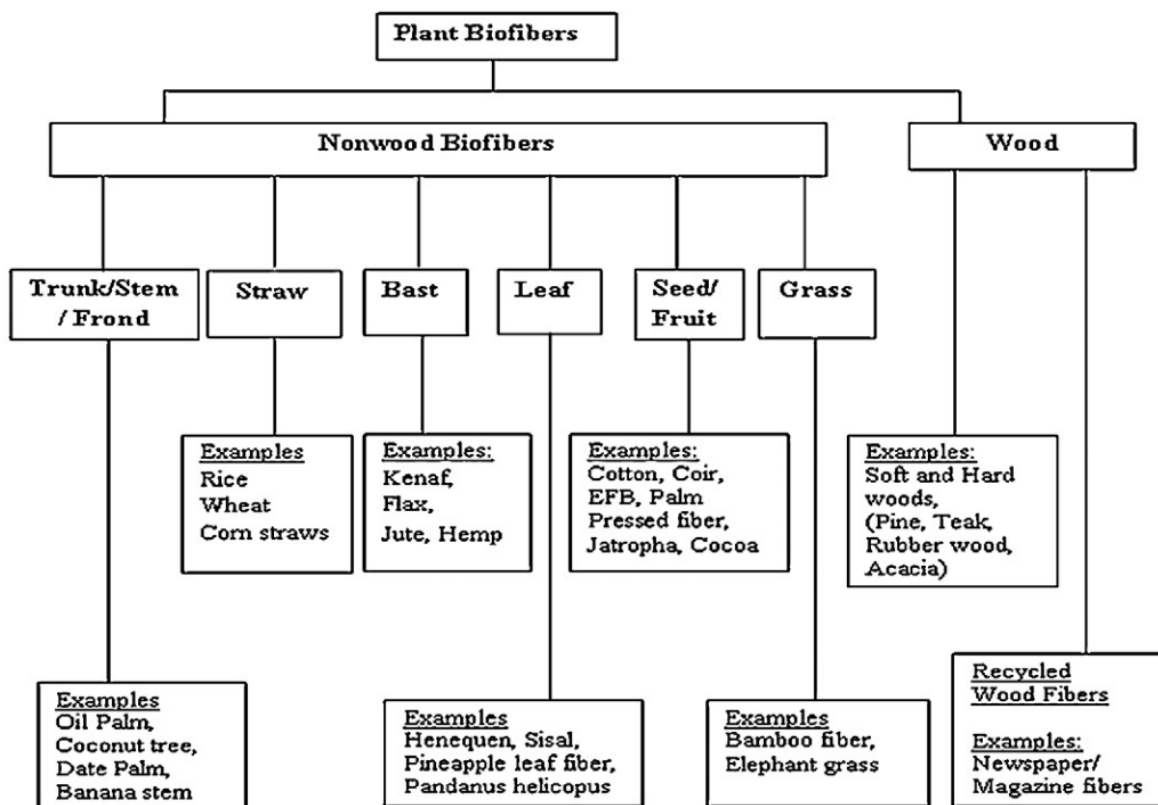


Figure 1.2 Schematic representation of reinforcing bio-fibres classification (Abdul-Khalil, 2012)

Plant fibres are composed of cellulose, hemicellulose and lignin. There are also small percentages of other compounds, such as pectin, waxes, ash and water-soluble substances. The chemical and physical structure of the fibre is the decisive variable when it comes to their functionality in technical applications (Müssig, 2010).

Plant fibres are themselves natural composite materials consisting of a matrix of amorphous lignin and hemicellulose reinforced by microfibrils (microfibrils) of crystalline cellulose. Each single strand of fibre has a diameter of at least 10 micrometres, while the microfibrils have a diameter of about 10 nanometres and are in turn formed by 30-100 macromolecules of cellulose (Dittenber and Gangarao, 2012).

The main component of plant fibres is cellulose. It is synthesised in plants from more simple carbohydrates. Cellulose is a natural linear polymer obtained by polycondensation of glucose units ($C_6H_{12}O_6$) (Nelson and Cox, 2000).

The structural hierarchy of plant fibres starts from the polymer chains made up of thousands of glucose units (see Fig.1.3). Cellulose chains in some places are arranged parallel and, by means of strong intermolecular hydrogen bonds, they are capable of forming very stable and hydrophobic crystal structures with a high tensile strength. In addition to the crystalline regions, there are some less ordered amorphous zones which decrease considerably the mechanical properties of the fibre itself, from that of the crystalline cellulose. The cellulose macromolecules build up to form microfibrils (Müssig, 2010). Hemicellulose, the second most abundant heteropolymer (Akin *et al.*, 1990), is made up of a large number of polysaccharides different in both composition and structure. Unlike cellulose, it is easily hydrated, it has a low molecular weight and a branched structure. Hemicellulose constitutes the main component of the matrix. The significant differences between cellulose and hemicellulose have been mentioned in several studies for their considerable importance during the manufacturing process and for functional attributes (Müssig, 2010). Lignin is an organic complex formed by aliphatic and aromatic groups and it is responsible for the strength, rigidity and protection from microbial attacks outside of the cell walls. Pectin is a heteropolysaccharide, that contributes to the structure of the matrix. Despite its relative low fraction, it has a fundamental role in the process of transformation of the plant fibres.

The physical properties of natural fibres depend essentially on two factors, (1) the chemical composition and (2) the microfibrillar angle, or, average angle of orientation of microfibrils, relative to the axis. The latter affects numerous mechanical properties of the fibre, in particular, a small angle leads to a high strength and stiffness, while higher angles promote the ductility (John and Anandjiwala, 2008).

The main advantages of natural fibres include the following:

- Low cost.
- Low specific weight, which means a higher specific strength and specific stiffness compared with the glass fibres.
- They are from a renewable resource and their production requires low levels of energy. Thus during the production phase, the relative volumes of emitted greenhouse gases are very low and in particular, the balance between CO_2 captured in the growth phase and CO_2 emitted during the combustion phase (in the case the fibres are used as combustible) is equal to zero.

- Better working conditions when compared with synthetic fibres; dermatological and respiratory problems are reduced.
- They are biodegradable and biocompatible, hence the life cycle of the fibre ends without by-products or waste. As said previously, thermal recycling is possible where the fibres are used as fuel.
- They have high electrical resistance.
- They have good properties of thermal and acoustic insulation.
- They do not lead to any serious abrasion of the processing equipment.

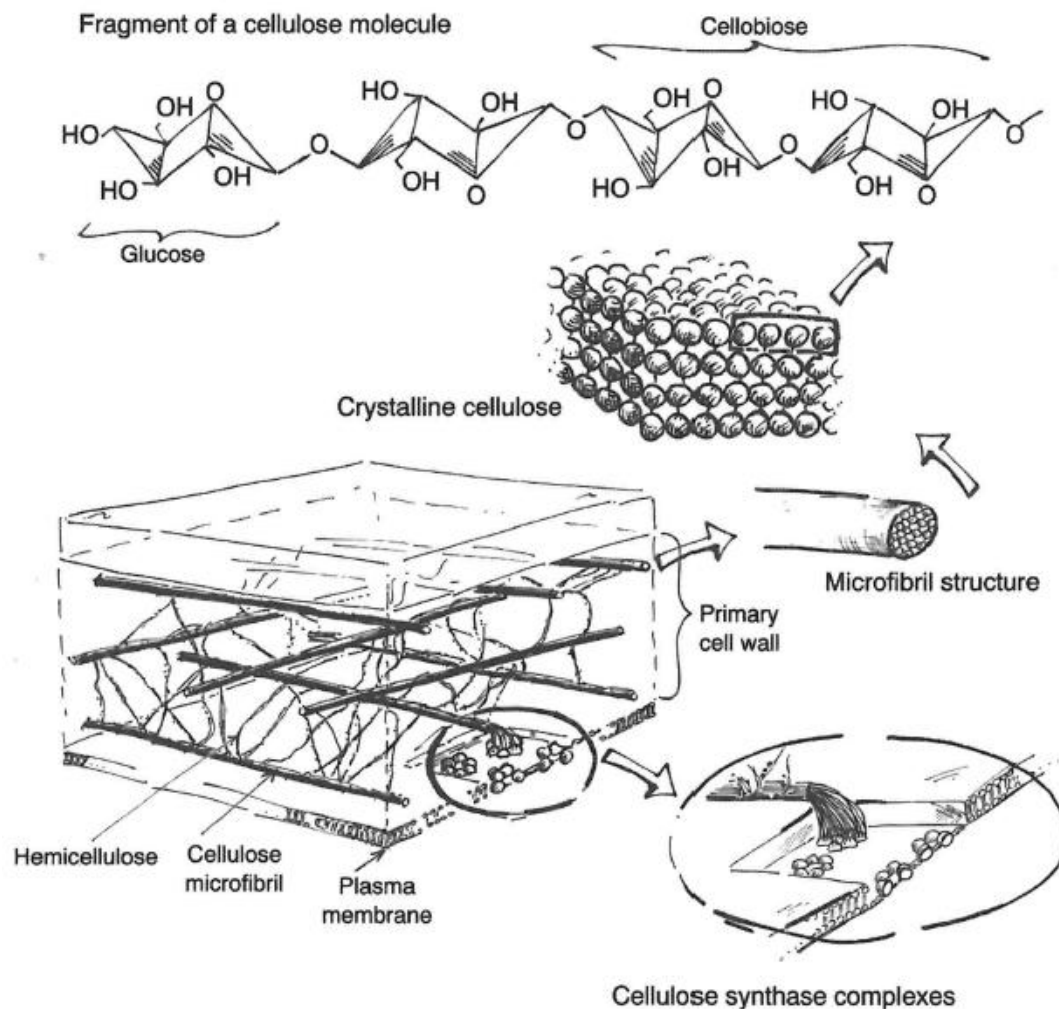


Figure 1.3 Schematic diagram of the hierarchy of a typical plant cell wall (Müssig, 2010)

In terms of disadvantages these can be listed as; climatic/soil conditions affecting the uniformity of the chemical composition and of the physical structure, poor resistance to moisture (causing swelling and dimensional instability), poor resistance to high temperatures and low durability. It is clear that the advantages outweigh the disadvantages and in the case of the latter, it is possible to find remedies based on the chemical treatments of the fibres and

their surfaces. In the following table, Table 1.2, physical data related to the typical reinforcing fibres, both vegetable and synthetic, are shown.

Table 1.2 Physical data of the most important fibres for composites (Mohanty et al., 2005)

Fiber	Density [g/cm³]	Diameter [μm]	Tensile strength [MPa]	Young's Modulus [GPa]	Elongation at break [%]
Flax	1.5	40-600	345-1500	27.6	2.7-3.2
Hemp	1.47	25-500	690	70	1.6
Jute	1.3-1.49	25-200	393-800	13-26.5	1.16-1.5
Kenaf	-	-	930	53	1.6
Ramie	1.55	-	400-938	61.4-128	1.2-3.8
Nettle	-	-	650	38	1.7
Sisal	1.45	50-200	468-700	9.4-22	3-7
PALF	-	20-80	413-1627	34.5-82.5	1.6
Abaca	-	-	430-760	-	-
Oil Palm EFB	0.7-1.55	150-500	248	3.2	25
Oil palm mesocarp	-	-	80	0.5	17
Cotton	1.5-1.6	12-38	287-800	5.5-12.6	7-8
Coir	1.15-1.46	100-460	131-220	4-6	15-40
E-glass	2.55	<17	3400	73	2.5
Kevlar	1.44	-	3000	60	2.5-3.7
Carbon	1.78	5-7	3400-4800	240-425	1.4-1.8

In summary, the mechanical properties of plant fibres are generally lower than those of synthetic origin. The strength and tensile modulus of natural fibres are less than those of synthetic fibres, but the difference between the two categories of fibres is attenuated if the mechanical properties are factored to the density.

1.3 Applications of natural fibres

The use of natural fibres is not new. Before man-made synthetic fibres, the only alternative for reinforcing composite materials was in vegetable or mineral fibres, and the associated technologies were quite advanced (Brown, 1947). The driving force for the use of this type of fibre, however, has changed. It has gone from having a purely technical purpose to having

both technical and environmental purpose (Müssig, 2010). In the past, natural fibres have been used in various applications; from shellac compounded by wood flour in the field of photography during the 1850s, to the use of flax fibre reinforced phenolic resin for airscrews in aeronautics in the 1930s (McMullen, 1984). Further, from fibre-reinforced soy-protein plastic discovered by Henry Ford in 1941 used in a prototype car (Materials,2010), to the monocoque construction of Trabant which includes the bonnet, the roof, the wings and the doors made by a thermosetting phenolic resin reinforced with cotton fibres, in 1958, in the automotive industry. Nowadays, composite materials reinforced with natural fibres are widely used in the construction industry and in the automotive field.

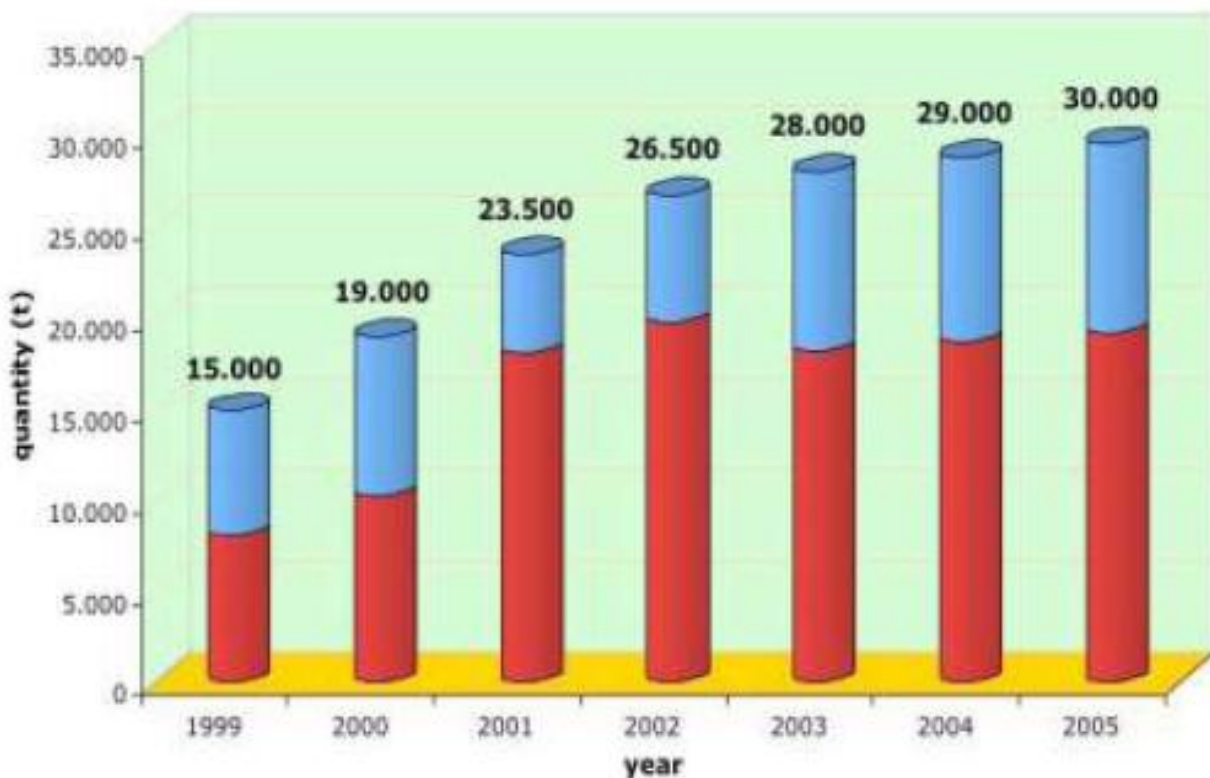


Figure 1.4 Usage of natural fibres in the automotive industry in Germany. Utilization in thermoplast (red) and thermoset (blue) (Nova-Institut, Germany)

The automotive industry is one of the most avid users of natural fibre composites designed especially for indoor applications, such as doors panels, seats, covers, hat rack, dashboards, brake pads and windshields. The DEFRA (Department of Environment, Food and Rural Affairs) of 2002, expects a growth in the use of natural fibres for automotive components, of about 54% per year. In the U.S. about 1.5 million vehicles are using natural plant fibres, such as jute, hemp and kenaf, to reinforce polymer matrices (Alves *et al.*, 2010). Further evidence for this comes from the chart above which shows the trend in the use of natural fibres in the automotive industry in Germany (Figure 1.4).

The driving force for the automotive industry towards using natural fibres is mainly due to their low cost and their low density. The low cost includes the acquisition of raw materials and the disposal of the product at the end of its life. In fact, they can be easily recycled or used as fuel. In the U.S. the number of landfills for the disposal of waste produced by the car industry has been reduced from 8000 to 2314 over a 10-year period (1988-1998) (Anil *et al.*, 2003). A comparative LCA study, conducted by the authors Joshi *et al.* (2004), shows that, at the same performance level, natural fibres reinforced composites have higher fibre content than glass fibre reinforced composites, which reduces the cost of the polymeric matrix and the amount of pollutants at the end of the life-cycle. The low weight furthermore ensures a significant reduction of the fuel consumption (Mohanty *et al.*, 2005).

Directive 2000/53/EC on “End of Life Vehicles” (ELVs), became law in 2000. The purpose of this directive is the reduction of waste arising from ELVs and the increasing of the recovery of the vehicle. This law set the year 2005 as the deadline for achieving the objective of recycling 85% of the weight of the vehicle. This percentage was increased to 95% for 2015 (Reuter *et al.*, 2006). The most practical way to work towards the legislation is to use thermo-chemical treatments, such as pyrolysis or gasification, in order to reduce the environmental impact of solid waste and to establish a new source of energy. This new energy source results from the decomposition of organic material. Another method is to employ innovative recycling concepts and renewable raw materials based on natural compounds (Sroggi, 2008).

The first companies that lead the development of natural fibres in automotive components are German, such as Audi, BMW, Mercedes-Benz and Daimler Chrysler. Nevertheless, now virtually every automobile industry develops and inserts natural based composites inside their vehicles (Mohanty *et al.*, 2005). In 1996, Mercedes-Benz included, in its E-Class, many components made from natural fibres, such as an epoxy resin reinforced with jute fibres for door panels, in 2000, Audi launched the A2 equipped with door trim panels made of polyurethane reinforced with flax and sisal fibres and, since 2003, BMW uses epoxy resin impregnated composites with a content of natural fibres, such as flax and hemp, by 70%. Recently, consideration is being made into the use of these materials in outdoor applications. In 2004, Daimler Chrysler replaced the glass fibres with plant fibres of abaca to manufacture spare tyres for Mercedes-Benz A-Class and, in 2008, Lotus has succeeded in replacing the same synthetic fibre by hemp fibre to make lighter body parts (Koronis *et al.*, 2007). In Table 1.3, other examples of automotive manufacturers utilising natural fibres are shown.

Table 1.3 Current well-established applications of natural fibres in automotive vehicles (Mohanty et al., 2005)

Automotive manufacturer	Model and application
Audi	A2, A3, A4, A4 Avant, A6, A8: Seat back, side and back door panel, boot lining, hat rack, space tire lining
BMW	3, 5 and 7 series and others: door panels, headliner panel, boot lining, seat back
Daimler/Chrysler	A, C, E, S class: door panels, windshield/dashboard, business table, pillar cover panel. A class, Travego bus: exterior under body protection trim. M class: instrumental panel (now in S class: 27 parts manufactured from bio fibres, weight 43 kg)
Fiat	Punto, Brava, Marea, Alfa Romeo 146, 156
Ford	Mondeo CD 162, Focus: door panels, B-pillar, boot liner
Opel	Astra, Vectra, Zafira: headliner panel, door panels, pillar cover panel, instrumental panel
Peugeot	New model 406
Renault	Clio
Rover	Rover 2000 and others: insulation, rear storage shelf/panel
Saab	Door panels
SEAT	Door panels, seat back
Volkswagen	Golf 4, Passat Variant, Bora: door panel, seat back, boot lid finish panel, boot liner
Volvo	C70, V70
Mitsubishi	Space star: door panels. Colt: instrumental panels

As said previously, the market of natural fibre composites is not confined to the automotive industry, but fits comfortably into various sectors. The numerous applications, in which the natural fibres are used nowadays, are summarised in Figure 1.5.

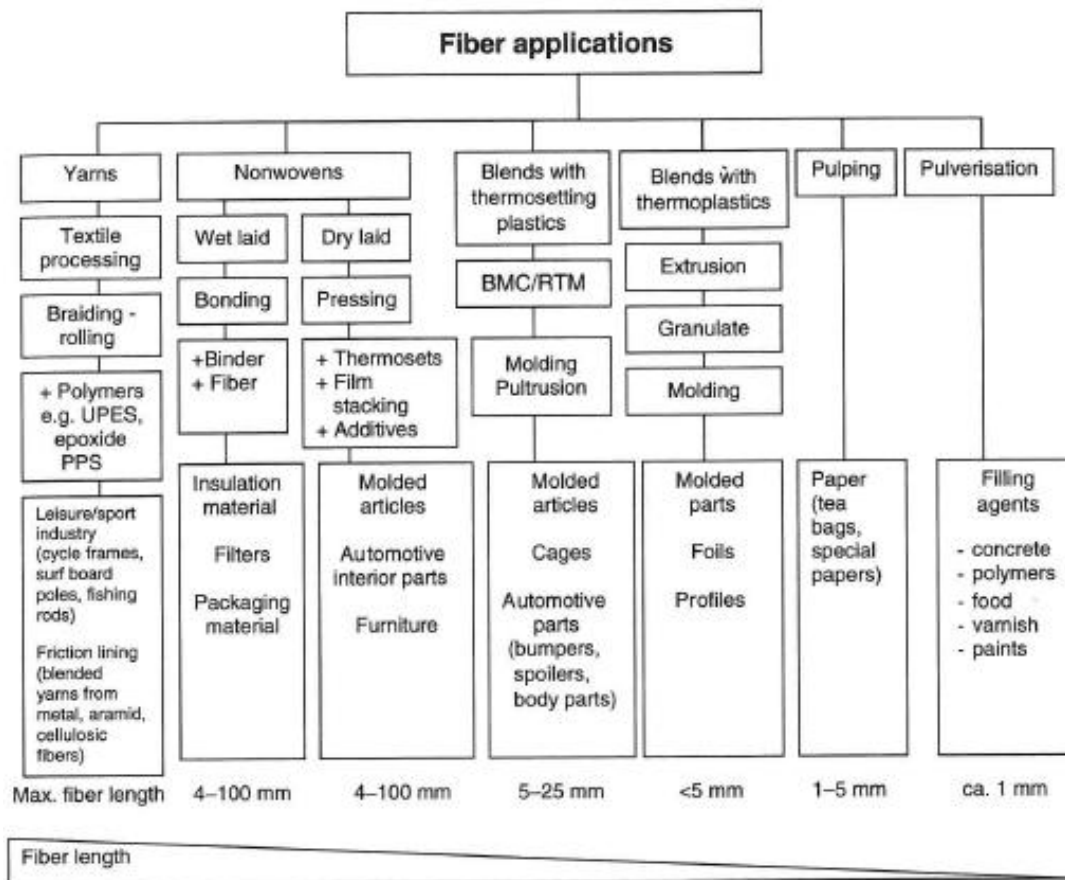


Figure 1.5 Promising nontextile applications of blast fibres (Mohanty et al., 2005)

1.4 Flax fibres

The scientific name of flax is *Linum usitatissimum*. Flax is a natural composite fibre formed mainly of cellulose and lignin (Müssig, 2010) and it is categorised as vegetable bast fibres (Stillfried, 2012). In Table 1.4 is shown the chemical composition of flax fibres as reported by different authors.

Table 1.4 Chemical composition of flax fibres (Yan et al., 2013)

Cellulose [%]	Hemi-cellulose [%]	Pectin [%]	Lignin [%]	Wax [%]	Moisture content [wt.%]	Authors
64.1	16.7	1.8	2.0	1.5	10.0	(Lewin and Pearce, 1998)
67	11	-	2.0	-	-	(Lilholt et al., 1999)
73.8	13.7	-	2.9	-	7.9	(Khalil et al., 2000)
65	-	-	2.5	-	-	(Troger et al., 1998)
62-72	18.6-20.6	2.3	2-5	1.5-1.7	8-12	(Dittenber and G., 2012)
71-75	18.6-20.6	2.2	2.2	1.7	10.0	(Cristaldi et al., 2010)

This ligno-cellulosic fibre is one of the most promising alternatives to replace glass fibres as reinforcement in engineering composites (Zafeiropoulos *et al.*, 2001). The high content of crystalline cellulose makes it strong and stiff. Its incorporation into composites results in an improvement of properties, such as, the stiffness, the tensile strength, the light weight, the manageability and the anisotropy (Baiardo *et al.*, 2004, Baley *et al.*, 2006). The following Table 1.5 shows that the physical and mechanical properties of flax fibres are comparable to those of glass fibres.

Table 1.5 Physical properties, tensile properties and specific tensile properties of flax and glass fibres (Bos *et al.*, 2004, Hull and Clyne, 1996)

Property	E-glass	Flax fibres
Diameter [μm]	8-14	10-80
Density [g/cm^3]	2.56	1.4
E-modulus [GPa]	76	50-70
Tensile strength [GPa]	1.4-2.5	0.5-1.5
Elongation to fracture [%]	1.8-3.2	2-3
Specific E-modulus [GPa per g/cm^3]	30	36-50
Specific tensile strength [GPa per g/cm^3]	0.5-1	0.4-1.1

In Table 1.6, are shown the results of a study from LCA-comparative concerning non-renewable resources required for their production. This table compares flax and glass fibre properties. It can be seen that the energy required for the cultivation, the extraction and the production of flax fibres is about 5 times lower than for the manufacture of glass fibres, which is heavily dependent on non-renewable oil-based energy sources. As a consequence of this, in the case of glass fibres, the emissions of greenhouse gases will be significantly higher (Joshi *et al.*, 2004). The low density, the low price, the low amount of energy required, the biodegradability and the ease of processing flax has led to a continuous growth in use, starting from 1990, in larger volume engineering markets (Celli, 2012). Moreover, at the end of the life-cycle of flax fibres energy recovery is possible to since they have a good calorific value (Stamboulis *et al.*, 2001). Globally 350k tonnes of flax are produced every year (Scheifele *et al.*, 2001) and according to a report of the Flax Council of Canada (2012), the demand of flax fibres in Europe is increasing by more than 50% every year.

Given the increase in the prices of the oil, considering the energy consumption and taking into account new environmental standards, traditional materials can no longer meet market demands. For this reason, the future for flax fibre reinforced composites is promising and

thorough research will be necessary for the optimisation of each single process step; from plant breeding to the technologies associated in obtaining the final product.

Table 1.6 Non-renewable energies requirements for the manufacture of glass and flax fibres (Joshi et al., 2004)

Nonrenewable energy requirements [MJ/kg]			
Glass fibre mat		Flax fibre mat	
Raw materials	1.7	Seed production	0.05
Mixture	1.0	Fertilizers	1.0
Transport	1.6	Transport	0.9
Melting	21.5	Cultivation	2.0
Spinning	5.9	Fibre separation	2.7
Mat production	23.0	Mat production	2.9
Total	54.7	Total	9.55

Chapter 2

Surface treatments and biomineralisation

The purpose of this chapter is to provide an initial overview of the main surface treatments that are carried out on natural fibers to ensure a better fit to the matrix. Following this are subsections covering concepts related to biomimetics and biomineralisation. The final argument concerns the phenomenon of nucleation and growth that occurs in the process of biomineralisation.

2.1 Reinforcement – matrix interface in composites based on natural fibres and characterisation methods

The interface plays a key role as regards the load bearing and fracture behaviour of a fibre reinforced composite. Excellent properties for both reinforcement and matrix are not sufficient for a wholly functioning composite. In order to increase the mechanical performance of the matrix with the reinforcements, specific features of the interface should be optimised. In fact, external loads are transferred from the matrix to the reinforcements via the interface and a weak interface will result in a very weak composite. Generally, strongly bonded fibre/matrix interfaces give high strength and stiffness to the composite, while weak interfaces ensure a high resistance to reinforcement fracture, but exhibit low properties of composite strength and stiffness (American Society of Testing and Materials, 1969). The problem of weak adhesion may arise when a hydrophobic polymeric matrix is reinforced by hydrophilic natural fibres. The result is poor wetting that creates poor adhesion of the fibres to polymeric materials as well as a high affinity to moisture. These are the biggest drawbacks to the use of natural fibres in composites (Gound, 2011). Surface treatments are often applied to fibres to lower the interfacial energy. This means that treatments will decrease interfacial tension at the surfaces (Gauthier *et al.*, 1998). The interface can also form a real distinct phase inside the composite; in some cases this phase is characterised by only few atoms, while in others the interphase can be considerably thicker. In this way, between the matrix and the reinforcement there is a discontinuity in both physical and chemical properties and the characteristics of the interface is determined by the treatment applied (Matthews and Rawlings, 2000).

During composite manufacture, there is a stage in which the matrix is in a liquid state, or in a viscous state, so it can flow onto and wet the reinforcements. Wettability is the main concept

during this stage. Wettability defines the ability of a liquid to spread over a solid surface and the degree of wettability is determined by a force balance between adhesive forces (which depend on the interactions between solid particles and liquid particles) and cohesive forces (they are attractive forces between particles of the liquid which tend to prevent the spreading). Wettability between a liquid and a solid surface can occur in a gas medium, or in an immiscible liquid medium. Wettability is completely described by the contact angle that is the angle made by the tangent to the interface liquid/fluid and the tangent to the solid surface. Good wettability is described by a contact angle smaller than 90° and it means that the liquid wets the solid, while a contact angle wider than 90° describes a situation in which the liquid does not wet the solid and it translates in poor wettability. In the case of water, good wettability is hydrophilicity while poor wettability is hydrophobicity. From a thermodynamic point of view, good wettability occurs when the interfacial tension of the wetting substance is lower than that of the substrate. Figure 2.1 shows a drop of liquid on a dry surface making a contact angle (Matthews and Rawlings, 2000).

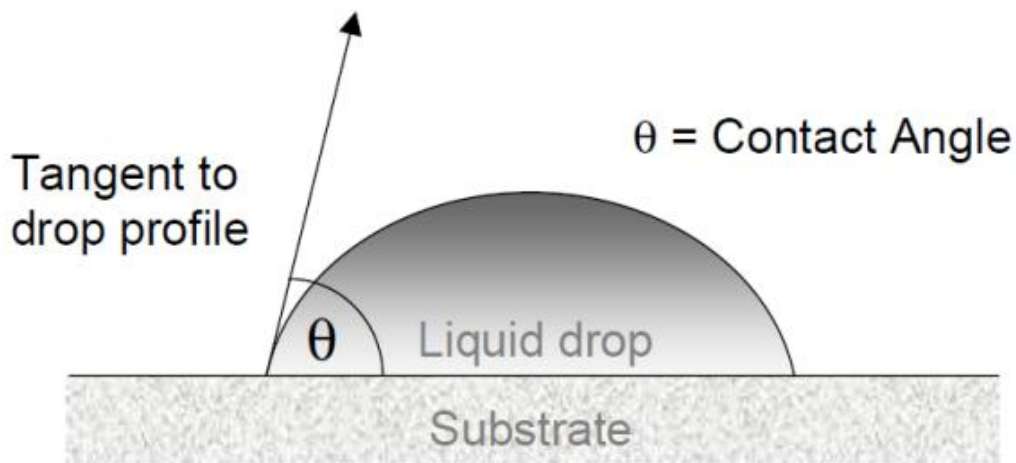


Figure 2.1 A liquid over a solid in equilibrium with a contact angle θ

All surfaces have an associated energy and the surface tension quantifies this energy. The surface tension is the ratio between the work required to obtain an infinitesimal increase of area and the infinitesimal increase of area itself, hence the unit of measure is referred to as the energy per unit area. The surface tension of solid-gas, liquid-gas and solid-liquid interfaces are γ_{SG} , γ_{LG} , γ_{SL} , respectively. For each increase of area or interface, dA , between solid and liquid, an addition of energy is required for the new solid-liquid and liquid-gas interfaces. Hence, the following:

$$(\gamma_{SL}dA + \gamma_{LG}dA) \quad (2.1)$$

is the energy required for the formation of the new solid-liquid and liquid-gas interfaces. The energy recovery due to the decrease of solid-gas interface is given by:

$$(\gamma_{SG}dA) \quad (2.2)$$

In order to have a spontaneous spreading of the liquid on a solid surface:

$$(\gamma_{SL}dA + \gamma_{LG}dA) < (\gamma_{SG}dA) \quad (2.3)$$

and dividing by dA , (2.3) gives (2.4):

$$\gamma_{SL} + \gamma_{LG} < \gamma_{SG} \quad (2.4)$$

The Spreading Coefficient SC , can be defined by the following equation:

$$SC = \gamma_{SG} - (\gamma_{SL} + \gamma_{LG}) \quad (2.5)$$

SC has to be positive for wetting. It is worth mentioning the Young's equation (2.6) is able to describe the balance of forces that occurs inside and outside the wet drop on a dry solid surface;

$$\gamma_{SL} + \gamma_{LG}\cos\theta = \gamma_{SG} \quad (2.6)$$

where the contact angle is given by Equation (2.7):

$$\theta = \arccos\left(\frac{\gamma_{SG} - \gamma_{SL}}{\gamma_{LG}}\right) \quad (2.7)$$

The bond between the matrix and the reinforcement occurs once the matrix is in contact with the reinforcement. The main bonds are mechanical, electrostatic, chemical and reactive. Moreover, they can coexist or change, from one to another, during the manufacturing stages of the composite.

Mechanical bonding consists of the interlocking of two surfaces if there exists an appropriate surface roughness. This kind of bonding is not usually adequate for technical applications, though it provides good resistance to shear. Electrostatic bonding occurs when the surfaces have opposite charges. Since this is a short range bond, it is affected by the intimacy of contact between the matrix and the reinforcement. The chemical bond is characterised by real chemical bonds between different groups existing both in the matrix and in the reinforcement.

On a surface there are compatible groups required for forming the appropriate bonds with groups available on the opposite surface. Often, dressing the fibre with coupling agents is necessary. For example, silanes are widely used as coupling agents for hydrophilic natural fibres so as to ensure good bonding with the non-polar and relatively hydrophobic polymeric matrix (Abdelmouleh *et al.*, 2007). Interdiffusion, or reactive bonding, takes place when atoms or molecules from both the matrix and the reinforcement interdiffuse mutually at the interface, resulting in molecular entanglements in the case of polymers. More generally, reactive bonding depends on the number of molecules involved per unit area at the interface and on the thickness over which the molecules have diffused. This type of bond is frequent in composites made by metal or ceramic matrix composites because they are processed under high temperatures and the diffusion coefficient is affected by temperature. In particular, the diffusion coefficient (D_d) increases exponentially with the temperature according to the following Arrhenius-type equation (2.8)(Matthews and Rawling, 2000):

$$D_d = D_0 \exp\left(-\frac{Q_d}{RT}\right) \quad (2.8)$$

where D_0 is the pre-exponential factor independent of temperature and Q_d is the activation energy.

It is now important to write a general overview of the physical and chemical properties of natural fibres to better understand the significance of each treatment. It must be pointed out that both the physical and chemical properties of natural fibres are highly variable as a function of growth location, the conditions during growth and the extraction methods. All this affects the fraction of cellulose, the degree of polymerisation, the orientation of filaments, the crystallinity and the geometrical properties (such as diameter, specific area and aspect ratio). However, the properties can be changed by means of appropriate treatments. For example, a progressive increase in the degree of crystallinity can be achieved by eliminating less organised regions through dissolution with chemicals or under attack of microorganisms. Using this method, it is possible to obtain a 100% degree of crystallinity.

The main component of natural fibres is cellulose. It is made up of anhydro-D-glucose repeat units which have three hydroxyl groups (OH) that are able to form both intermolecular and intramolecular hydrogen bonds. Hence they have a hydrophylic nature. It has to be stressed that the characteristic of hydrophilicity is found both on the surfaces and in the bulk of natural fibres. Cellulose swells in polar media, such as water, dimethylformaldehyde and dimethylsulfoxide through its structural organisation, which allows for the entrapment of molecules, and because of its hydroxyl groups, which form hydrogen bonds with water molecules. Non-polar media, such as benzene, toluene and aliphatic hydrocarbons encourage hydroxyl groups into the structure that is full of holes (Gauthier *et al.*, 1998). The amount of

water adsorbed into the fibre depends on an equilibrium between its concentration inside the fibre and its partial pressure in the medium. Water absorption is affected by the purity of the cellulose (untreated fibres can absorb at least twice as much water as treated fibres) and by the degree of crystallinity. This is because only OH groups from the amorphous regions are available to interact with water. The crystalline regions are rigid and already electrostatically bonded, making it harder for them to readily interact with water (Gauthier *et al.*, 1998). Methods used for the treatment of natural fibres are of the physical, physico-chemical and chemical type, but the aims of treatments are usually the same; (1) the removal of contaminants from the surface and (2) improved properties of adhesion between the matrix and reinforcement in the composite. Physical treatments are typically used to separate single filaments in order to raise the reinforcement surface area and thus increase the adhesion of fibres to hydrophobic matrices. Methods for improving interfacial adhesion include; ultrasound, ultraviolet and electrical discharge methods, such as corona and cold plasma, which alter the polarity of the natural fibre surface (Mukhopadhyay and Figueiro, 2009). Cold plasma is one of the most interesting modern technologies. It is generated by applying a potential difference between two electrodes placed in a chamber containing a rarefied gas. The applied cold plasma cleans the surface to promote adhesion of coupling agents, and ablates or etches to make a rougher surface, which in turn increases the interlocking, the crosslinking or branching of molecules, subsequently strengthening the surface layer. The surface can also be modified by means of functional groups or free radicals that are able to interact with the functional groups at the matrix interface (Mukhopadhyay and Figueiro, 2009). Thanks to the low operating temperature used in the cold plasma method, surface treatment leaves the bulk properties generally unchanged. For these reasons, this method is particularly suitable for the treatment of temperature sensitive materials, such as synthetic polymers and natural fibres. Moreover, this is a clean treatment because it does not need solvents, it uses a low concentration of reactants and it works under atmospheric pressure (Zhou *et al.*, 2011). The gases used to increase the hydrophobicity of natural fibres may be sulphur-hexafluoride, or more generally, fluorocarbon-based gas (Hochart *et al.*, 1999) and hexamethyldisiloxane (Vautrin-UI *et al.*, 2000).

Physico-chemical treatments include surface fibrillation, also called mercerisation, and other methods applied during the manufacturing of the composite (Mohanty *et al.*, 2005).

Amongst the various processing treatments available, the use of enzymes during manufacture of natural fibres leads to the removal of organic compounds or pollutants (Islam, 2013). This technology has many benefits including; cost reduction, the improvement of the product quality and the energy and water saving benefits (Bledzki *et al.*, 2010).

Coupling agents are typically used in chemical treatments of natural fibres. Coupling agents are substances, commonly polymers, which are added in low concentrations as a superficial treatment to make the fibres more compatible in composites applications. They have the

chemical ability to interact with both the hydroxyl groups (OH) of the cellulosic fibre and with functional groups at the matrix interface, creating thus, molecular continuity across the entire interfacial regions of the composite (Mohanty *et al.*, 2005). The bonding is typically covalent, secondary (such as hydrogen bonding and van der Waals forces), polymer molecular entanglements and mechanical interlocking. Mechanical interlocking is itself often due to the change in the roughness and structure of the fibre surface (Ashori, 2008). In addition, the use of coupling agents minimises the sensitivity of the fibre to moisture. This occurs as the coupling agents limit the presence of hydroxyl groups. The most commonly used coupling agents in natural fibre composites in a polymeric matrix are copolymers containing maleic anhydride (anhydride groups may react with hydroxyl groups of the cellulose forming ester bonds, while the other end of the molecule may entangle with the polymeric resin), sodium hydroxide, acetic acid, acrylic acid, peroxide potassium permanganate, benzoyl chloride, silanes, isocyanates and titanates. A few chemical methods are described below.

Silanes are multifunctional molecules that are able to make a bridge between cellulose molecules via hydrogen bonds, and within the polymer via stable covalent bonds (Maya and Anandjiwala, 2008). The general chemical formula of silane is X_3SiR and when choosing the functional groups X and R, each combination of cellulose/resin should be evaluated. In particular the chemical properties of both surfaces have to be known. R is the organic functional group that reacts with the polymer, while X is the group that interacts with the cellulose. It is important that X groups are able to hydrolyse in aqueous solution in order to form more reactive silanol groups that can form hydrogen bonds with the hydroxyl groups of the cellulose. Silanol molecules have a high affinity for each other; during the hydrolysis process, silanol molecules interact with each other and start forming polysiloxane oligomers of SiOSi bonds. This step should be minimised to leave silanols free for adsorption to the natural fibre. Once silanes molecules are hydrolysed, the next stage involves adsorption on the fibre surface. Here, the reactive monomers and oligomers react with the hydroxyl groups by means of hydrogen bonds. Finally, when heated surface grafting may be possible, where hydrogen bonds between silanols and hydroxyl groups are replaced by reversible covalent SiOC bonds. The competition of alkoxy hydrolysis and silanol condensation with hydroxyl groups of the natural fibre depends on the temperature, the solvent and the concentration of silanes (Xie *et al.*, 2010). A schematic of the mechanism is presented in Figure 2.2.

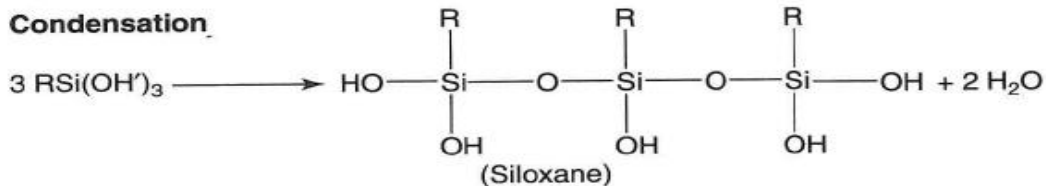
Among the different types of silanes, aminosilanes are the most commonly used as coupling agents for both thermoplastic and thermoset polymeric matrices (Xie *et al.*, 2010).

Isocyanates are one of the more promising coupling agents for thermoplastic matrices reinforced by natural fibres and in particular, the use of poly(methylene)-poly(phenyl) isocyanate (PMPPIC) has shown the best results in respect of mechanical properties.

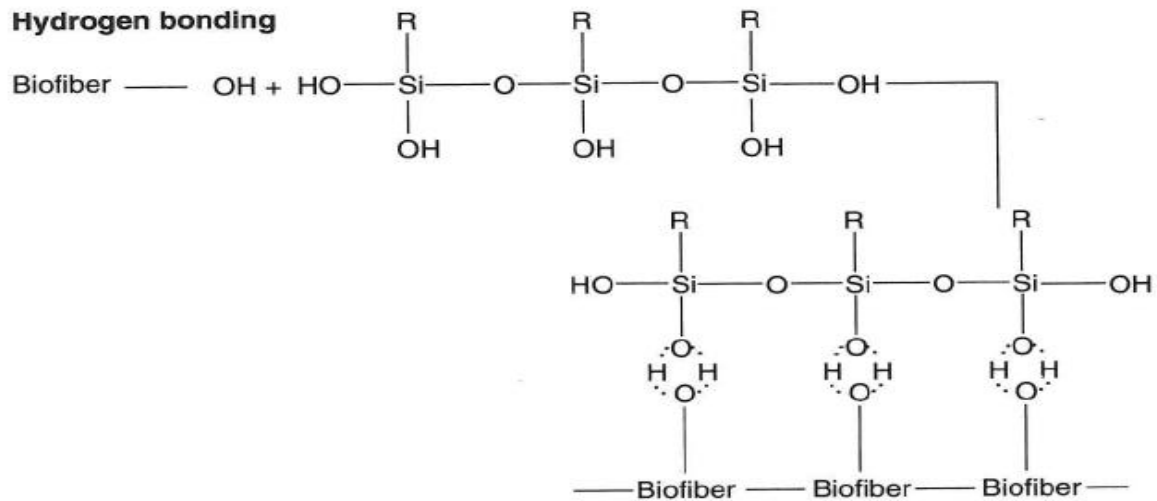
Hydrolysis



Condensation



Hydrogen bonding



Surface grafting

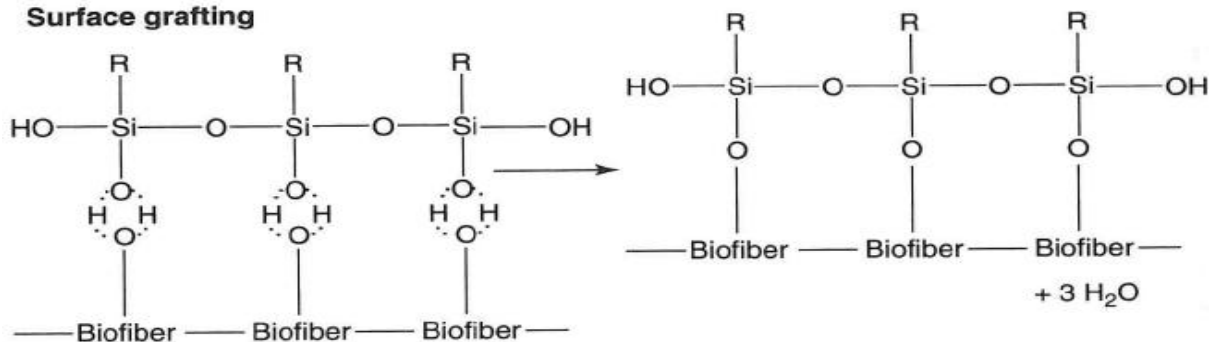


Figure 2.2 Schematic representation of the mechanism of interaction of silane with the natural fibre (Mohanty et al., 2005)

This improvement was found to be due to the strong covalent bonds formed with the hydroxyl groups within the cellulose (Pickering and Ji, 2004). The isocyanate group $-N=C=O$ is highly reactive with $-OH$ groups and can form the urethane group shown in Figure 2.3.

It is important to take into account that the presence of moisture is a big disadvantage for the isocyanate reaction. Isocyanate groups tend to react more readily with water than with the hydroxyl groups of cellulose (Jayamol *et al.*, 2001).

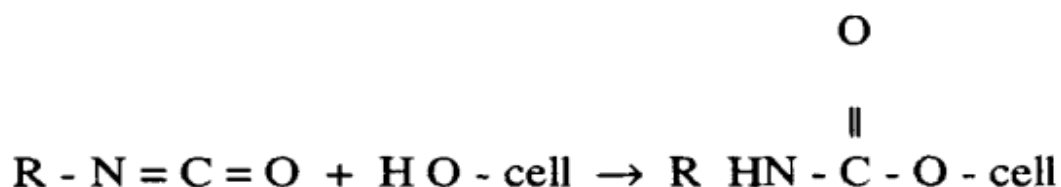


Figure 2.3 Formation of the urethane group between cellulosic fibre and isocyanate (Jayamol *et al.*, 2001)

Sodium hydroxide plays an important role in the formation of charged intermediate species on the fibre surface, allowing for the nucleophilic addition of compounds, such as alkyl halides, epoxides, benzoyl groups, acrylonitrile and formaldehyde, in the reactions of etherification and benzylation. Concerning the latter reaction, the inclusion of the benzoyl group ($C_6H_5C=O$) into the fibre promotes hydrophobic behaviour. Benzoyl chloride is used the most. Figure 2.4 shows the mechanisms of these reactions (Susheel *et al.*, 2009).

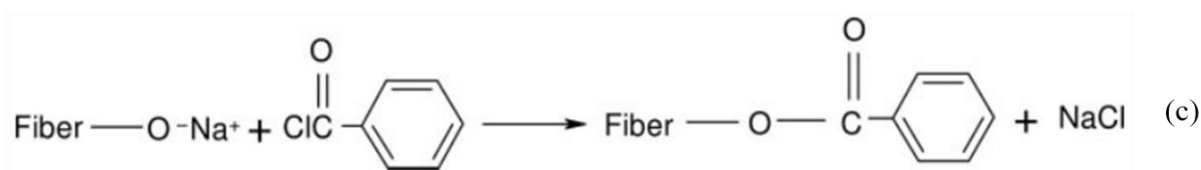
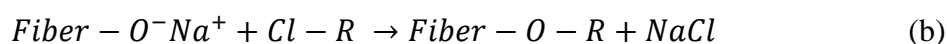
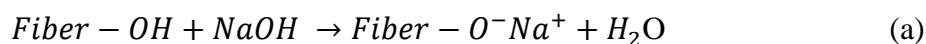


Figure 2.4 Alkaline pre-treatment for the activation of the cellulose hydroxyl groups (a) and reaction schemes for the etherification (b) and benzylation (c) (Susheel *et al.*, 2009)

Acetylation of natural fibres is a treatment resulting in higher dimensional stability and stabilisation against moisture. These characteristics arise through the substitution of hydrophilic hydroxyl groups with acetyl groups from acetic anhydride in acetic acid (CH_3COOH) (Susheel *et al.*, 2009). The mechanism of the reaction is presented in Figure 2.5.

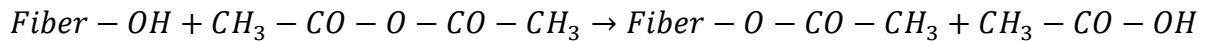


Figure 2.5 Acetylation of natural fibre with acetic anhydride (Sreekala *et al.*, 2000)

The use of organic peroxides is another common treatment used to inhibit natural fibre hydrophilicity by removing hydroxyl groups from the fibre. This method is particularly useful due to its easy processability resulting from the easy decomposition of peroxides into free radicals (RO·), which are capable of reacting with both hydrogen groups of the matrix and the hydroxyl groups of the natural fibre. The reactions are shown in Figure 2.6.

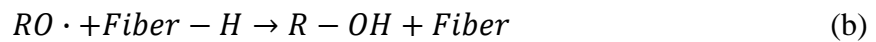


Figure 2.6 The mechanism of the peroxide treatment of the cellulose; decomposition of the peroxide (a) and reaction between the free radical and the cellulose of the fibre (b) (Susheel *et al.*, 2009)

Chemical treatments that make the natural fibre surface more compatible to a hydrophobic matrix can be applied using different methods to the fibre surface and/or by modifying the cell wall. The spraying method forms a surface coating, but the inside of the cell wall is left untreated. If deemed necessary to modify the fibre surface and the cell walls, the impregnation method may be used (Xie *et al.*, 2010). The impregnation method is a surface and bulking treatment that considerably improves the properties of the composite more than surface methods. However, it has disadvantages including; high consumption of energy during the drying process, difficulty in controlling the molecular size to allow molecules to enter the cellulose structure and, in the case of short fibres, the problem of fibres aggregation that hinders dispersion within the cell walls (Xie *et al.*, 2010).

An example of surface and bulking treatment is the impregnation of natural fibres in a liquid monomer; these monomers polymerise *in-situ* by the administration of heat, radiation or through the presence of a catalyst (Jayamol *et al.*, 2001).

Another method of surface chemical modification is termed graft polymerisation of natural fibres (already covered in part in the section on silanes coupling agents). Grafting can be carried out before compounding a composite, whereby coupling agents are added by means of solution or vapour, or, during compounding at the mixing temperature of the matrix. The efficiency of grafting depends on the type of the initiator, on the monomer to be grafted and on the operating conditions. The degree of grafting can be changed by varying the ratio of monomer/cellulose, the reaction time and the concentration of the initiator, though it is

important to take into account the accessibility of cellulose free radicals to the monomers (only amorphous regions are available for the diffusion of monomers), the life-time of free radicals formed on the cellulose and the cellulose-monomer interaction. The first stage of the grafting process involves the activation of free radicals on the cellulose. The activation of radicals occurs in several ways; by physical means, chemical means (such as dehydrogenation, depolymerisation or the formation of an unstable metal complex), radiative means (through the administration of a high-energy ionising radiation) and by enzymatic means. The second and final stage involves treatment with solution or vapour from monomers; such as vinyl, acrylonitrile, methyl methacrylate or styrene, compatible with the matrix. The resulting copolymer has suitable properties both for increasing interfacial adhesion and for reducing the affinity of the natural fibre to moisture (Jayamol *et al.*, 2001).

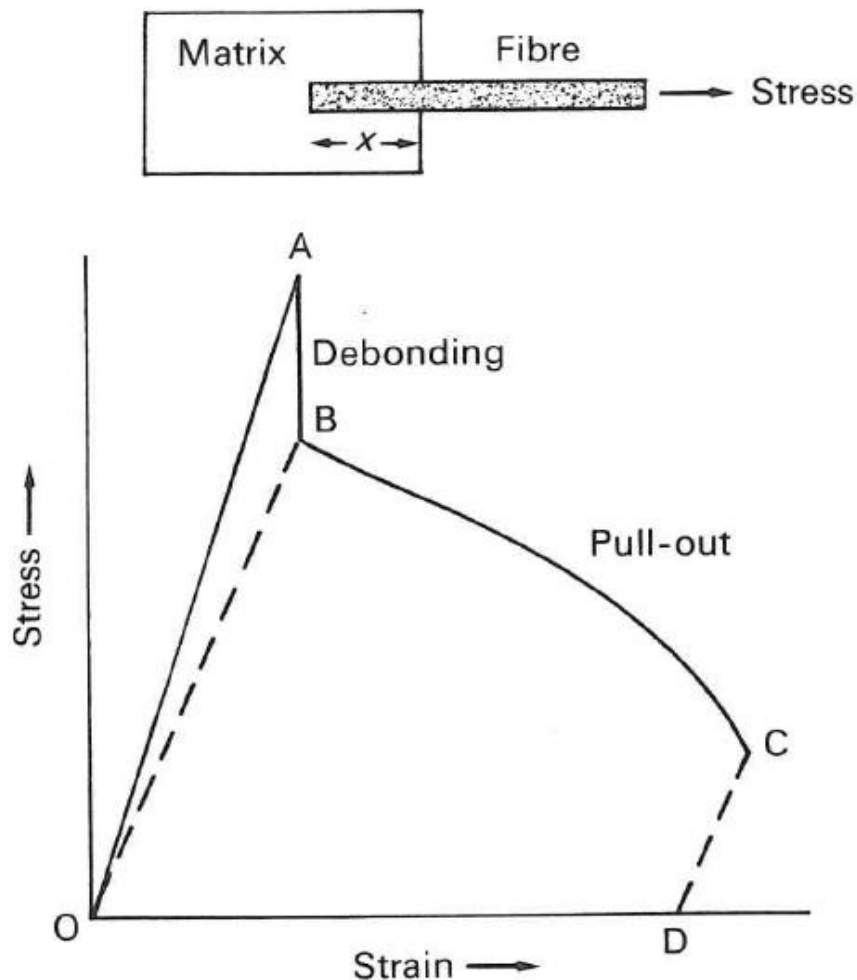


Figure 2.7 Pull-out test principle and corresponding graph (Matthews and Rawlings, 2000)

Several methods can be used for micromechanical characterisation as a means of determining the adhesion strength of fibre in a polymer matrix. The test methods for assessing the adhesion between a single fibre and the matrix are the most common. These tests are based on the calculation of the maximum value of stress transferred from the matrix to the fibre. The presence at the same time of many factors, such as adhesive forces, cohesive forces and the properties of the interface, makes these tests difficult to carry out. The complexity of the fibre-matrix interphase is demonstrated by the large number of the mechanical characterisation methods available and their variations adapted to each individual application (Herrera-Franco and Drzal, 1992). Below, the most common single fibre-based methods are described. Other characterisation tests have been reported in (Narkis *et al.*, 1988, Outwater and Murphy, 1969, Wu, 1989).

The pull-out method involves testing a single fibre partially embedded into a matrix block whereupon the free portion of the fibre is axially pulled out of the matrix. In Figure 2.7 a schematic representation of the pull-out test is shown and below the resulting graph that includes the debonding phase and the pull-out phase.

The length of the embedded fibre, its diameter and the force/speed applied are variables which affect the value of the interfacial shear strength. The following equation (2.9) provides a model to calculate the arithmetic mean of the interfacial shear strength. The assumption behind this equation is that the shear stress is uniformly distributed throughout the embedded fibre surface.

$$\tau = \frac{F}{\pi dl} \quad (2.9)$$

In (2.9), F is the maximum load measured prior to debonding of the fibre, d is the diameter of the fibre and l is the fibre embedment length (Matthews and Rawlings, 2000).

When a single fibre is fully embedded in a matrix block, single-fibre fragmentation testing is possible. In this test, the fibre is subjected to a tensile load and the transfer of the stress from the matrix to the fibre depends on the strength of bonding between them. The fibre is subdivided into a number of fragments (the energy is dissipated at the expense of the deformation and breakage), which become smaller during the loading process until the lengths of fibre fragments are so small that the tensile stresses induced in the fibre can no longer reach the fibre tensile strength. In other words, the lengths of the fragments do not allow transfer of the tensile strength to the fibre (Mohanty *et al.*, 2005). The Figure 2.8 below shows the loading process.

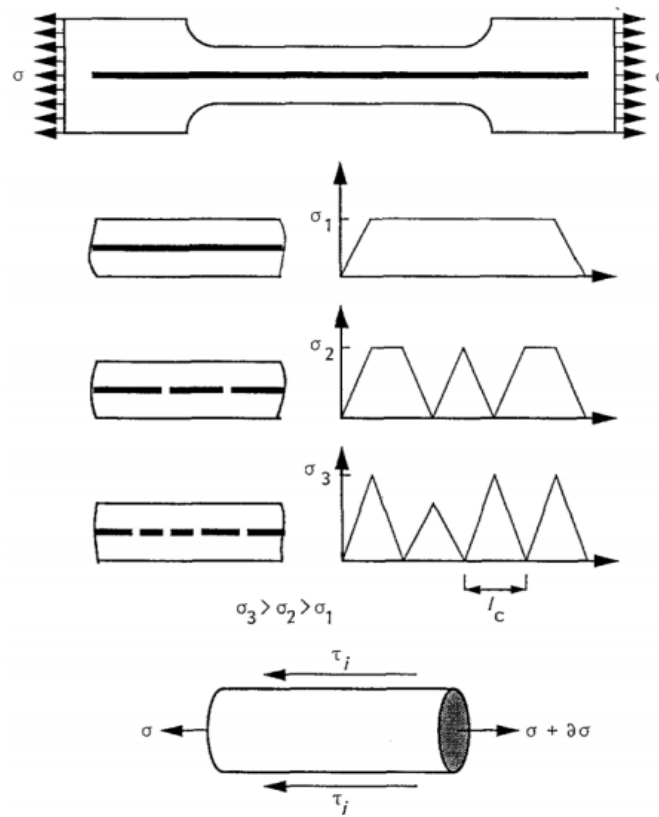


Figure 2.8 Schematic representation of the single-fibre fragmentation method

This final length, also called critical length, is the indirect variable used in the calculation of an interfacial shear stress. The shear stress is defined according to Equation (2.10) developed by Kelly and Tyson (1965):

$$\tau = \frac{\sigma_f}{2} \left(\frac{d}{l_c} \right) \quad (2.10)$$

where σ_f and l_c are the maximum tensile stress of the fibre and the critical length, respectively, and d is the diameter of the fibre. The statistical distribution of the fibre fragments required to carry out the value of the critical length, fits the Weibull Distribution. For this reason the equation above has been modified including Weibull's parameters as (Drzal *et al.*, 1980):

$$\tau = \frac{\sigma_f}{2\beta^2} \Gamma\left(1 - \frac{1}{\alpha}\right) \quad (2.11)$$

in which, α and β are the shape and the scale parameters of the Weibull distribution, respectively, and Γ is the gamma function (Mohanty *et al.*, 2005).

Micro or nano-indentation testing is another common method for assessing the strength of interfacial bonding. The test works at the cross sectional area; the sample must thus have an

adequate thickness and the surface should be polished to a finish suitable for microscopic examination.

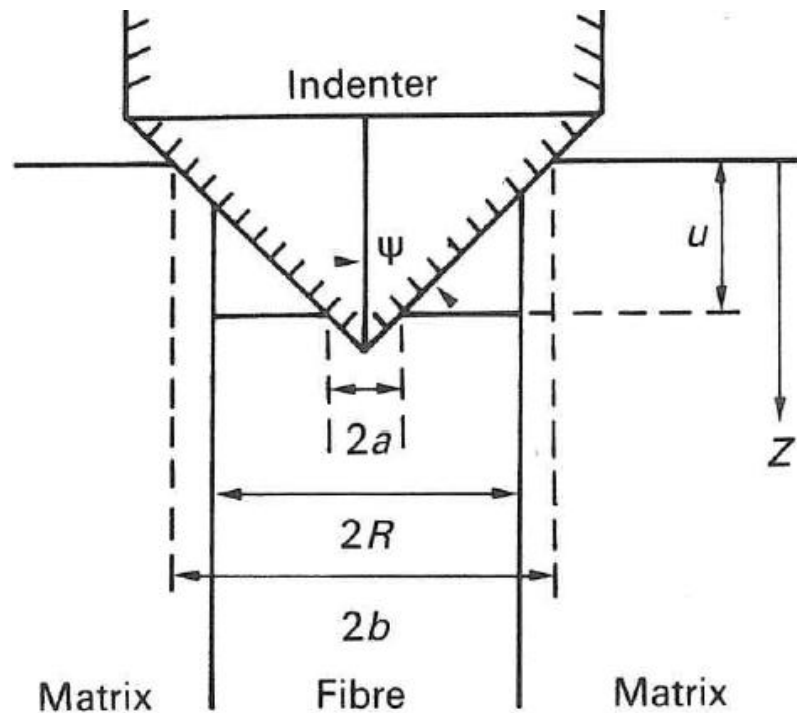


Figure 2.9 Schematic representation of the micro-indentation method (Matthews and Rawlings, 2000)

Considering Figure 2.9, it can be seen that the indenter is loaded axially at the centre of the cross section of the fibre and, depending on the force applied, the fibre is pressed down and forced to slide along the fibre-matrix interface. Considering a distance u from the original point at which the area of the fibre, normal to the axis of the indenter, lies in the plane of the surrounding matrix surface, the following equation (2.12) can be used for the calculation of the interfacial shear stress.

$$\tau = \frac{F^2}{4\pi u R^3 E_f} \quad (2.12)$$

where F and E_f are the force applied and the Young's modulus of the fibre, respectively, R is the radius of the fibre and u is the sliding distance. For a standard pyramidal indenter, the distance u can be calculated as:

$$u = (b - a) \cot 74^\circ \quad (2.13)$$

where b is half the diagonal length of the indentation on the matrix surrounding the fibre, while a is half the diagonal of the indentation on the fibre (Matthews and Rawlings, 2000).

2.2 Biomimetics

It is well known that synthetic chemistry, which includes an enormous knowledge reflecting *reaction know-how*, has been and still has very successful in the field of materials engineering. Nevertheless, the chemistry of biological systems is leading the development of numerous research endeavours in various sectors of engineering. These include processes and systems similar to the synthetic chemistry, but at higher levels of organisation.

The recent interests that researchers have on biomaterials produced by means of biological processes, is due to the presence of several factors including, environmental regulations and increases in the cost of energy and oil. Moreover, biological materials have attractive and complex structures that result in an excellent combination of toughness, high elastic modulus and high strength. Whilst traditional synthetic composites tend to decrease in toughness with an increase of the elastic modulus (Mann, 1996), biological composites are able to increase toughness while maintaining stable properties of stiffness. The concept of using biological systems as models for the design of engineering materials is continuously rising and this can be evidenced by the number of publications. Between the years 2000 and 2005, there have been 111822 publications made on biological materials and 2553 on biological composites. These data can be comparable to the considerably lower number of publications on the same topics between 1950 and 1999 (Brown, 2005). A new field of research, called Biomimetics, has emerged as a result of the more in-depth knowledge accrued on biological structures and function. Biomimetics is an interdisciplinary collaboration between chemists, engineers, biologist, material scientists and nanotechnologists with the ultimate aim of studying biological structures and their physical and chemical properties (Sarikaya and Aksay, 1995), in order to incorporate their technology into new materials and products (Heuer *et al.*, 1992). In other words, biomimetics seeks to integrate biological features from unique functional biostructures, into the design and the synthesis of artificial systems (Romano, 2012).

Applications for biomimetics, as enhanced composites materials, can be found in the diverse fields of engineering (Kokubo *et al.*, 1999, Thummalapalli and Donaldson, 2012), medicine (Petrini *et al.*, 2013, Lu *et al.*, 2013, Ma, 2008, Bitton *et al.*, 2009), nanotechnology (Hilt, 2004, Peppas, 2004) and robotics (Wang *et al.*, 2010, Shahinpoor, 2003). It is worth mentioning a classical example of inspiration from nature for the development of bioinspired engineering products; the invention of *Velcro* (Vincent, 2006). *Velcro*, or hook and loop fastener, was developed by the Swiss engineer George de Mestral, in 1948, and was inspired by the strong interlocking properties of the seeds of the burdock plant, which uses hooks to catch onto anything with a closed loop.

In the field of composite materials, inspiration may come from the unique mechanical characteristics of materials existing in nature. Shells and teeth are good examples, because their high tensile strength is comparable to engineering ceramics, such as silicon carbide and alumina. In Table 2.1, the mechanical properties of a few selected synthetic and biological materials are presented. In this table, it can be noted that the mechanical properties of the femur bone of a bovine are similar, or higher to that of short glass fibre reinforced polyethylene terephthalate and to glass bead reinforced polybutylene terephthalate (Mann, 1996).

Table 2.1 The mechanical properties of synthetic and biological materials (Mann, 1996)

Material	Tensile Strength [MPa]	Tensile Modulus [GPa]	Work of fracture [J/m ²]
Continuous fibre PEEK/AS4, perpendicular	73	8.3	-
Polybutylene terephthalate/Glass beads	95	4.9	-
Polyethylene terephthalate + short glass fibre	165	20	3200
Bone	220	20	1700
Dentine	250	12	550

Figure 2.10 provides a qualitative comparison between natural materials and common engineering materials correlating elastic modulus to density.

Therefore, synthetic composite materials can be mechanically improved by designing their microarchitectures in mimicry of designs found in many biological materials. Researchers are trying to design materials, or hybrid materials, with the same characteristics of biostructures and this would provide benefits not only from a technological perspective, but also from an economic perspective. This is because many of the raw materials involved in the manufacture of biomimetic products can be sought directly from nature itself. There is also a potential environmental benefit, since biological processes operate in a closed-cycle which eliminates problems associated with waste and pollution.

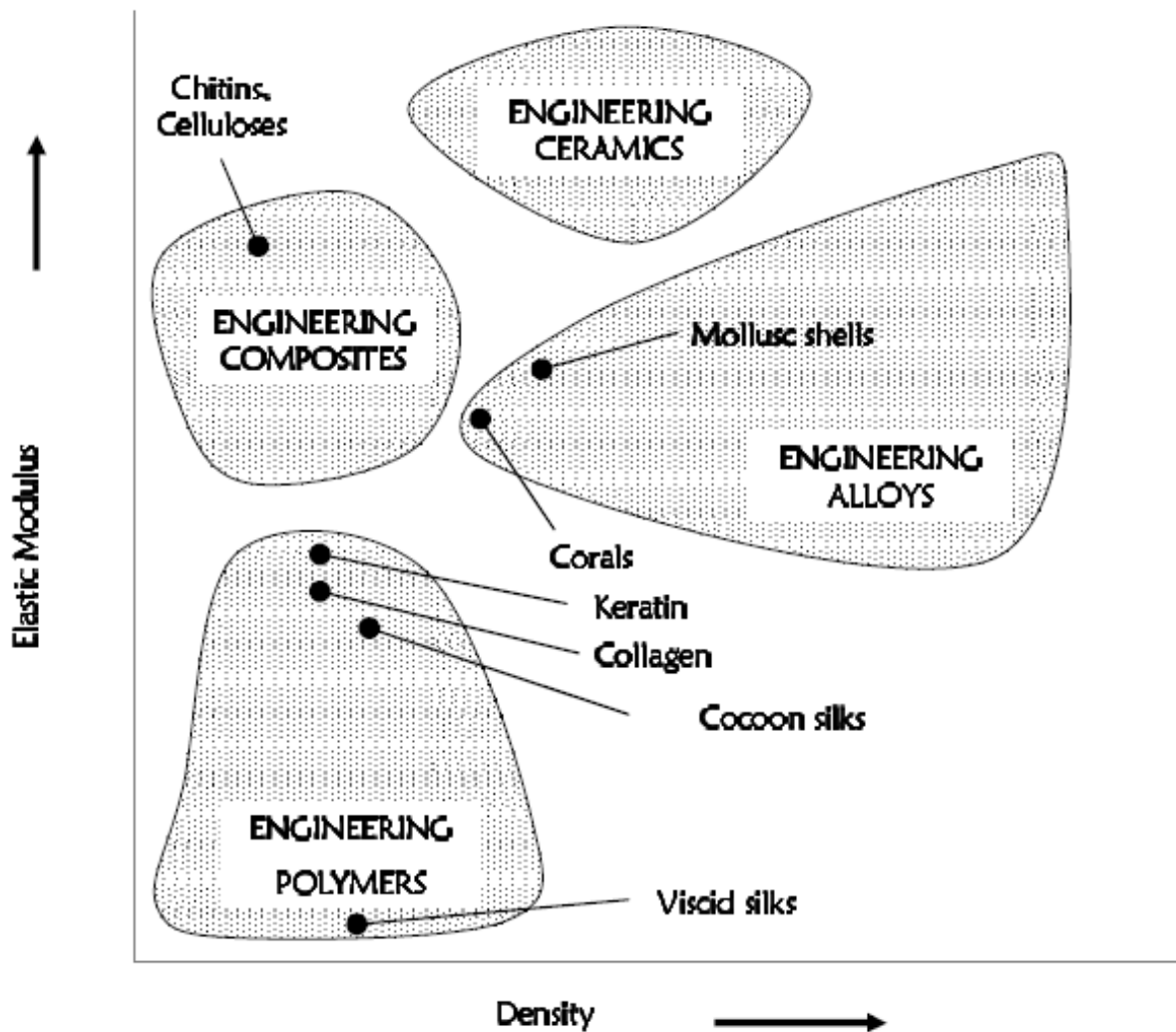


Figure 2.10 Elastic modulus/density relationships for natural materials and engineered materials (Alam, 2013)

2.3 Biomineralisation

Biomineralisation is an extremely complex process through which organisms form minerals. The process of biomineralisation causes the conversion of ions in solution to mineralised solids through cell activities. Biomineralisation is assumed to be the interaction of the organic regions of these organisms with the inorganic components and it allows for the formation of specific crystal structures. These are termed 'biominerals' and contain both mineral and organic components making them essentially, composite materials. The organic component forms the glue-like matrix which changes the properties of the mineral compound. These properties include the phase, the morphology and the growth dynamics. The final properties of the natural composite are different from those of the pure mineral (Weiner and Dove, 2003). The aim in studying biomineralisation is in understanding how organisms are able to control a process that allows them desirable properties. There is in fact controllability at the

nanoscale on the size of the crystals, on the shape and on the crystallographic orientation. The final result is a material with remarkable mechanical properties such as ultra-high strength and fracture toughness (Weiner and Dove, 2003). Therefore, a biomineral consists of nanometre-sized crystals glued together by a network of organic molecules (proteins, polysaccharides and/or lipids) (Zhang *et al.*, 2013), produced by the organism that controls the process of biomineralisation. Each single crystal may possess a different morphology if compared with its inorganic counterpart. It is reported that calcium carbonate formed by biomineralisation processes in abalone shells is able to increase its fracture energy by almost 3000 times the equivalent of inorganic calcium carbonate (Massimino, 2010). The organic component of the composite releases the mechanical energy by means of a phenomenon named weaving. The macromolecules, that constitute the softer fraction of the biomineral, spread the external load applied about the entire structure, but at gradually decreasing length scales such that there is a significant dissipation of mechanical energy (Fratzl, 2007). The final biomineral is a material with the properties of both rigidity and ductility (Massimino, 2010). Another important characteristic of biomineralised materials is the ability of resistance at the corrosion and abrasion.

In nature, about 50% of biominerals contain a form of calcium (Lowenstam and Weiner, 1989), and this can be explained by its function of primary importance in cellular metabolism (Lowenstam and Margulis, 1980, Simkiss and Wilbur, 1989, Berridge *et al.*, 1998). In particular, calcium carbonate presents itself in different crystalline forms, these being calcite, aragonite and vaterite. Approximately 25% of biominerals include a form of phosphate and most of them originate from a controlled mineralisation process. Another widespread biomineral is silica, which exists in hydrated form as water is needed for the organic component to retain strong bonds to the silica. It should be noted that each category of mineral includes at least one hydrated phase and crystalline phases often have a previous hydrated form. This is due to the lower energy barrier required for nucleation and growth (Weiner and Dove, 2003).

The nucleation and growth of crystals in aqueous solution requires a certain level of supersaturation. It is for this reason that biological systems isolate a determined zone from the external environment in order to create the best conditions for biomineralisation. In particular, they are able to regulate the flow of matter, ions (usually cations) and components, maintaining the constraint of the electroneutrality. In fact, in a solution of electrolytes; cations and anions are not independent but rather, the amount of each of them is strictly connected to the constraint of electroneutrality in the solution. In particular, if an electrolyte $M_v^+X_v^-$ is dissolved in a medium with a high dielectric constant, like water, the dissociation into v^+ positive ions with a charge z^+ and v^- negative ions with a charge z^- occurs. The following equations (2.14) and (2.15), in which charges are shown in a normalised units ($z^+=1$ for a proton), summarise the concept of electroneutrality (Praustnitz *et al.*, 1999). In particular,

(2.14) represents the equilibrium dissociation of an electrolyte and (2.15) the constraint of electroneutrality of the solution.



$$\nu_+z_+ + \nu_-z_- = 0 = \nu_+z_+ - \nu_-|z_-| \quad (2.15)$$

Ions involved in the process of biomineralisation may include Na^+ , K^+ , Ca^{2+} , Mg^{2+} , HCO_3^- , Cl^- and SO_4^{2-} . Solutions with high ionic strengths have to be studied in terms of ionic activity and not in terms of concentration. Hence to define supersaturation an accurate activity coefficient model is required. In the study of equilibrium between ions in a solution, it is necessary to take into account two important concepts. The first is that inside the solution the dissociation forces generate a quantity of particles, or ions, greater than the same solution without these forces. This affects the calculation of colligative properties which depend on the number and not on the quality of distinct particles that form the solution. The second concept is that among this quantity of ions inside the solution, only a certain quantity can participate in a determined phenomenon, such as a chemical process or a physico-chemical process. This is because some particles are solvated by the solvent which shields them electrically. Therefore, the activity a , is the effective concentration in a solution, or rather the actual number of particles involved in a phenomenon. The activity of the solute is different with respect to the initial analytical concentration and, considering an i -species, they are related by the following equation (2.16):

$$a_i = \gamma_i \cdot c_i \quad (2.16)$$

where γ_i and c_i are the activity coefficients of the i^{th} species and the concentration of the i^{th} species, respectively. The ideal electrolytic solution has an activity coefficient equal to 1 for each i -species and this can be obtained by a solution with a high level of dilution. In this case, ions are too far apart to influence each other. According to the relationship above, if the activity coefficient tends to unity, the activity of the i^{th} species tends to the value of the concentration of the i^{th} species. The activity coefficient is dependent on the concentration of the electrolyte, but at the same concentration, electrolytes containing ions with multiple charges affect the activity coefficients of ions more heavily if compared to electrolytes containing ions with a single charge (Praustnitz *et al.*, 1999). For this reason, the ionic strength of the solution can be introduced by (2.17):

$$I(\text{mol/Kg}) = \frac{1}{2} \sum m_i z_i^2 \quad (2.17)$$

where i is the ionic species, m_i and z_i are the concentrations expressed by molality and the charge of the ion. Table 2.2 shows the molality of the main ions present in seawater. According to this data, the ionic strength measured is $I = 0.72 \text{ mol kg}^{-1}$ (Clegg and Whitfield, 1991).

Table 2.2 Concentration of major ions in oceanic seawater (Clegg and Whitfield, 1991)

Component	Molality [mol/Kg]
Na ⁺	0.486
Mg ²⁺	0.055
Ca ²⁺	0.011
K ⁺	0.010
Cl ⁻	0.566
SO ₄ ²⁻	0.029

The charged particles, or ions, interact according to the Coulomb's law (2.18):

$$F_{el} = \frac{(z_+z_-)}{4\pi\epsilon_0\epsilon_r r^2} \quad (2.18)$$

where z^+ is the charge on the cation and z^- is the charge on the anion, r is the distance between ions, ϵ_r and ϵ_0 are the dielectric constant of the medium (solvent in this case), in which charges are immersed, and the dielectric constant of the vacuum, respectively. Given that within an electrolyte solution there are both positive and negative ions, it is difficult to calculate the activity coefficients of individual ions (Praustnitz *et al.*, 1999). To circumvent this conundrum the mean ionic activity coefficient (described by the equation (2.19)), can be used:

$$\gamma_{\pm} = (\gamma_+^{\nu_+} \cdot \gamma_-^{\nu_-})^{\frac{1}{\nu}} \quad (2.19)$$

where $\nu = \nu_+ + \nu_-$. Moreover, defining the mean ionic molality, m_{\pm} , as:

$$m_{\pm} = (m_+^{\nu_+} \cdot m_-^{\nu_-})^{\frac{1}{\nu}} \quad (2.20)$$

it is possible to obtain the mean ionic activity, a_{\pm} , as:

$$a_{\pm} = [(a_{+})^{v_{+}} \cdot (a_{-})^{v_{-}}]^{\frac{1}{v}} = m_{\pm} \gamma_{\pm}^{(m)} \quad (2.21)$$

where $\gamma_{\pm}^{(m)}$ is the molality activity coefficient. Based on the principles of electrostatics, Debye and Hückel proposed a semi-empirical relationship (2.22) for the calculation of the activity coefficient in aqueous solutions:

$$\ln \gamma_{\pm}^{(m)} = \frac{-A \gamma |z_{+} z_{-}| I^{1/2}}{1 + I^{1/2}} + bI \quad (2.22)$$

where z_{+} and z_{-} are charges on ions, I is the ionic strength and A , b are the parameters of Debye-Hückel equation.

Two classes of biomineralisation processes exist; biologically induced mineralisation and biologically controlled mineralisation. The difference lies in the degree of biological control. Biologically induced mineralisation is characterised by the heterogeneity of the structure, the morphology and the particle size. Moreover, the biomineral includes certain amounts of impurities. Cell surfaces promote the nucleation and growth of extracellular phases in an open environment, instead of in a defined control volume, and the mineral formed is dependent on both the organism and the environment. In other words, the same organism in different environmental conditions is able to induce the precipitation of different compounds. In biologically controlled mineralisation the organism controls all stages by means of macromolecules. This includes the nucleation, the growth, the shape, the structure, the polymorphism, the orientation and the final location of the deposited mineral. It occurs inside a well-defined control volume, where the composition of the solution is tightly regulated. In this case, the organism does not modify ambient supersaturation conditions in order to induce mineralisation (often the minerals are deposited under conditions of undersaturation), but rather, it exploits the interactions between organic molecules and minerals. As an example, the calcium ion is regulated by certain biological systems at concentrations of about 10^{-7} M. It is worth stressing that due to the low solubility of the major minerals involved in the biomineralisation processes, it is difficult to mimic this mechanism artificially, since it is not easy to manipulate conditions of supersaturation (Weiner and Dove, 2003).

The tiny particle sizes guarantee high mechanical properties, thanks to the intimate contact between the matrix and the reinforcement. This is similar to synthetic nanocomposites, except that such composites have high energy demands in manufacture due to the high temperatures and pressures often required. Moreover, the release of nanoparticles can pose risks to human health and to the environment (Brinton *et al.*, 1993).

For these reasons, biomineralisation is gaining increasing interest as a potential technology for coating and high-performance composites (Alam, 2013). The application of molecular biology and protein chemistry into material engineering provide an important interface

between traditional methods in materials design and structural biology. Efforts to reach this aim have led to significant step forward, but there remains a lack of understanding as to the role of the interface between the mineral and organic constituents (Li and Kaplan, 2003). Artificially controlling the process of biomineralisation *in-vitro*, similar to that found in nature (*in-vivo*), would allow for the development of lightweight products with excellent mechanical properties for a variety of applications (Belcher *et al.*, 1998). These applications may range from automotive to electronics, or from prosthetics to construction.

2.4 Crystal engineering

The study of biomineralisation is undoubtedly a very difficult task. An organism is characterised by different complex compounds, such as enzymes and macromolecules. In the process of biomineralisation there exists a complicated synergy of events. The making of a compartment around the nucleation site is to control the crystal shape, to manage ion channels for regulating the flow of matter, and to make available organic macromolecule functional groups for controlling crystal orientation (Massimino, 2010). To simplify this biological process we can divide it into four phases (Mann, 1996); (1) molecular organisation (2) molecular recognition at the interface with the solution (3) regulation and the control of the crystal orientation and (4) the real cell process. The first is the preliminary stage to mineralisation and consists of the formation of a compartment of organic walls around a nucleation point. The second exposes functional groups which act as fingerprints for the nucleation of the inorganic compound. The third phase consists of the equilibrium phase change. This is to control the morphology and through the introduction of impurities that may block crystallite attachment, a specific orientation of mineral crystals can be forced during growth. The final phase involves the implementation of networks to form a nanocomposite with superior mechanical properties. Organic molecules provide strong control from the start to the end of the growth of crystals. The second and the third phases of the process require some further focus since these phases include the nucleation and growth of crystals. In effect, crystal engineering examines the intermolecular interactions during these processes, in order to develop molecular solid-state structures with desired physical and chemical properties (Anthony *et al.*, 1998).

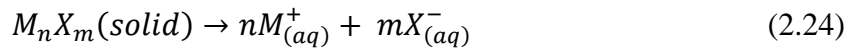
Crystallisation is a first-order phase transition in which a molecule goes from a solvated state with a high Gibbs free energy, to a state with lower Gibbs free energy in the crystalline lattice (De Yoreo and Vekilov, 2003). All characteristics of the latter state depend on the criterion of minimum energy, or lower-energy state (Kashchiev, 2000). In biological mineralisation, organisms are able to change the energetic barriers so as to control the growth kinetics and then the final equilibrium state. The driving force of both the nucleation and growth is the difference between the quantity of the Gibbs free energy at the initial state, that corresponds

to the solution without the crystalline phase, and the quantity at the final state. This corresponds to the solution plus the crystalline phase. The resulting quantity of which may be expressed by the difference in the chemical potential (Gibbs free energy per molecule or atom) between the initial and final state of each crystallising species (2.23) (De Yoreo and Vekilov, 2003).

$$\Delta\mu = \frac{G_{old} - G_{new}}{M} \equiv \mu_{old} - \mu_{new} \quad (2.23)$$

where G_{old} and G_{new} are the Gibbs free energy of the old and the new phases, respectively, M is the total number of molecules in the system, and μ_{old} and μ_{new} are the chemical potential at the equilibrium of the old and the new phases, respectively. The greater the difference between the chemical potentials of the same species in the two states, the greater the driving force for crystallisation (Mullin, 1992). A brief description of the thermodynamic drivers of the nucleation and growth follow (Mann, 2001).

The solubility, at a given temperature, is the maximum amount of solute that dissolves in a solvent. Considering the following general reaction (2.24) of an ionic solid containing univalent ions:



it is possible to obtain the equilibrium constant, also called solubility product, K_{sp} , as:

$$K_{sp} = [M^+]^n [X^-]^m \quad (2.25)$$

in which $[M^+]$ and $[X^-]$ are the effective concentrations (activities) of ions in a solution in equilibrium with the solid phase. Given the hypothesis of a slightly soluble salt, the concentration of the solid $[M_n X_m]$ that will settle to the bottom, is considered constant at the equilibrium, hence it is incorporated inside the solubility constant. This solubility product is a measure of the activity product at the equilibrium (Mann, 2001).

Moreover, knowing that the Gibbs free energy per molecule of a solution, ΔG_{sol} , can be described by (2.26):

$$\Delta G_{sol} = -K_B T \ln K_{sp} \quad (2.26)$$

where T is the temperature, K_B is the Boltzmann constant and K_{sp} is the equilibrium constant, or solubility constant, it is possible to write the change in chemical potential as follows:

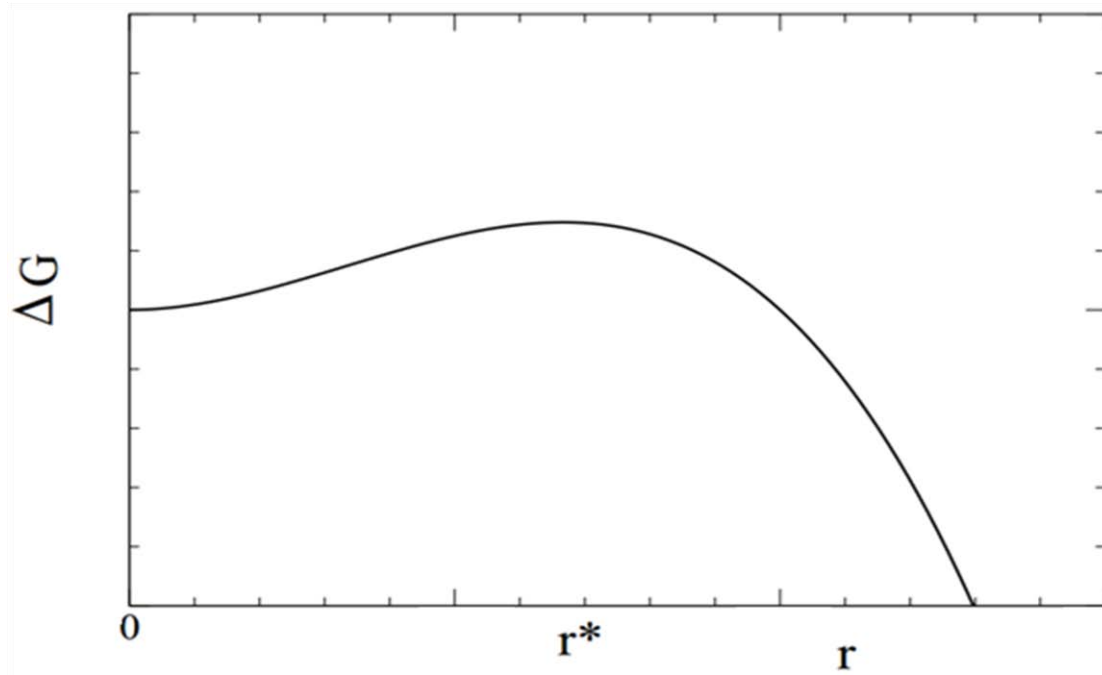
$$\Delta\mu = -K_B T \ln AP - \Delta g_{sol} = K_B T \ln \frac{AP}{K_{sp}} = K_B T \ln \sigma \quad (2.27)$$

where $\Delta\mu$ is referred to the whole system ($\Delta\mu = \sum \Delta\mu_i$), AP is the activities product and σ is the supersaturation. The factors which affect AP and K_{sp} are the temperature and the composition of the solution, but the latter is the main variable used by biological systems in order to control the crystal growth (De Yoreo and Vekilov, 2003). From (2.27) can be seen as the supersaturation is the thermodynamic driving force for inorganic precipitation (Mann, 2001). Crystallisation is the formation of a crystalline solid by means of the processes of nucleation and growth. In the case of a phase transition from a liquid to a solid state, nucleation consists of the formation of crystal clusters, which will form the nuclei required for the subsequent growth phase. The formation of these clusters is due to a spontaneous process that minimises the Gibbs free energy. Despite that in biomineralisation processes, this does not often occur (homogeneous nucleation), its description is necessary in order to understand nucleation at the surface of an organic matrix. Therefore, considering a homogeneous nucleation, the Gibbs free energy of formation of a nucleus, ΔG , constitutes a contribution of volume (or bulk), ΔG_b , and one of surface (or interface), ΔG_i . The difference of which is the function in the graph below (Figure 2.11). In the equations under the graph, σ is the supersaturation, ΔG_v is the free energy per mole associated with solid-liquid phase change and V_m is the molar volume.

The plot shows a maximum point that corresponds to the value of the critical radius, or critical size, of the nucleus over which there is a significant decrease in the free energy. In order to achieve crystallisation, this energetic barrier must be overcome. The maximum of the function is when the derivative $d\Delta G/dr = 0$, from which one can derive the expression for the critical radius. Before the critical size, the contribution of the interfacial energy is dominant. Hence it will lead to an increase of the total free energy and consequently to the dissolution of the nucleus. Over the critical size, the bulk contribution becomes such that the energy connected to the increase of the surface can be neglected. The value of the critical size can be modified by altering the concentration of compound supersaturation and the value of the interfacial energy. At the same concentration the smaller the value of surface tension, the smaller will be the critical radius (De Yoreo and Vekilov, 2003). In order to demonstrate the strong influence of the values of supersaturation and the surface tension, the equation for the homogeneous nucleation rate is shown below (Abraham, 1974, Neilsen, 1964):

$$J_n = A \exp\left(-\frac{\Delta G^*}{K_B T}\right) = A \exp\left(-\frac{B \alpha^3}{\sigma^2}\right) \quad (2.28)$$

Equation (2.29) is for the nucleation rate of a spherical nucleus with the explicit terms of supersaturation, σ , and surface tension, α . In (2.29), A is the pre-exponential factor, ΔG^* is the value of the free energy barrier at the critical size and the parameter B includes all factors other than supersaturation and interfacial energy.



$$\Delta G = \Delta G_i - \Delta G_b \quad [\text{free energy/mol}]$$

$$\Delta G_i = 4\pi r^2 \sigma$$

$$\Delta G_b = (4/3)\pi r^3 \Delta G_v / V_m$$

Figure 2.11 Qualitative trend of ΔG as a function of the radius of the nucleus. The combination of the functions ΔG_i and ΔG_b , which equates to ΔG , present a point of maximum at a critical cluster size r^* . The equations for the contribution of the bulk and interface energy are also presented (Mann, 2001)

The nucleation rate is seen to be a function of the 2nd and 3rd powers in the exponential, of the supersaturation and of the surface tension, respectively (De Yoreo and Vekilov, 2003). Once it has surpassed a critical size, the growth of the crystal depends on the flux of molecules attaching to the crystal surface and the flux of molecules detaching from the surface. In other words, the growth rate is limited by the mass transport to the surface. Variables which affect both the kinetics of attachment and detachment and the shape of crystals are many. They include the temperature, the strength of bonding of the crystal, the pH, the ionic strength of

the compound, the bulk concentration, the barrier to desolvation, the amount of impurities at the surface of the crystal and the presence of particular compounds.

Therefore, the crystallisation mechanism is characterised by a large number of factors which provide a wide number of opportunities for the modification of the nucleation and growth processes. This explains why it is challenging to understand the variables involved in biological mineralisation.

2.5 Calcium carbonate

Calcium carbonate is a chemical compound with the formula CaCO_3 . This substance is a white solid at ambient temperature and is slightly soluble in water (0.014 g/l at 293 K). Calcium carbonate is one of the most common natural compounds on earth. It can be found in rocks, such as limestone, travertine, chalk and tufa; and in marine sediments or organisms, such as shells, corals and sponges. In the marine environment, organisms biomineralise by abiotic precipitation and either biologically induced or controlled precipitation (Morse *et al.*, 2007). Given the wide availability in nature, this compound is generally extracted by mining or quarrying, though it can also be produced industrially from calcium oxide.

The reaction initially involves the formation of calcium hydroxide by reaction between calcium oxide and water. Following this reaction, carbon dioxide is injected into the slurry for the precipitation of calcium carbonate. This chemical compound decomposes under heat (thermal decomposition, also said calcination), or by reaction with a strong acid. In both cases, it releases carbon dioxide (Teir *et al.*, 2007).

Pure calcium carbonate has three different crystalline forms: calcite, aragonite and vaterite (Feng *et al.*, 2000). The conventional configurations are rhombohedral, orthorhombic and hexagonal, respectively (Stillfried, 2012). At ambient temperature and pressure, calcite is the thermodynamically most stable, followed by aragonite (slightly less stable than calcite) and vaterite. There are also metastable forms, such as amorphous calcium carbonate (ACC) which is highly unstable (Addadi *et al.*, 2003), the crystalline monohydrate form and the hexahydrate calcium carbonate (Stillfried, 2012). The former is often present as transient precursor of more stable crystalline calcite and aragonite (Addadi *et al.*, 2003). Many studies have demonstrated the influence of the crystalline morphology of calcium carbonate by the presence of proteins (Feng *et al.*, 2000), (Aizenberg *et al.*, 1996) and amino acids (Orme *et al.*, 2001), (Briegel *et al.*, 2012).

Chapter 3

Experimental work

The aim of this chapter is to provide, initially in Section 1, a background of previous work on the topic and a description of the experiments carried out. From Section 2 to Section 5, the experiments are detailed from the microscale to the macroscale. Section 2 will focus on molecular dynamic simulations, performed using the software Ascalaph Designer, for the calculation of the intermolecular energy of the system. Section 3 will describe the method used for the manufacture of the natural fibre reinforced composites and the SEM (scanning electron microscope) micrographs taken to evaluate the differences in the morphology of calcium carbonate. The last two paragraphs are about mechanical testing. The results and the discussion of each experiment are provided in the last part of each corresponding paragraph.

3.1 Background on previous work

The main idea behind this work is in creating natural fibre coral-mimicking composites with improved mechanical properties over unmineralised fibre-reinforced composites. We try to functionalise natural fibres by nucleating and precipitating calcium carbonate as a coating on the fibre surface and through mimicking biomineralisation. The objective is to assess the viability of using such fibres as advanced reinforcements for rubber.

Alam *et al.*, (2013) published a work in which are described the effects of fibre-surface morphology on the mechanical properties of Porifera-inspired rubber-matrix composites. Flax fibres were soaked in acetic acid solutions containing ground calcium carbonate. In particular, one solution contained 1 g CaCO₃, 30 ml acetic acid and 400 ml distilled water, whilst the other solution contained four times more the amount of CaCO₃ with 10 ml acetic acid and 400 ml distilled water. The composite was made with fibres aligned unidirectionally in a matrix of SBR (styrene-butadiene rubber) (Alam *et al.*, 2013). The manufacture of fibres using the solution with 1 g CaCO₃ resulted in smaller mineralised patches than the solution containing 4 g CaCO₃. The fibre coating characterised by small mineralised precipitates provided superior mechanical strength to the composite than the un-mineralised fibre composite. It has been hypothesised that this phenomenon is essentially due to the increase of surface roughness on the fibres, which leads to an improvement of the mechanical interlocking. Moreover, it was observed that there is a critical thickness of the surface treatment over which the properties of the whole composite exhibit inferior mechanical properties than the material made by un-

treated fibres (Alam *et al.*, 2013). Since the composite was compression moulded, the effects of pressure on the surface treatment were studied using the finite elements models based on scanning electron microscope micrographs. In particular, three structures were studied; (1) the natural fibre surface with small mineralised patches treatment, designed as cuboids, (2) the total covering, designed by an enveloping cylindrical shell, and (3) as in (2), but with a crack perpendicular to the fibre axis. The structure with small mineralised regions allows for higher operating pressure during compression moulding. The space between them lowers the local stresses, induced during the manufacture, that in turn increases the critical point at which the fibre starts failing. The same benefit can be obtained with a determined size of the crack running through the total covering of the fibre (case (3)). Moreover, it is shown that treatment (1) provides efficiency in terms of volume of material used (since only under the critical volume fraction of calcium carbonate is possible to perceive the improvement) and also in view of minimising damages during manufacture (Alam *et al.*, 2013).

Stillfried *et al.* (2013) published a work on the improvements of the flexural properties of flax fibres treated with a *Crispatotrochus*-mimicking coating. It was shown that a thin-film of calcium carbonate as a coating on the fibre surface increases the ability of the material to absorb mechanical energy and to resist buckling. In this case, a solution of water with poly(acrylic) acid 25 wt% was prepared and 0.5 g ground calcium carbonate were dissolved into it. After mixing 50 ml of the resulting mixture with 400 ml of distilled water, 35 g of flax fibres were soaked. The fibres were cut to 2 cm lengths and separated from each other. The results of the bending tests, carried out using a Messmer Buchel-bending resistance tester (rate 5°/s and gauge length 5 mm), show an important improvement of the mechanical performance in flexion over uncoated fibres. In particular, at the same angle (45°), treated fibres have a seven times higher flexural stress, σ_f , and a six times higher flexural modulus. Considering the factorisation by density, these parameters were five times and four times higher, respectively, to uncoated fibres. Equation (3.1) quantifies the flexural stress:

$$\sigma_f = \frac{Fl}{W} \quad (3.1)$$

where F is the load applied to the fibre, l is the length of the cantilever in bending, and W is the section modulus (for details about calculations see Stillfried *et al.*, 2013). The wide gap, between flexural properties factorised by density of coated and uncoated fibres, underlines the usefulness of this surface treatment in improving the performance of engineered natural fibres, in which both strength and stiffness are highly desirable (Stillfried *et al.*, 2013). Moreover, it has been demonstrated there is an increase of absorption of mechanical energy of about ten times more than the flax fibres without the coating. All these considerations are

quantified in the following Table 3.1, where the values are presented as mean values \pm the standard deviation.

Table 3.1 Flexural properties of un-treated and treated flax fibres characterized by 500 nm coating thickness (Stillfried *et al.* 2013)

	Uncoated	Coated	Coated/Uncoated
σ_f [MPa]	69.7 ± 25.1	548.4 ± 176.9	7.9
σ_f/ρ [KN m Kg ⁻¹]	47.0 ± 17.0	240.2 ± 77.5	5.1
E_f [GPa]	0.83 ± 0.3	5.08 ± 1.6	6.1
E_f/ρ [MN m Kg ⁻¹]	0.56 ± 0.2	2.22 ± 0.71	4.0
U_f [MJ m ⁻³]	2.9 ± 1.1	29.6 ± 9.5	10.2

In Table 3.1, E_f is the flexural modulus and U_f is the mechanical energy. A finite-element analysis was carried out in order to assess the dependence of coating thickness on the flexural modulus of the natural fibres. The simulations showed there is an optimal coating thickness at 80 nm, after which the flexural modulus decreases (Stillfried *et al.*, 2013). Once again, as published in the work of Alam *et al.* (2013), it was demonstrated that higher coating thicknesses than the critical size contribute to decrease the mechanical properties of the fibres, or more generally, of the composite.

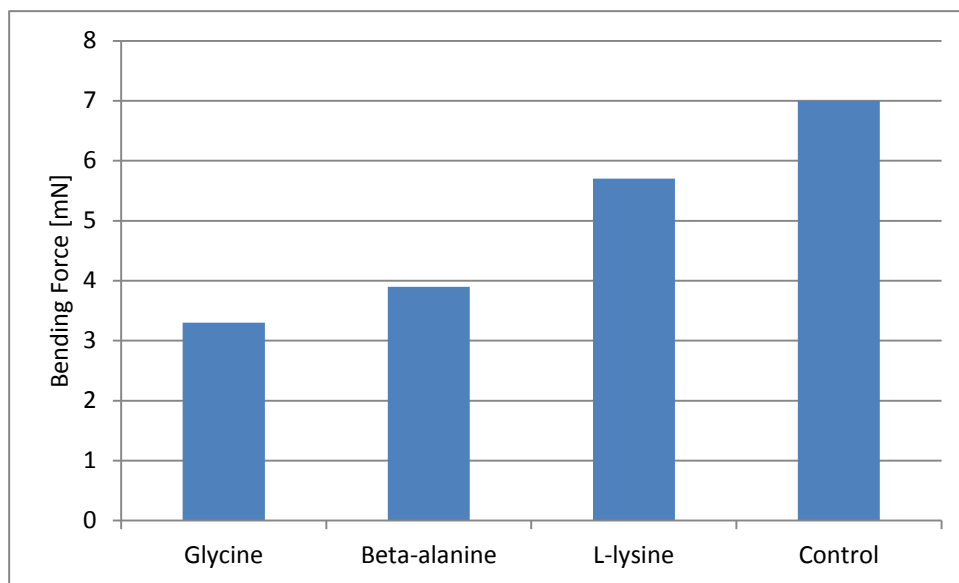


Figure 3.1 Bending tests results (Fagerlund *et al.* 2013)

This thesis work is a step forward in the studying of surface coatings made by deposits of calcium carbonate on natural fibres to improve the mechanical properties of the final

composite. In particular, the work starts from the results obtained by a research group in the laboratory of “Paper Coating and Converting” at Åbo Akademi University in Turku (Finland). The final results of this research are presented in Figure 3.1.

It is seen that the process of biomineralisation of calcium carbonate is affected by the types of amino acid present; in other words, depending on the organic molecule, the crystalline morphology of calcium carbonate changes (Fagerlund *et al.*, 2013). As a consequence, the change of crystal morphology involves a change in the roughness of the natural fibre surface. This means that mechanical interlocking between the matrix and the fibre is dependent on the crystal morphology of the mineral deposited on the fibre surface. The histogram in Figure 3.1 shows the bending tests carried out after soaking the flax fibres in solutions of calcium carbonate in solutions with different amino acids. The crystals increased the bending resistance of the fibres compared to uncoated fibres. As it can be seen from the graph above, the control (pure calcium carbonate fibre coating) is the most resistant to bending load, but it expresses also a certain degree of brittleness. The fibres treated with amino acid addition, contrarily, decrease the chances of brittle failure and thus the amino acids increase the durability of the fibre coating. In particular, the sample, made by an artificial biomineralisation process in the presence of L-Lycine, is both strong and flexible (Fagerlund *et al.*, 2013).

In this thesis work, the three amino acids from the previous work were taken into account (Glycine, β -alanine and L-lycine) and three different concentrations for each amino acid were considered for the manufacture of the natural fibres reinforced composite ($30 \cdot 10^{-3}$ M, $50 \cdot 10^{-3}$ M, $100 \cdot 10^{-3}$ M). The tests carried out are explained in the following sections of this chapter.

3.2 Molecular modelling: molecular dynamic simulations

The software Ascalaph Designer was used with the aim of calculating the intermolecular energy of the system under consideration. The algorithm within the software for the molecular dynamic simulations is designed for the simulation of interactions between biomolecules. This was modified, in order to make it able to calculate the intermolecular energy between inorganic molecules and organic macromolecules. It is important to clarify that the reliability of these modifications has to be further demonstrated by writing a new script specifically for the interactions between inorganic compounds and organic macromolecules. The results may be also affected by the equations of the force field, which in the case of the interaction between inorganic and organic molecules are less accurate than e.g. a universal force field. For the construction of the molecular models, the charges of atoms of calcium carbonate molecules were changed in agreement with the work of Wang and Becker (2009); the charges that ensure the electroneutrality of the molecule of calcium carbonate are shown in the Table 3.2. In this way, a more accurate predictive model was developed. Three-dimensional

boundary conditions were used in the simulations. All simulations were carried out using NPT ensembles, where the number of particles, N , the pressure, P , and the temperature, T , were kept constant. In particular, the temperature was fixed at 298.15 K, under vacuum conditions.

Table 3.2 Partial charges implemented in the algorithm for a non-ideal system (Wang and Becker, 2009)

Atom	Partial Charge
Ca	+2.000
C	+1.123
O	-1.041

There were no constraints imposed to molecules as all of them were free to move inside the simulation cell. The time step implemented in all molecular dynamic simulations was 2.5 fs (femtosecond), which is equivalent to 10^{-15} s. The system was allowed to equilibrate until 100000 number of steps, which is equivalent to 250 ps simulation time, following the simple Equation (3.2) below:

$$MDs\ time = Nsteps \cdot Tstep \quad (3.2)$$

where $MDs\ time$ [ps] is the molecular dynamic simulation time, $Nsteps$ [adm] is the number of steps and $Tstep$ [fs] is the time per step.

Initially, the intermolecular energy between a single molecule of amino acid and a single molecule of calcium carbonate was calculated (Table 3.3).

Table 3.3 Intermolecular energy between calcium carbonate and different amino acids

	Glycine + CaCO ₃	L-lycine + CaCO ₃	β-alanine + CaCO ₃
Intermolecular energy [cal/mol]	-510 / -515	-575	-510 / -515

The negative intermolecular energy means that there are attractive between the molecules. It can be seen that the range of the intermolecular energy is comparable to Van Der Waals' forces, London forces, ion-induced dipole and dipole-dipole interactions. L-lycine expresses more intermolecular energy (in modulus) than Glycine and β-alanine; the difference between L-lycine and Glycine/β-alanine systems is about 60 cal/mol. The construction of the simulation systems were done using the following simple calculations; for the construction of the system, the number of molecules was necessary.

The number of moles were calculated multiplying the molarity by the volume (for these simulations 1 lt of solution was considered) for all systems, following the Equation (3.3):

$$\frac{m}{M_{mol}} \cdot \frac{1}{V} = M \quad (3.3)$$

where m [g] is the mass of the compound, M_{mol} [g/mol] is the molar mass of the compound, V [lt] is the volume of the solution and M [mol/lt] is the molarity expressed in the number of moles of the solute into the volume of the solution. Rearranging the (3.3), it was found the the number of moles and, multiplying by the Avogadro's number ($N_A = 6,023 \cdot 10^{23}$), the number of molecules of each concentration was calculated. The values of the number of molecules of amino acids constituting the system are given by the following equations:

$$n_{AA,30}[n. molecules] = 30 \cdot 10^{-5} [mol] \cdot 6.023 \cdot 10^{23} \left[\frac{n.molecules}{mol} \right] = 1.8069 \cdot 10^{20} \quad (3.4)$$

$$n_{AA,50}[n. molecules] = 50 \cdot 10^{-5} [mol] \cdot 6.023 \cdot 10^{23} \left[\frac{n.molecules}{mol} \right] = 3.011 \cdot 10^{20} \quad (3.5)$$

$$n_{AA,100}[n. molecules] = 100 \cdot 10^{-5} [mol] \cdot 6.023 \cdot 10^{23} \left[\frac{n.molecules}{mol} \right] = 6.023 \cdot 10^{20} \quad (3.6)$$

where $n_{AA,30}$, $n_{AA,50}$, $n_{AA,100}$ are the number of molecules of amino acid in the system $30 \cdot 10^{-5}$ M, $50 \cdot 10^{-5}$ M, $100 \cdot 10^{-5}$ M, respectively. 1 g calcium carbonate was considered, hence considering the molecular mass of calcium carbonate, the number of moles is given by Equation (3.7):

$$mol_{CaCO_3}[mol] = \frac{1 [g]}{100.09 \left[\frac{g}{mol} \right]} = 9.99 \cdot 10^{-3} \quad (3.7)$$

In the same way, as in the calculation of the number of molecules of amino acids, the number of molecules of calcium carbonate is given by Equation (3.8):

$$n_{CaCO_3}[n. molecules] = 9.99 \cdot 10^{-3} [mol] \cdot 6.023 \cdot 10^{23} \left[\frac{n.molecules}{mol} \right] = 6.017 \cdot 10^{21} \quad (3.8)$$

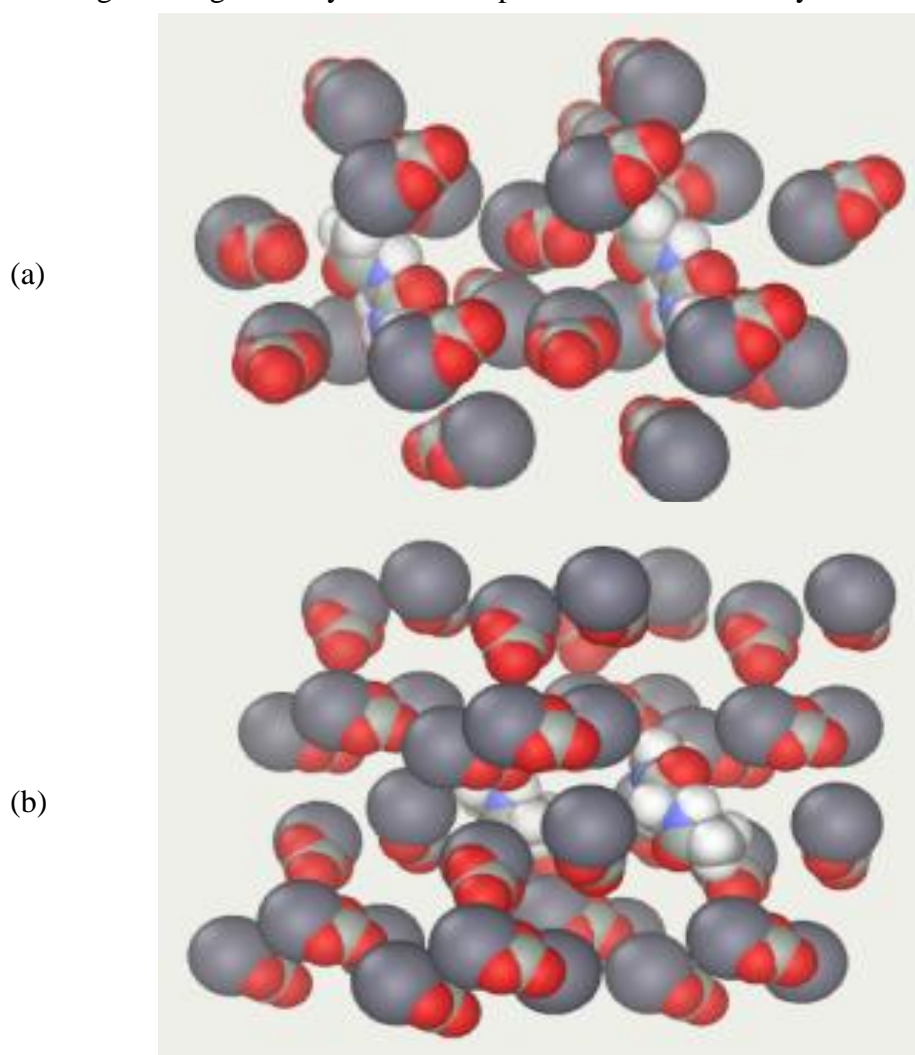
where n_{CaCO_3} , is the number of calcium carbonate molecules. In order to build the system, ratio R between the number of amino acid molecules and the number of calcium carbonate molecules was calculated. This ratio describes, the number of molecules which have to be drawn in the simulation cell. In particular, in the case of $30 \cdot 10^{-5}$ moles, for each 33 molecules

of calcium carbonate, a molecule of amino acid has to be drawn; whilst for $50 \cdot 10^{-5}$ moles, for each 20 molecules of calcium carbonate one amino acid has to be drawn. Finally, for $100 \cdot 10^{-5}$ moles, one amino acid molecule is drawn for each 10 molecules of calcium carbonate. The values of R , expressed in decimal numbers, and the real number of molecules in the simulation systems are shown in Table 3.4.

Table 3.4 Values for the ratio R and number of molecules drawn in the system

Number of moles [mol]	R (n_{AA}/n_{CaCO_3})	n.molecules A.A.	n.molecules CaCO ₃
$30 \cdot 10^{-5}$	0.03	2	66
$50 \cdot 10^{-5}$	0.05	2	40
$100 \cdot 10^{-5}$	0.1	2	20

For the comparison, the system devoid of amino acid was also taken into account. This system was designed by replacing each molecule of amino acid with a molecule of calcium carbonate. Figure 3.2 gives only a few examples of the simulation systems built.



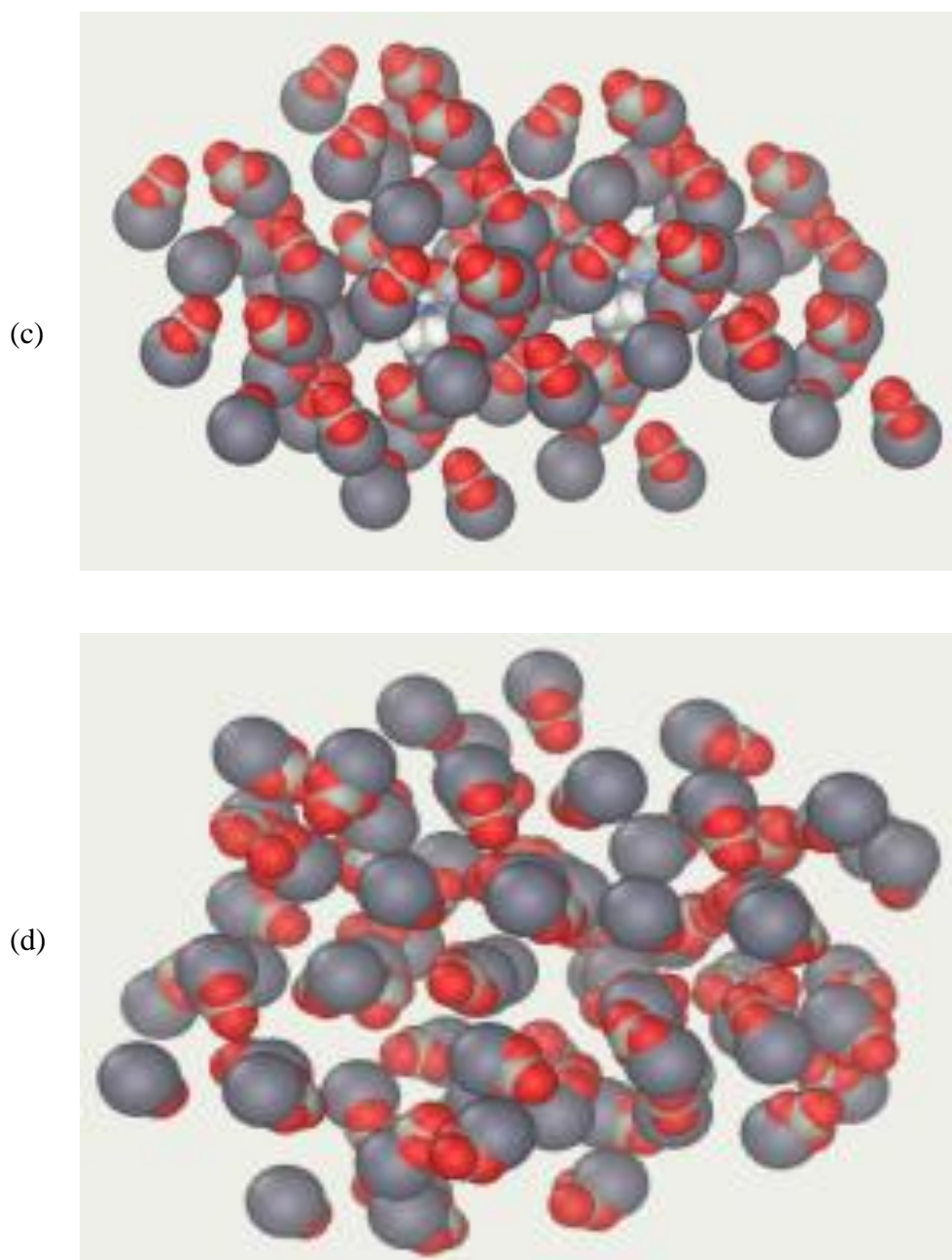


Figure 3.2 Qualitative pictures for the simulation systems with molecules of Glycine at $100 \cdot 10^{-5} M$ (a), $50 \cdot 10^{-5} M$ (b), $30 \cdot 10^{-5} M$ (c). Control system for $30 \cdot 10^{-5}$ moles (d)

Since the calcium carbonate molecules were hand-drawn, the geometrical configuration of these molecules was performed with the geometry optimiser within the software. It was a simple but necessary adjustment for an initial molecular geometry.

Figure 3.3, Figure 3.4 and Figure 3.5 show the total intermolecular energy as a function of the number of steps.

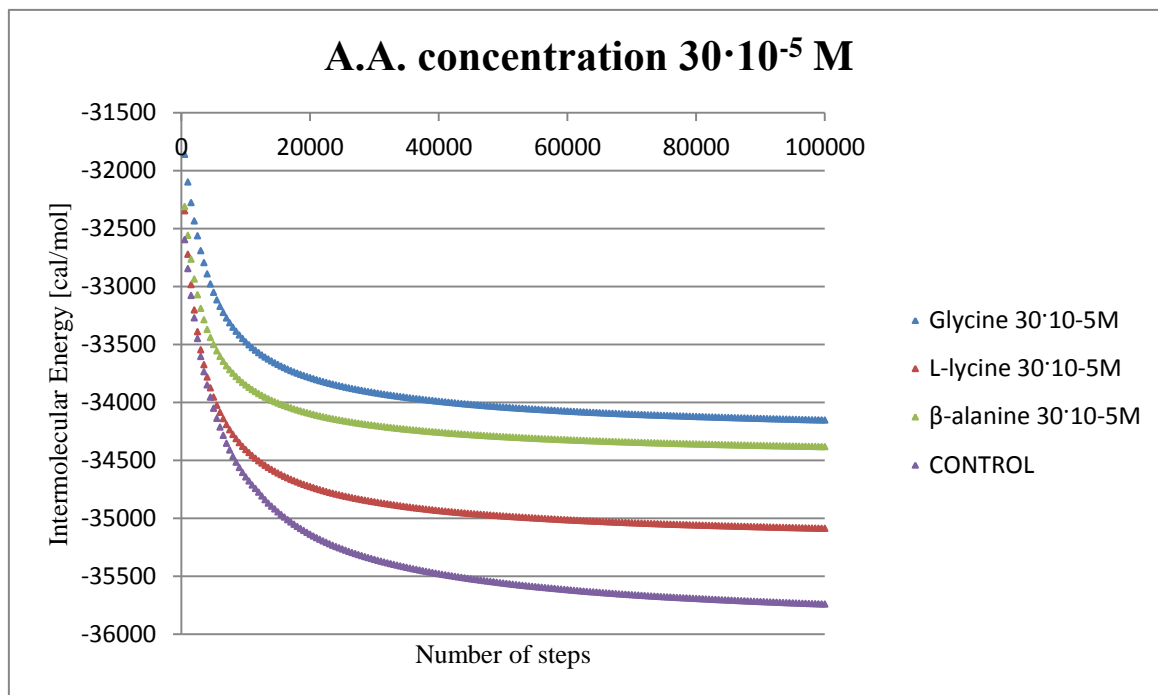


Figure 3.3 Intermolecular energy as a function of the number of steps for the simulation systems at $30 \cdot 10^{-5} \text{ M}$

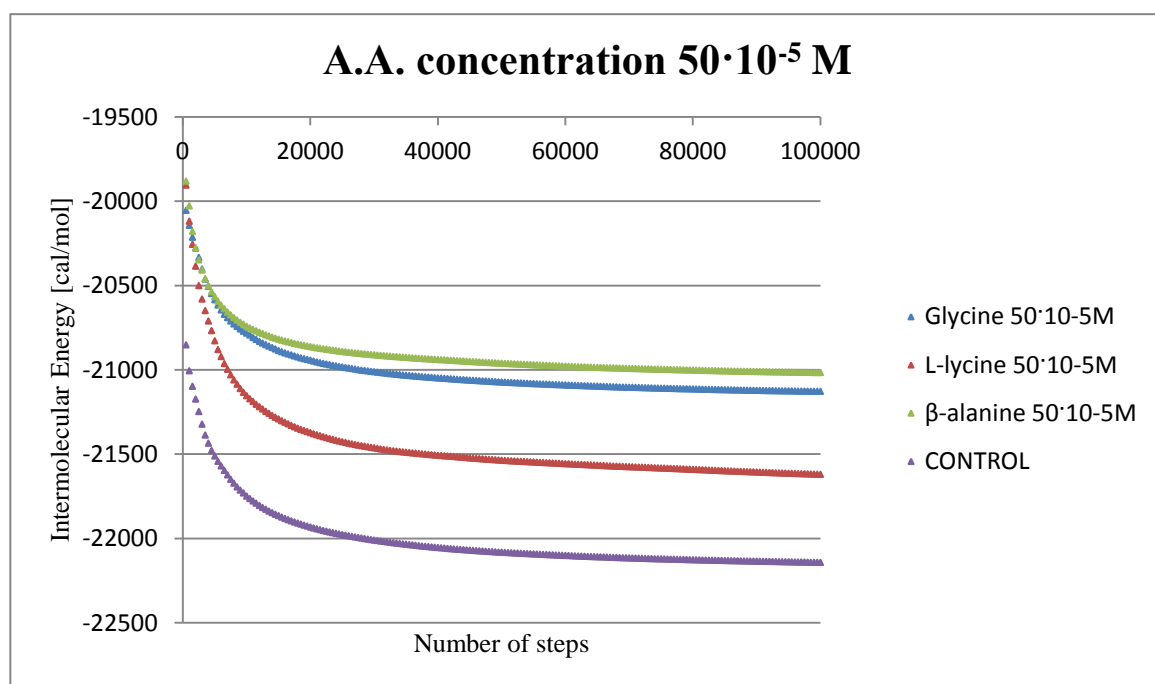


Figure 3.4 Intermolecular energy as a function of the number of steps for the simulation systems at $50 \cdot 10^{-5} \text{ M}$

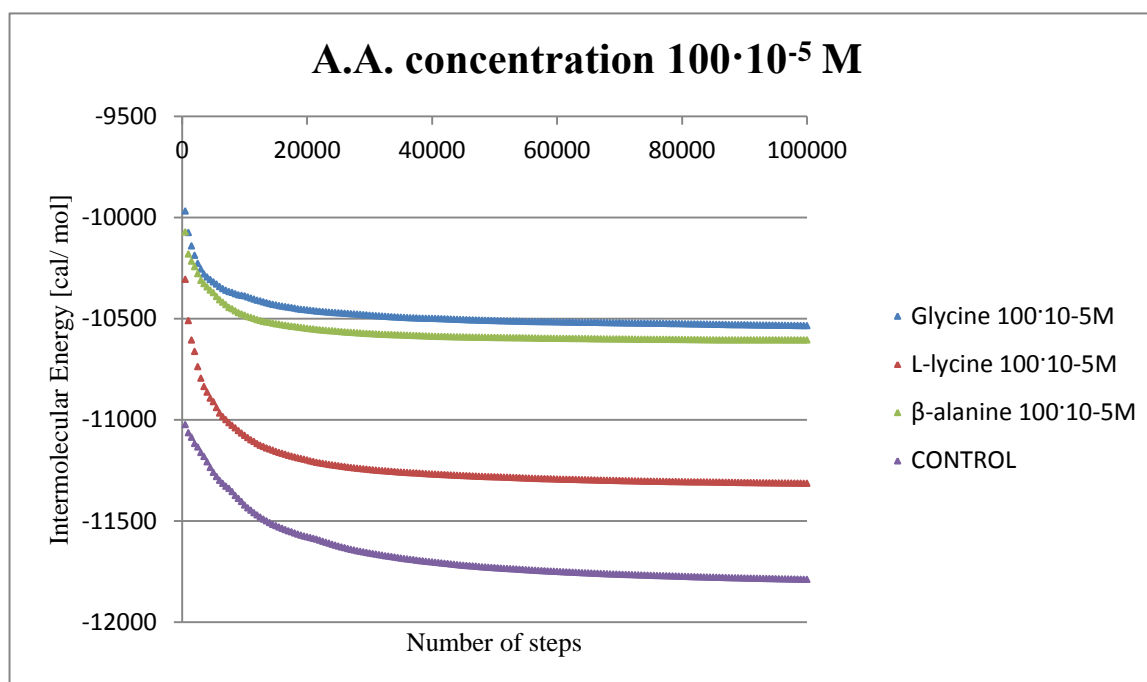


Figure 3.5 Intermolecular energy as a function of the number of steps for the simulation systems at $100 \cdot 10^{-5} \text{ M}$

The higher the intermolecular energy the greater the interaction between molecules. In all simulations, the control system turned out to be the strongest in terms of dissociation energy of the total system. In all concentrations, L-lysine shows the highest intermolecular energy among simulation systems with amino acids creating also a more compact structure than observed in the β -alanine and Glycine systems. This means that this organic molecule is able to minimise the energy of the system more effectively than the other amino acids. In other words, the calcium carbonate particles become more stable with the presence of L-lysine.

Between the β -alanine and Glycine systems there is a gap of only about 250 cal/mol and their behaviour is very similar at the equilibrium (corresponding to 100000 number of steps).

Comparing the values in Table 3.3, it is clear that the intermolecular energy is a linear function of the number of molecules. Hence, there are no synergistic effects within the structures that raise the intermolecular energies further. Moreover, it seems to exist a correspondence with the data for the bending tests (Figure 3.1). Although at different length scales, the control turned out to be the strongest in terms of bending force (mN) and intermolecular energy, respectively. In bending tests, the control sample is followed by the L-lysine sample as in the results of the simulation. Also in the bending tests β -alanine and Glycine systems show similar characteristics.

3.3 Manufacture of natural fibre reinforced composites and SEM (Scanning Electron Microscope)

For the manufacture of the crystallised-natural fibre reinforced composite, materials and chemicals were obtained from commercial sources and they were used without further purification. Flax fibres, the reinforcement of the matrix, were from FLAXLAND, UK. The latex used as the matrix for the composite was E-SBR latex (Emulsion polymerised Styrene-Butadiene Rubber). Table 3.5 provides the properties of the E-SBR latex.

Table 3.5 Physical and mechanical properties of E-SBR

Property	Minimum value	Maximum value	Units measure
Density	0.94	0.95	Mg/m ³
Elastic limit	12	21	MPa
Tensile Strength	10	25	MPa
Young's modulus	0.002	0.01	GPa
Elongation	250	700	%
Glass transition temperature	210	215	K

Before the production of fibre reinforced composite samples, flax fibres were mineralised in solutions containing different types of amino acid monomers at three different concentrations. The three different concentrations for each amino acid used (β -alanine, Glycine, L-lysine) were the same concentrations used in the molecular dynamics simulations ($30 \cdot 10^{-5}$ M, $50 \cdot 10^{-5}$ M, $100 \cdot 10^{-5}$ M), but based on 0.25 lt of solution.

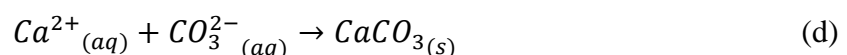
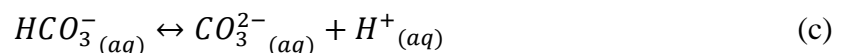
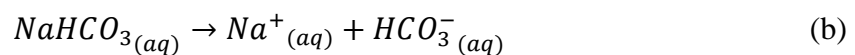
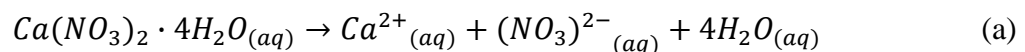


Figure 3.6 Precipitation reaction of calcium carbonate

In this way, nine samples were made, using three different amino acid used at three concentrations. Equation (3.3) was used to calculate the amount in grams of amino acid in 0.25 lt of solution. In order to deposit the calcium carbonate onto the fibre surfaces, calcium nitrate tetrahydrate and sodium bicarbonate (Sigma-Aldrich) were used. The reaction mechanism by which calcium carbonate deposits onto fibres surfaces is shown in Figure 3.6. Reactions (a) and (b) represent the dissociation of salts into the solution, whilst the reaction (c) provides the equilibrium between the bicarbonate ion and the carbonate ion. Finally, in the reaction (d), the formation reaction of calcium carbonate is given. The driving force of the precipitation reaction of calcium carbonate is given by the formation of an insoluble salt at the expense of the less stable soluble salts (Conte, 2014); in other words, among soluble salts, there will be the formation of the salt with the lowest solubility. The solubility at 293 K of the calcium nitrate, sodium bicarbonate and calcium carbonate are 121.2 g/100ml, 95.5 g/l, 0.014 g/l, respectively. In Table 3.6 details about the amount of compounds inside the solutions are shown; solutions are expressed in molarity of amino acid.

Table 3.6 Details of solutions

Solution	Ca(NO₃)₂·4H₂O [g]	NaHCO₃ [g]	Glycine [g]	L-lysine [g]	β-alanine [g]	Distillate water [ml]
30·10 ⁻⁵ M	1	1	0.00563025	-	-	250
30·10 ⁻⁵ M	1	1	-	0.01096425	-	250
30·10 ⁻⁵ M	1	1	-	-	0.0066822	250
50·10 ⁻⁵ M	1	1	0.00938375	-	-	250
50·10 ⁻⁵ M	1	1	-	0.01827375	-	250
50·10 ⁻⁵ M	1	1	-	-	0.011137	250
100·10 ⁻⁵ M	1	1	0.0187675	-	-	250
100·10 ⁻⁵ M	1	1	-	0.0365475	-	250
100·10 ⁻⁵ M	1	1	-	-	0.022274	250

The procedure for the preparing the solutions follows: 1 g calcium nitrate tetrahydrate, 1 g sodium bicarbonate and the fixed amount of amino acid were added into 250 ml of distilled water. After 30 min of mixing over a magnetic stirring, 35 g flax fibres were soaked into the solution and the entire contents was mixed for 2 min. Subsequently, the solution with flax fibres was left to dry at room temperature for ten days, in order to allow for the deposition of calcium carbonate onto the fibres surfaces.



Figure 3.7 Representation of a step during the manufacture of the composite: the spreading of the first thin layer of latex where some flax fibres have been placed on top

After mineralising flax fibres, 17.5 g combed flax fibres obtained from each dried solution were weighed for the production of flax fibres reinforced composite tiles of the size of about 10 cm length, 10 cm width and 3 mm thickness. These fibres were stretched in order to make a composite material reinforced with unidirectional fibres.

Two aluminium blocks (15 cm length, 12 cm width and 5 mm thickness) were used for compression moulding and were covered by parchment paper to avoid sticking of the composite material through bonding of the latex. 100 ml SBR latex was weighed and deposited over the parchment paper. The fibres were placed over the latex layer after stretching fibres one more time (Figure 3.7). It is very important to carefully align the fibres in the same direction, otherwise the results of mechanical testing may be affected by fibre anisotropy. Another thin layer of latex was spread over flax fibres and again another layer of fibres was put over it. This procedure was repeated until all 17.5 g flax fibres were used. Finally, the other aluminium block covered with the parchment paper was placed on top. Through a manual press, the excess of latex was removed and the composite tile was formed. Figure 3.8 shows a schematic drawing of the final configuration.

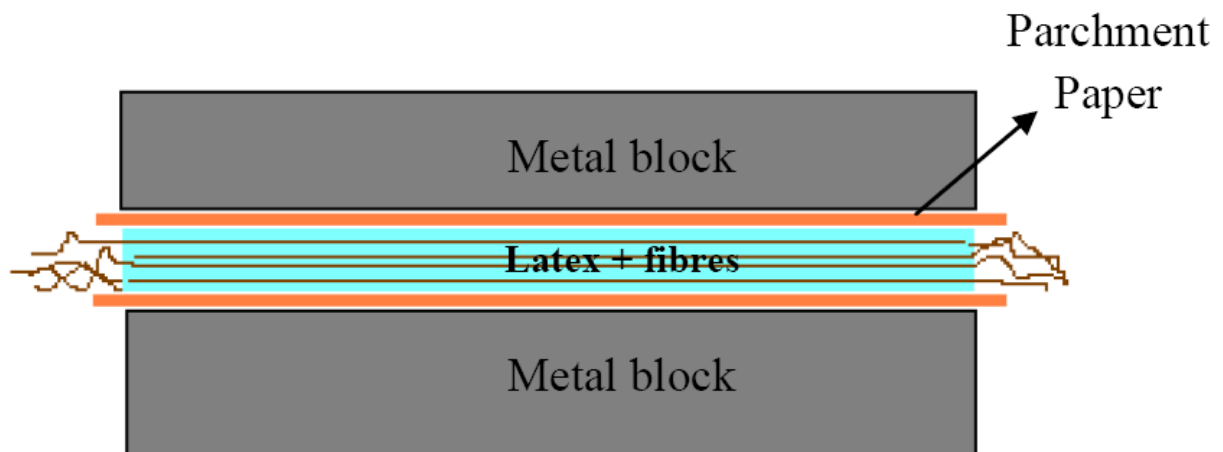


Figure 3.8 Schematic representation of the moulding process (Stillfried, 2012)

The final composite tile, with the two aluminium blocks still in contact, was put into an oven at 80 °C for one hour, after which the block on the top was removed. The assembly was left into the oven at the same temperature for three hours and after this time has passed, the bottom metal block was also removed. The parchment paper allows the transmission of heat to dry the latex-fibre mixture. Water molecules are able to penetrate through the paper thus drying the tile.

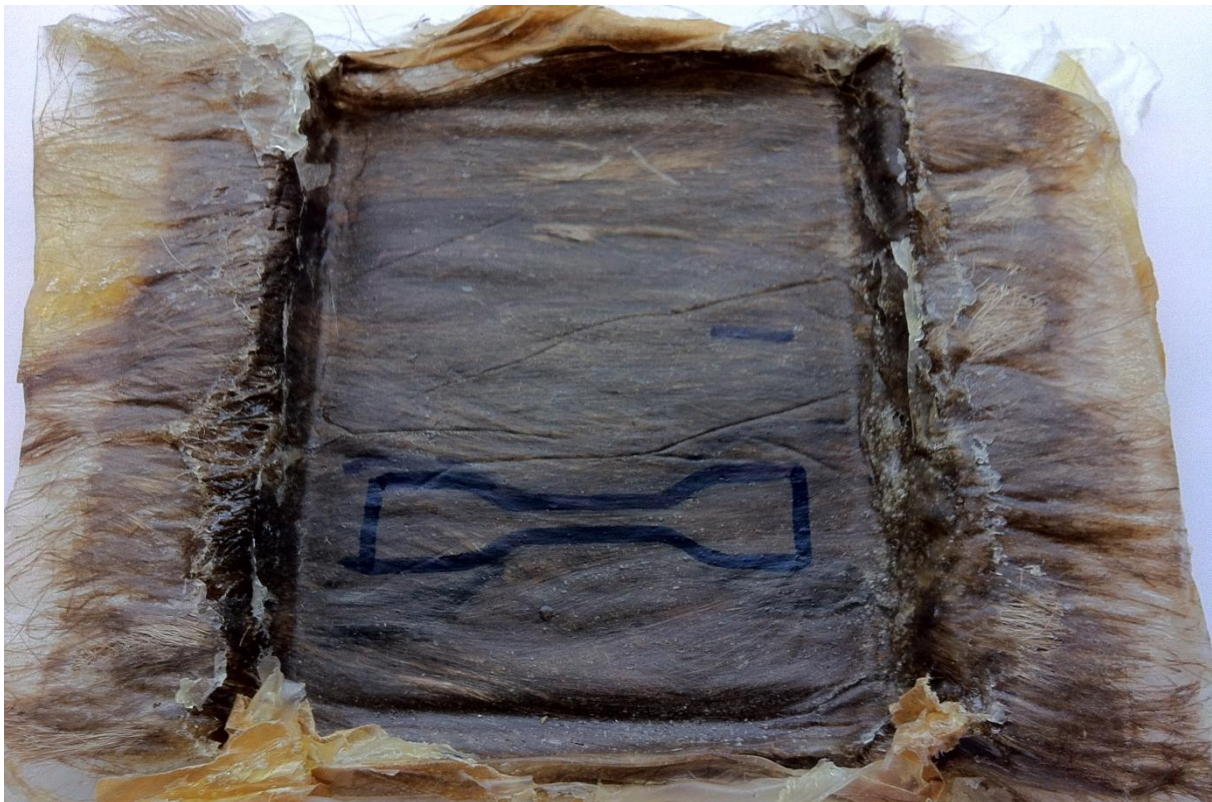


Figure 3.9 Mineralised flax fibres reinforced composite tile

To ensure complete drying, the composite was kept into the oven at 80°C for another twelve hours. After this time has elapsed, the paper was easily removed from the composite and this was left for an hour more into the oven. The tile was then taken out of the oven and allowed to cool. This procedure was repeated for all samples described in Table 3.6 and also for flax fibres without any treatment (control sample). It is worth mentioning that the whole procedure for the manufacture of the composite is an entirely manual procedure, hence the values obtained from the following mechanical tests may be subjected by operative errors, such as human errors. In particular, the maintenance of the same moulding pressure, which could otherwise affect the fraction of the latex in the composite, as well as ensuring fibre unidirectionality are complex tasks when carried out manually. The manufacture of the material may have affected the tensile testing data. In figure 3.9, an example of a final flax fibre reinforced composite tile is shown.

SEM pictures of mineralised flax fibres were taken to better understand the crystalline morphologies obtained by the different mineralisation treatments. In Appendix (Annex A) are shown the most representative SEM pictures in terms of crystalline morphology of calcium carbonate. There are some similarities with the SEM pictures of the research work done by Fagerlund *et al.* (2013). β -Alanine seems to form a surface with densely packed cones and some round undefined structures. The crystal structure affected by Glycine presents a similar configuration, but more rational with rectangle-shaped prisms. The structure affected by L-lysine shows a mushroom-like morphology and closer observation (5000x, 8000x) reveals the crystal structure was made up of thin layers (Fagerlund *et al.* 2013).

3.4 Tensile testing

All composite tiles, obtained by each mineralisation treatment of Table 3.6, were cut into “dog bone” form in order to subject them to tensile tests. Details about dimensions of the dog bone shaped composite sample (Figure 3.10) are presented in Table 3.7.

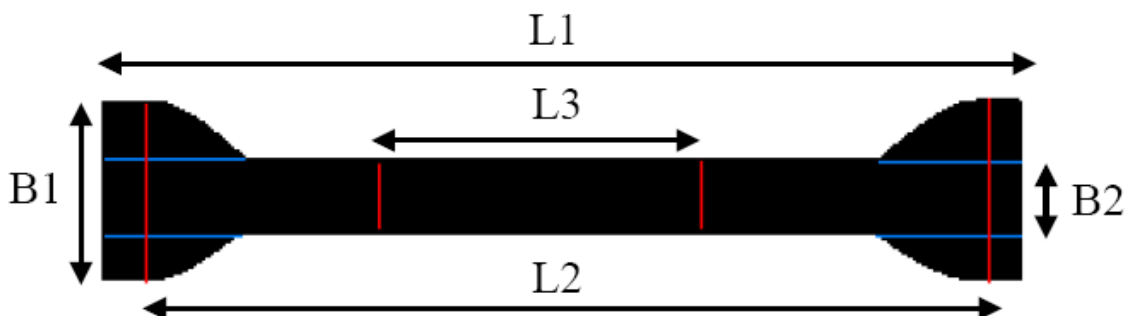


Figure 3.10 Dog bone shaped composite sample (Stillfried, 2012)

Table 3.7 Sample size

L1 [mm]	L2 [mm]	L3 [mm]	B1 [mm]	B2 [mm]
75	58 ± 2	25 ± 0.5	10 ± 0.5	5 ± 1

In Table 3.7; $L1$ is the overall length of the sample, $L2$ is the distance between the grips of the machine, $L3$ is the gauge length, $B1$ is the width of the ends of the samples and $B2$ is the width of the trunk of the sample. The thickness of samples is $3 \text{ mm} \pm 1 \text{ mm}$. Tensile tests were performed using a testing machine, model INSTRON 8872 (Figure 3.11a) at ambient conditions. The tensile test consists in subjecting the sample to an equal and opposite force applied orthogonally to its cross section (Figure 3.11b).

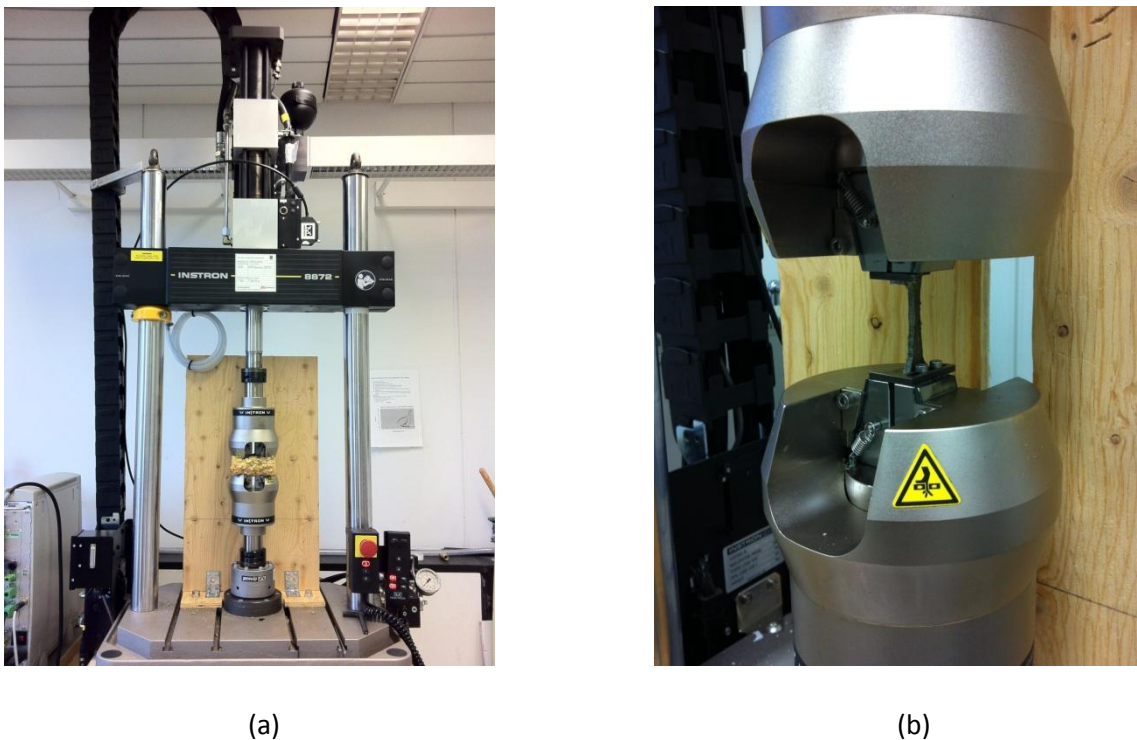


Figure 3.11 Testing machine model INSTRON 8872 (a) and particular during the pulling stage (b)

The system was set so that the machine is able to maintain a constant pulling velocity of 0.2 mm/min by varying the stress applied to the sample. During the tests, the outputs (the force applied and the corresponding position of the grips of the machine) were processed with Excel to obtain the values of the stress (or engineering stress) and strain (or engineering strain). It could be possible obtain a load-length of sample curve, but the data would not take into account the geometrical affects of the sample. Stress, σ [Pa], is defined as the ratio of the force applied, F [N], to the initial cross sectional area, A_0 [m²] (Equation 3.9), whilst the strain, ε [dimensionless], is defined as the change in length, Δl [m], per unit of the original length, l_0 [m] (Equation 3.10).

$$\sigma = \frac{F}{A_0} \quad (3.9)$$

$$\varepsilon = \frac{\Delta l}{l_0} \quad (3.10)$$

The stress - strain curve shows a linear elastic trend following the Hooke's law ($\sigma = E\varepsilon$) when the load applied is sufficiently low; the material stretches elastically and once the force is removed, it returns to its original length. This constant of proportionality, E [Pa], is named Young's modulus or the elastic modulus and it represents the slope of the straight line in a region of elastic deformation. The elastic part of the curve ends when the yield stress, σ_y [Pa], is reached. After this point the material begins to deform permanently (plastic region). In fact, the yield stress is the transition point from the elastic to the plastic range. The ultimate stress, σ_{ult} [Pa], refers to the maximum value of load withstood by the material before failing. Resilience represents the ability of a material to absorb energy when it is deformed elastically and to release the same amount of energy when the load is removed. The modulus of resilience, U [J/m³], allows the calculation of the maximum amount of energy per unit volume that can be absorbed by the material without creating an irreversible deformation (Equation 3.11):

$$U = \frac{\sigma\varepsilon}{2} \quad (3.11)$$

Three samples per each treatment shown in Table 3.6 (and for the control sample) were tested. It is important to clarify that each group of samples corresponds to a certain treatment and has a wide range of stress values (differences of about 30 MPa among samples belonging to the same group/treatment). This made it hard to differentiate between them. The median for each group was plotted as the sample set was low. Given the wide range of stress values of the samples, it was demonstrated that three samples are not enough for the consolidation of this theory. The evaluation of close values may be misleading. The reliability of these values can be ascertained only by increasing the number of samples in each test group. In Figure 3.12, 3.13 and 3.14 are reported engineering stress-strain curves for median sample from each group. In Annex C, the minimum and maximum values for the ultimate stress of all samples tested are reported. In each figure, the control sample (flax fibres reinforced composite without any treatment) is also reported. The plots are parametrised by the molarity of amino acid used. The stress values are given in MPa, whilst the strain values are shown in percentage of the real value ($\varepsilon_{\%} = (\Delta l/l_0) \cdot 100$). The trend of the curves shows similarities in all composites in that once the ultimate stress is reached, the samples experience severe structural failure. All composites that were subjected to the treatment showed good improvement over

the control sample. All composites tested with the $30 \cdot 10^{-5}$ M treatment of each amino acid show an higher gap between the ultimate stress and the fracture point.

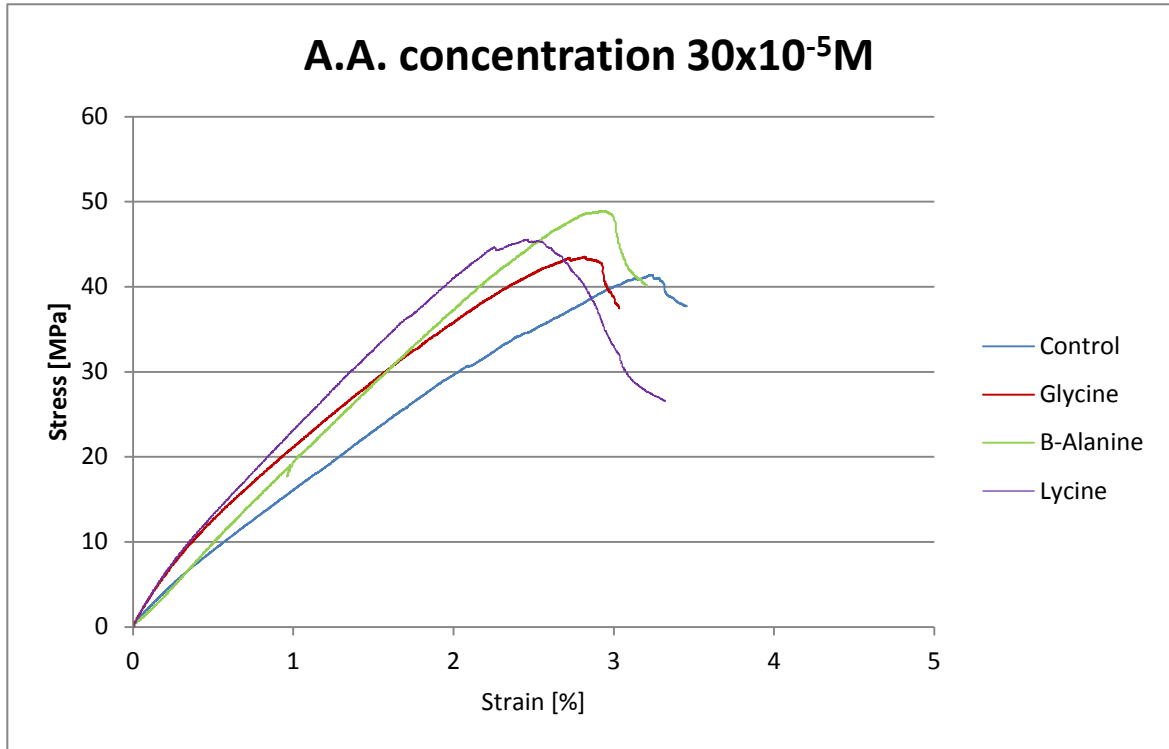


Figure 3.12 Stress - strain diagrams of composites ($30 \cdot 10^{-5}$ M)

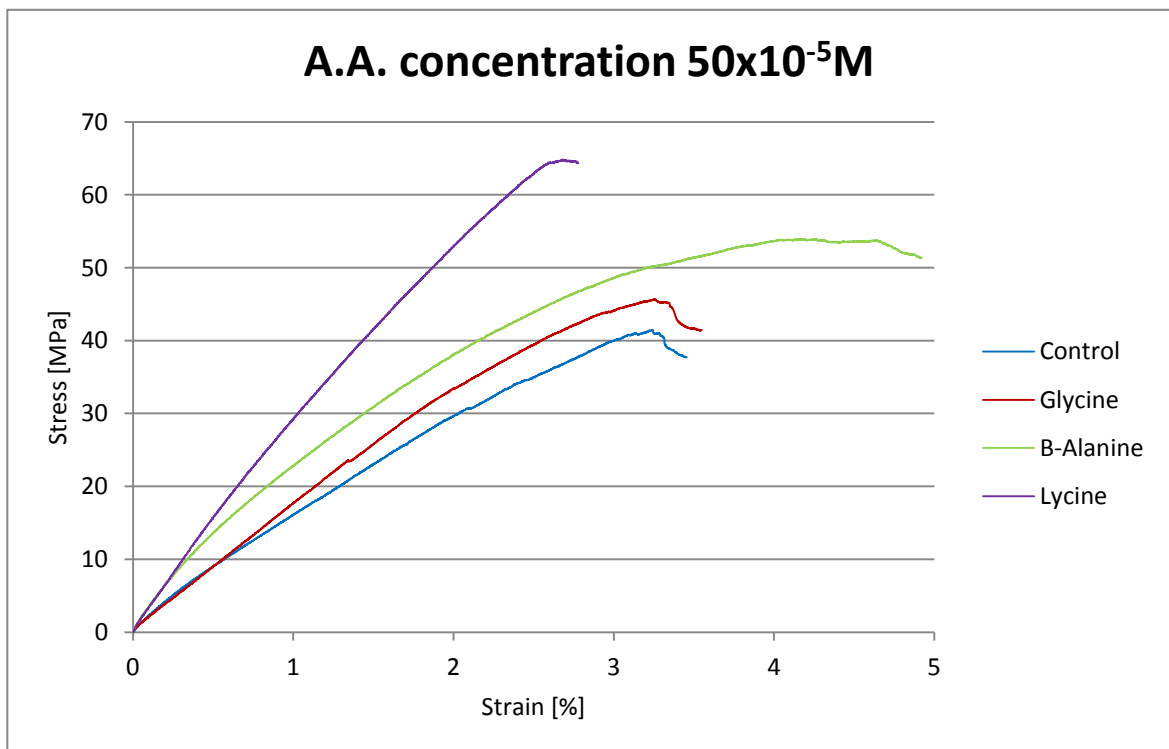


Figure 3.13 Stress - strain diagrams of composites ($50 \cdot 10^{-5}$ M)

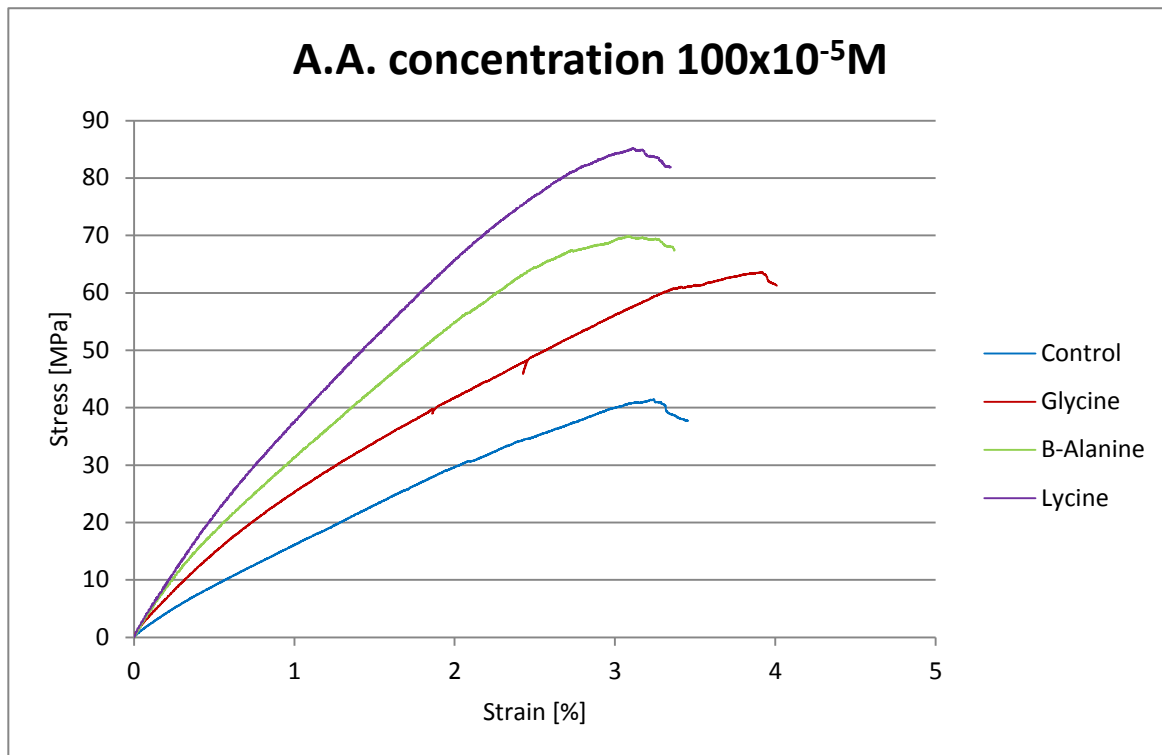
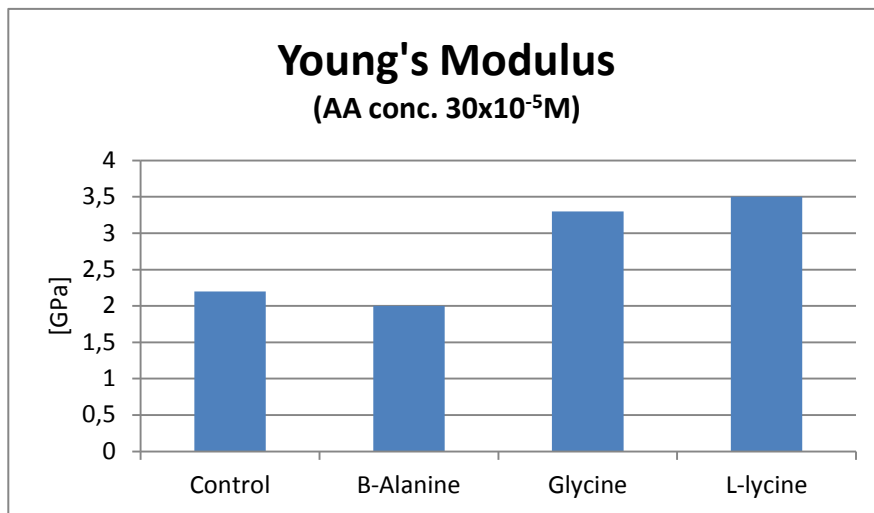


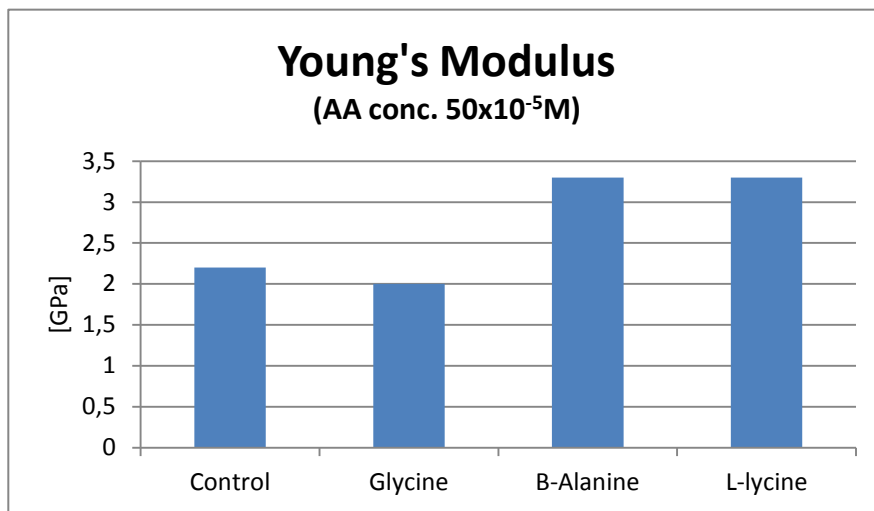
Figure 3.14 Stress - strain diagrams of composites ($100 \cdot 10^{-5} M$)

The composite treated with L-lysine at $50 \cdot 10^{-5} M$ and $100 \cdot 10^{-5} M$ has the best mechanical properties in terms of Young's modulus, stiffness and ultimate stress value. L-lysine provides the best mechanical properties also considering the $30 \cdot 10^{-5} M$, with the exception of the ultimate stress, but this value is very close to the highest value of the graph. Composites treated with Glycine and β -Alanine have similar curves to each other with negligible differences (about 5 MPa). There is the tendency for an increase in mechanical performance with the addition of amino acid. It was hypothesised that this could be due to the greater influence on the crystal morphology of calcium carbonate, hence on the mechanical interlocking between the matrix and the fibres. Values of the Young's modulus calculated from the stress-strain curves above are shown in the Figure 3.15. These graphs provide a clear indication of mechanical improvement within the elastic region. The elastic modulus reflects the stiffness of a material (Portela *et al.*, 2010), hence, at all concentrations, flax fibres mineralised with L-lysine exhibited more stiffness than the others. Notably, a value of the elastic modulus equal to 5.5 GPa at $100 \cdot 10^{-5} M$ was measured.

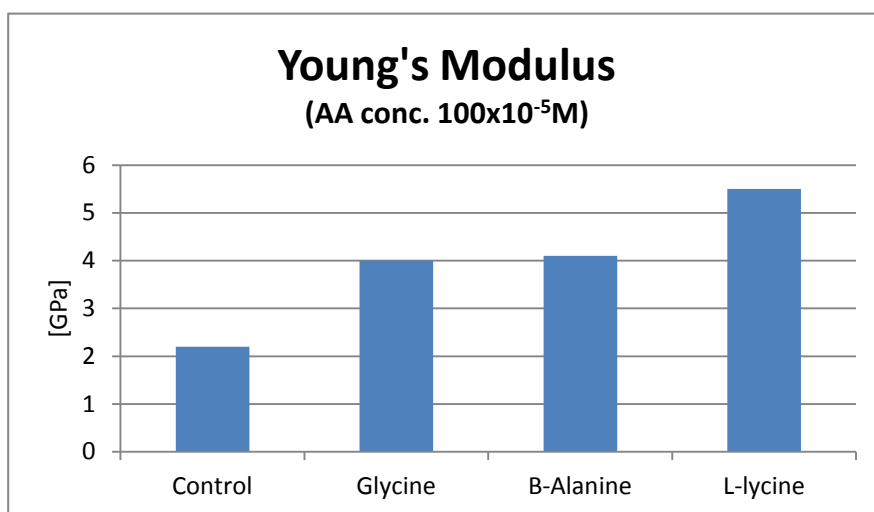
These results are in agreement with Fagerlund *et al.* (2013) and with the previous results obtained in molecular dynamic simulations, in which fibres treated with Glycine and β -Alanine revealed similar properties in terms of bending strength and intermolecular energy, while L-lysine had a greater influence on the mechanical properties of the whole composite.



(a)



(b)



(c)

Figure 3.15 Young's modulus of flax fibres reinforced SBR treated with different amino acids at $30 \cdot 10^{-5} M$ (a), $50 \cdot 10^{-5} M$ (b) and $100 \cdot 10^{-5} M$ (c)

In Table 3.8 are reported the values of the modulus of resilience calculated from stress - strain diagrams according to Equation (3.11). The following Equation 3.12 provides an analysis on the units of measure of the resilience modulus:

$$U = \frac{\sigma \varepsilon}{2} = \frac{[N]}{[m]^2} \cdot \frac{[m]}{[m]} = \frac{[N] \cdot [m]}{[m]^2 [m]} = \frac{[J]}{[m]^3} \quad (3.12)$$

The transformation from [N·m] to [J] is possible because the dimension [m] refers to a change in length or a displacement Δl ; in other words, a constant force on a point which moves a displacement in the direction of the force produces a work measured in [J].

Table 3.8 Modulus of resilience of flax fibres reinforced SBR treated with different amino acids at different concentrations

Concentration	Mineralisation treatment	Modulus of Resilience [J/m ³]
30·10 ⁻⁵ M	Control	4602
	L-lycine	2285
	Glycine	2424
	β-Alanine	49000
50·10 ⁻⁵ M	Control	4602
	L-lycine	5454
	β-Alanine	5454
	Glycine	6250
100·10 ⁻⁵ M	Control	4602
	Glycine	2000
	L-lycine	2272
	β-Alanine	9878

The modulus of resilience expresses an inverse proportionality to the elastic modulus. Even though Glycine and β-Alanine exhibited similarities in the previous tests, β-Alanine showed a significant ability to absorb mechanical energy in its elastic state.

3.5 Nano-indentation testing

Nano-indentation testing was carried out to measure the hardness of the composite. The indentation is made in a line over the cross section of the fibre embedded in an epoxy resin. The preparation of the samples follows. Some flax fibres obtained by each mineralisation treatment (see Table 3.6) were cut into 2-3 cm length and they were put into a small bowl vertically.

Table 3.9 Amount in grams and compounds used for the preparation of the epoxy resin for four cross-sections

Mixture	Compound	Amount [g]
A	Epon 812	11.68
	DDSA	15.43
B	Epon 812	16.14
	MNA	14.52

For the preparation of the epoxy resin, the following chemical compounds were used:

- Epoxy Embedding Medium (Sigma-Aldrich) 414 2 1000 ml Liquid 25038-04-4
- Epoxy Embedding Medium, Accelerator (Sigma-Aldrich) 414 250 ml Liquid 90-72-2
- Epoxy Embedding Medium, hardener MNA (Sigma-Aldrich) 414 1000 ml Liquid 5134-21-8
- Epoxy Embedding Medium, hardener DDSA (Sigma-Aldrich) 414 1000 ml Liquid 25377-73-5

Initially, two different mixtures were prepared in a fume cupboard following the amounts for four cross-sections reported in Table 3.9. The amounts detailed in the table were calculated for ten samples. The final resin was obtained mixing together 20 g A, 20 g B and 0.6 g accelerator.

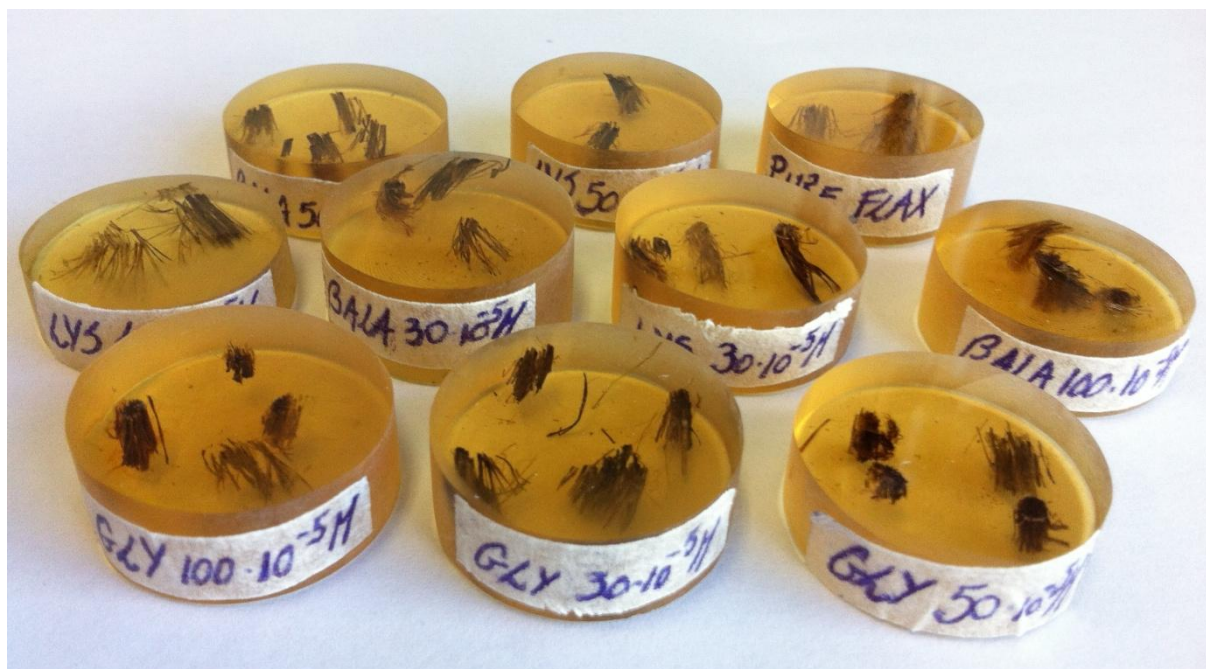


Figure 3.16 Cross-sections of mineralised flax fibres for nano-indentation testing

These quantities are always referring to four cross-sections. The resin was mixed in paper cups; first mix A in a cup and mix B in another cup for blending carefully with disposable

pipettes and spatulas. After putting blend A and B together in another clean paper cup, accelerator was added and the cup of mixed resin was put into a vacuum oven (200mbar, 10 min) for gas release. 8 g of the mixed resin were weighed and ten forms (one per each sample) with mineralised flax fibres placed vertically were filled evenly. The samples were put again into the vacuum oven (200mbar, 10 min) to release air bubbles. It is important to check that the samples stand nicely in the bottom of forms. Finally, all samples were put overnight (16-24 h) into an oven at 60°C without vacuum for hardening.

After hardening, the samples were taken out from the oven and let in the fume cupboard for a few minutes. The mixed resin with fibres were extracted from the forms and rinsed with warm water. The samples were marked with a pen (Figure 3.16).

The grinding instructions, followed for obtaining polished and flat cross-sections, are presented. Edges of samples were ground by hand so that they fit exactly into the holder.

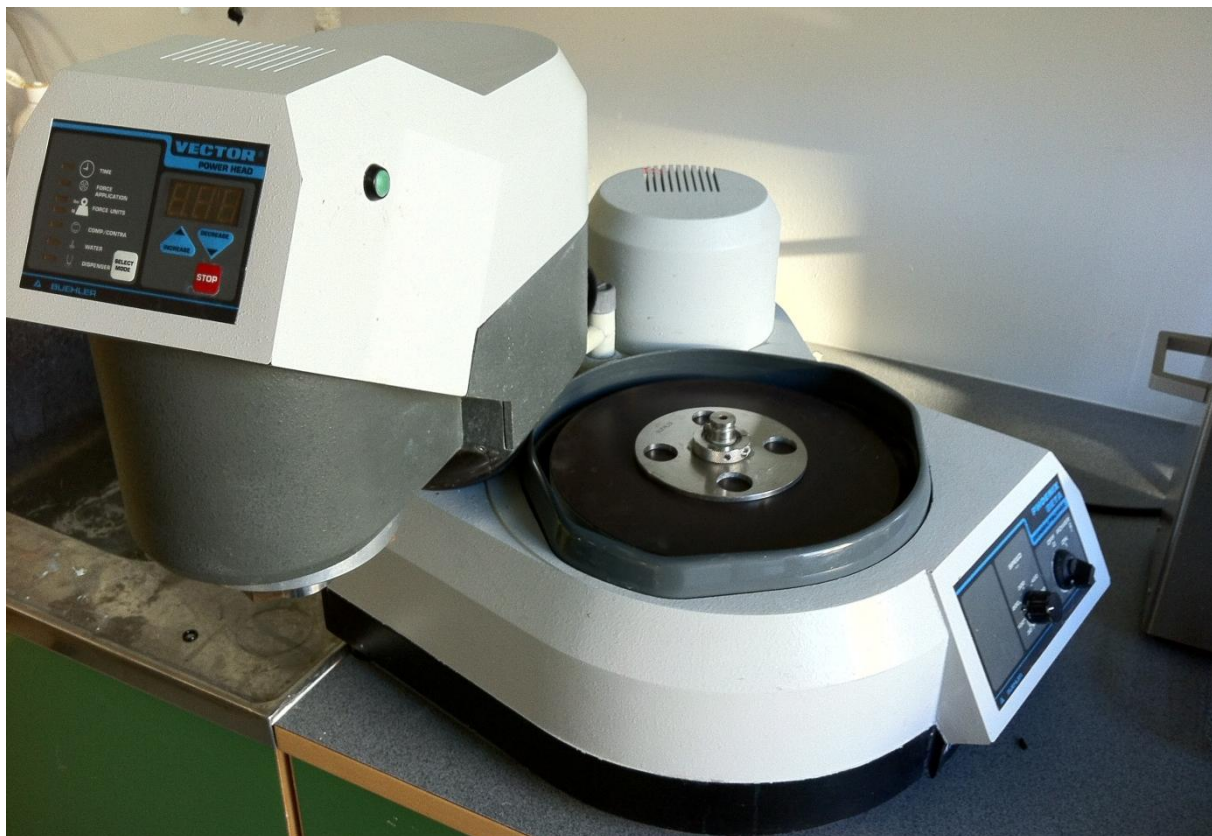


Figure 3.17 Grinding machine to smooth cross-sections of the samples

The grinding machine (Figure 3.17) was set with 5 N pressure and 50 rpm speed; P 320 was the grinding paper placed on the turntable and both the plate and the holder spun in the same direction (Comp mode). It was important to place the water tap on the grinding plate to avoid overheating. Once the right diameter of the samples was reached, the samples were inserted into the holder for the automatic grinding of the cross-sections. The machine was set with 20

N pressure, 30 s grinding time and 200 rpm speed. P 320 was used as grinding paper and again the plate and the holder spun at the same direction.

The surfaces were checked for smoothness. If the cross-sections had an irregular or scratched surface, the last grinding stage was repeated setting new parameters for the pressure and/or the grinding paper.

All samples were sent to the “Biological and Biomimetic Material Laboratory” of Nanyang Technological University in Singapore for nano-indentation testing. The hardness, H , was calculated following Equation 3.9:

$$H = \frac{F_{max}}{A_r} \quad (3.13)$$

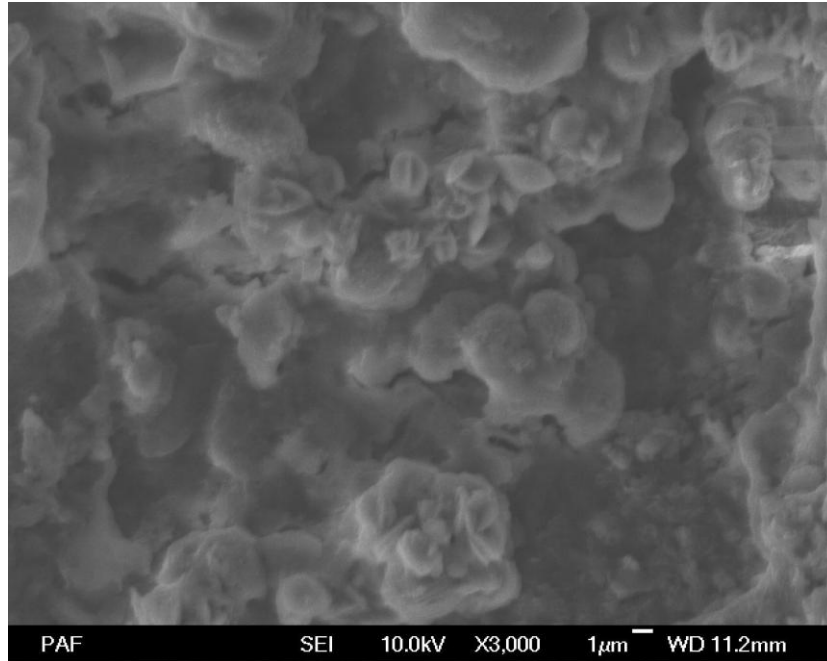
where F_{max} [N] is the maximum load applied with a corner-cube and A_r [m²] is the residual indentation area, and the Young’s modulus was measured as a function of the stiffness of the material. For further details about nano-indentation, see Section 2.1. Nano-indentation results demonstrate that, considering the flax fibres reinforced composite material formed by an epoxy resin matrix, there are not differences between samples. The hardness measured for all samples tested resulted in the same ($H = 0.2\text{-}0.3$ GPa) and the Young’s modulus values (around 8-9 GPa) do not allow for the determination of differences concerning mechanical properties. Nano-indentation results are reported in Annex B. For the evaluation of the residual indentation area, SPM (Scanning Probe Microscopy) images for probed regions of each sample are also reported. It is hypothesized that if the matrix of the composite is too tough, there are not important interlocking phenomena able to provide a significant difference between mineralised natural fibres and unmineralised. Probably, the mineralised layer upon natural fibres do not ensure the bonding between the epoxy resin matrix and the flax fibre; in other words, during the loading stage, in which the fibre is pressed down into the material, the fibre coating is removed because unable to support the load.

Conclusions

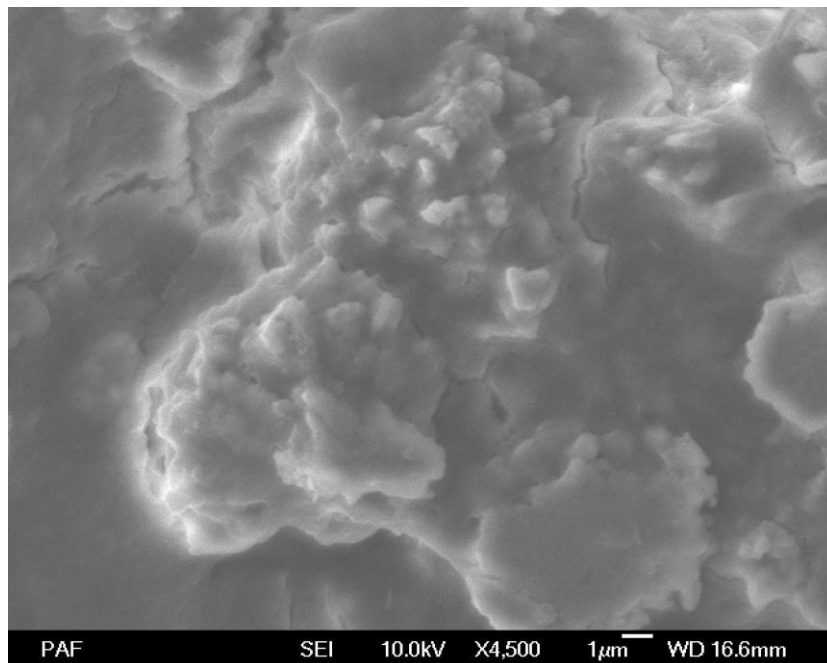
L-lysine has the strongest influence inside the calcium carbonate system in terms of intermolecular energy when compared to other systems containing Glycine and β -Alanine. These results correlate well to the work done by Fagerlund *et al.* (2013) in view of bending strength. The functionalisation and the mineralisation of natural fibre surfaces using a bio-inspired mineralisation approach was successful in that calcium carbonate was mineralised onto fibre surfaces with different crystal structure as demonstrated by SEM pictures. To reduce the chances of human error, manufacture of the composite tiles could follow a standardised procedure. In fact, the production of the natural fibre reinforced composite tile was quite difficult to do manually as the effects of moulding pressure and latex fractions can have a significant effect on the mechanical properties of natural fibre based composites. From tensile testing, it is ascertained that flax fibres mineralised with calcium carbonate and L-lysine yield the best composite mechanical properties. Mineralised fibres using Glycine and β -Alanine showed a very similar behaviour to each other. These results are also in agreement with Fagerlund *et al.*, (2013) and with molecular dynamic simulation results. In these researches, fibres treated with Glycine and β -Alanine showed similar characteristics of bending strength and intermolecular energy with a calcium carbonate system, while L-lysine demonstrated greater influence on the mechanical properties of bending fibres, as well as a more strongly bonded structure inside a calcium carbonate system. However, given there is a wide range in the stress values of the samples, the reliability of these values need to be double checked by increasing the number of test samples. Nano-indentation testing on flax fibre reinforced epoxy resin did not provide clear results. It is hypothesised that tough matrices make it hard to differentiate between the different mineralisation treatments.

Appendix

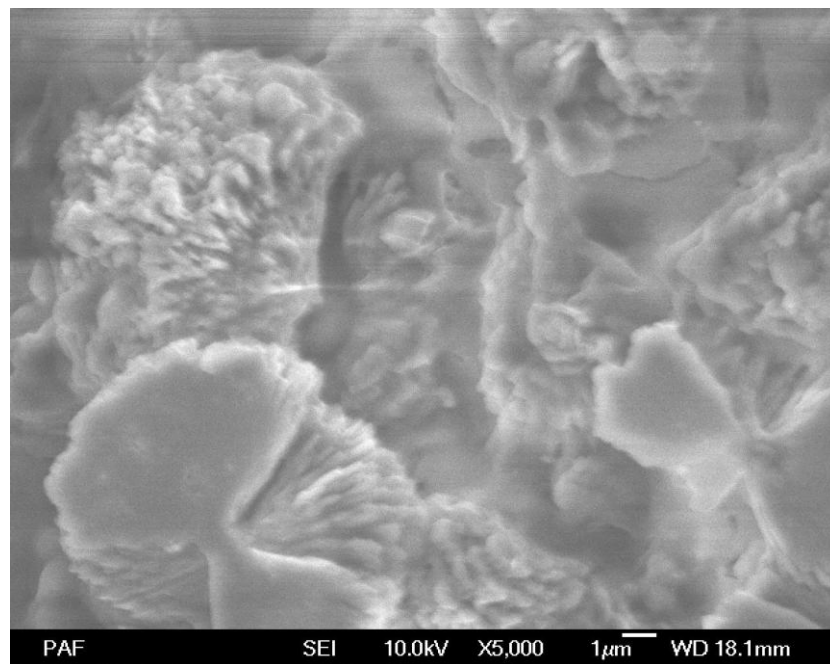
ANNEX A: SEM pictures of mineralised flax fibres.



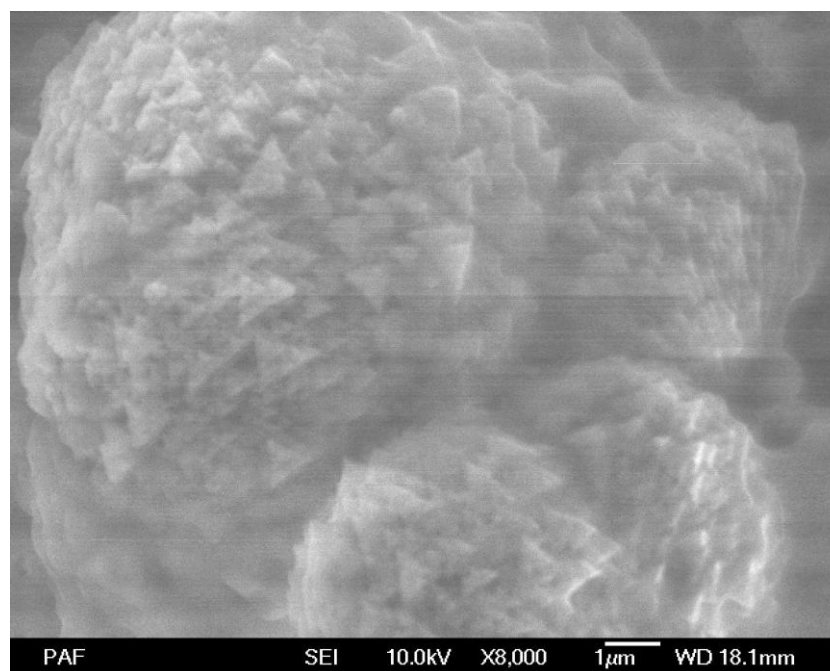
Flax fibres mineralised with β -Alanine ($30 \cdot 10^{-5} M$)



Flax fibres mineralised with Glycine ($100 \cdot 10^{-5} M$)

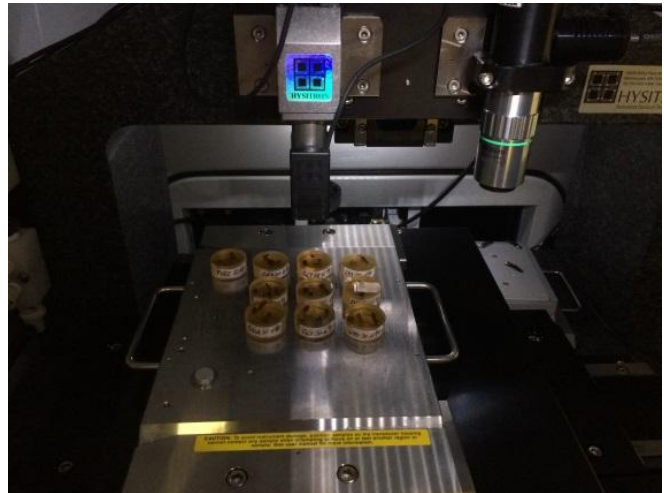


Flax fibres mineralised with L-lysine ($50 \cdot 10^{-5} M$)



Flax fibres mineralised with L-lysine ($50 \cdot 10^{-5} M$)

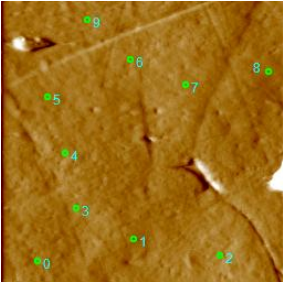
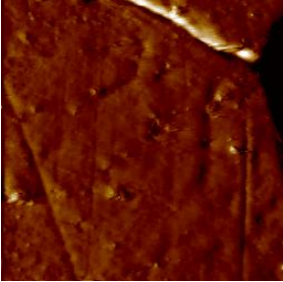
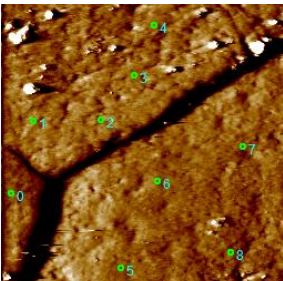
ANNEX B: Nano-indentation results

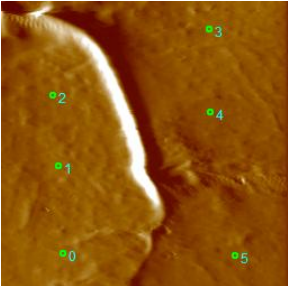
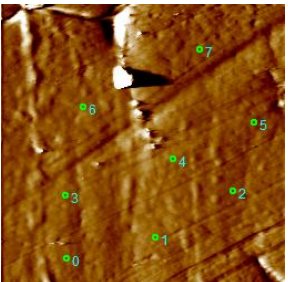
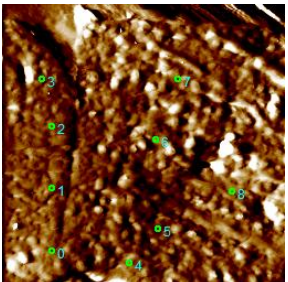
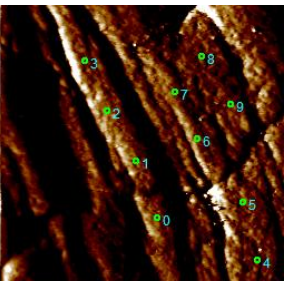
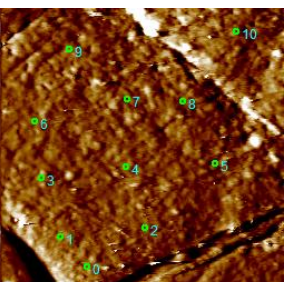
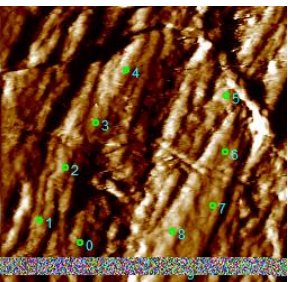


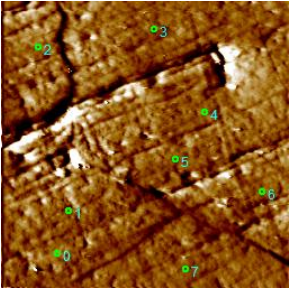
Max applied load. = 500 μ N

No. of indents/sample = 10

Load function (Loading-holding-unloading) = 5-2-5 seconds

Sample	SPM image of probed region	Results [GPa]
Pure		$E = 9.8 \pm 0.6$ $H = 0.3 \pm 0.0$
Bala 30		$E = 9.4 \pm 0.3$ $H = 0.2 \pm 0.0$
Bala 50		$E = 7.8 \pm 0.4$ $H = 0.2 \pm 0.0$

Bala 100		$E = 8.6 \pm 0.9$ $H = 0.2 \pm 0.0$
Gly 30		$E = 9.7 \pm 0.7$ $H = 0.2 \pm 0.0$
Gly 50		$E = 8.1 \pm 0.6$ $H = 0.2 \pm 0.0$
Gly 100		$E = 9.5 \pm 0.8$ $H = 0.3 \pm 0.0$
Lys 30		$E = 7.3 \pm 0.3$ $H = 0.2 \pm 0.0$
Lys 50		$E = 9.9 \pm 0.8$ $H = 0.2 \pm 0.0$

Lys 100		$E = 8.7 \pm 0.4$ $H = 0.2 \pm 0.0$
------------	---	--

ANNEX C: Minimum and maximum values for the ultimate stress

Ultimate stress [MPa]			
A.A. concentration	Amino Acid	Min	Max
30·10 ⁻⁵ M	Glycine	42	48
	β-Alanine	45	51
	Lycine	44	55
50·10 ⁻⁵ M	Glycine	38	52
	β-Alanine	44	54
	Lycine	52	65
100·10 ⁻⁵ M	Glycine	56	70
	β-Alanine	68	75
	Lycine	70	86
Control	-	22	51

References

- Abdelmouleh M, Boufi S, Belgacem M.N., Dufresne A., (2007). Short natural-fibre reinforced polyethylene and natural rubber composites: effect of silane coupling agents and fibres loading. *Composites Science and Technology*, Volume **67**, Issue 7-8, 1627-1639.
- Abdul-Khalil H.P.S., Bhat A.H., Ireana Yusra A.F., (2012). Green composites from sustainable cellulose nanofibrils: a review. *Carbohydrate Polymers*, Volume **87**, 963-979.
- Abraham F.F., (1974). *Homogeneous nucleation theory*. Academic Press, New York (U.S.A.).
- Addadi L., Raz S., Weiner S., (2003). Taking advantage of disorder: amorphous calcium carbonate and its roles in biomineralization. *Advanced Materials*, Volume **15**, Issue 12, 959-970.
- Aizenberg J., Lambert G., Addadi L., Weiner S., (1996). Stabilization of amorphous calcium carbonate by specialized macromolecules in biological and synthetic precipitates. *Advanced Materials*, Volume **8**, Issue 3, 222-226.
- Akin D.E., Deblois S., Harris P.G., Ljungdahl L.G., Wiegel J., Wilson J.R., (1990). *Microbial and Plant Opportunities to improve lignocelluloses utilization by ruminants*. Elsevier, New York (U.S.A.).
- Alam P., (2013). *Structural organisation and biomimesis of nature's polymer composites*. New developments in polymer composites research. Ed. Laske S. and Witschnigg A., 325-379.
- Alam P., Stillfried D.G., Celli J., Toivakka M., (2013). Effects of fibre surface morphology on the mechanical properties of Porifera-inspired rubber matrix composites. *Applied Physics A*, Volume **111**, Issue 4, 1031-1036.
- Alves C., Ferrão P.M.C., Silva A.J., Reis L.G., Freitas M., Rodrigues L.B., Alves D.E., (2010). Ecodesign of automotive components making use of natural jute-fiber composites. *Journal of Cleaner Production*, Volume **18**, Issue 4, 313-327.
- American Society for Testing and Materials (ASTM), (1969). *Interfaces in composites*. Meeting, York (U.S.A.).
- Anil N. Netravali, Shitij Chabba, (2003). Composites get greener. *Materials today*, Volume **6**, Issue 4, 22-29.

- Anthony A., Desiraju G.R., Jetti R.K.R., Kuduva S.S., Madhavi N.N.L., Nangia A., Thaimattam R., Thalladi V.R., (1998). Crystal engineering: some further strategies. *Crystal Engineering*, Volume **1**, Issue 1, 1-18.
- Ashori A., (2008). Wood-plastic composites as promising green composites for automotive industries. *Bioresource Technology*, Volume **99**, Issue 11, 4661-4667.
- Baiardo M., Zini E., Scandola M., (2004). Flax fibre-polyester composites. *Composites Part A: Applied Science and Manufacturing*. Volume **35**, Issue 6, 703-710.
- Baley C., (2002). Analysis of the flax fibres tensile behaviour and analysis of the tensile stiffness increase. *Composites: Part A*, Volume **33**, Issue 7, 939-948.
- Baley C., Yves Perrot, Frederic Busnel, Herve Guezenoc, Peter Davies, (2006). Transverse tensile behaviour of unidirectional plies reinforced with flax fibres. *Materials Letters*, Volume **60**, Issue 24, 2984-2987.
- Belcher A.M., Hansma P.K., Stucky G.D., Morse D.E., (1998). First steps in harnessing the potential of biomineralisation as a route to new high performance composite materials. *Acta Materialia*, Volume **46**, Issue 3, 733-736.
- Berridge M.J., Bootman M.D., Lipp P., (1998). Calcium – A life and death signal. *Nature*, Volume **395**, Issue 6703, 645-648.
- Bledzki andrzej K., Abdullah A. Mamum, Adam Jaszkiwicz, Karsten Erdmann, (2010). Polypropylene composites with enzyme modified abaca fibre. *Composites Science and Technology*, Volume **70**, Issue 5, 854-860.
- Boccaccini A.R., C. Kaya, K.K. Chawla, (2001). Use of electrophoretic deposition in the processing of fibre reinforced ceramic and glass matrix composites: a review. *Composites Part A: Applied Science and Manufacturing*, Volume **32**, Issue 8, 997-1006.
- Bos H.L., (2004). The potential of flax fibres as reinforcement for composite materials. *Ph.D Thesis*, Eindhoven University of Technology, Eindhove (NL).
- Brazel Christopher S., Stephen L. Rosen, (2012). *Fundamental principles of polymeric materials* (3rd ed.). John Wiley & Sons, New York (U.S.A.).
- Briegel C., Coelfen H., Seto J., (2012). Single amino acids as additives modulating CaCO₃ mineralization. In: *Advanced Topics in Biomineralization*. In Tech, Rijeka (Croatia).
- Brinton Thomas George, Komarneni Sridhar, Parker John, (1993). Nanophase and nanocomposite materials. *Materials Research Society Symposium Proceedings – Materials Research Society*, Boston, Massachusetts, (U.S.A.), December 1-3.

- Brown E.N., (2005). Biomimetic composites: inspiration to application – A review. *SEM Annual Conference and Exposition on Experimental and Applied Mechanics*, Los Alamos National Laboratory (U.S.A.).
- Brown W.J., (1947). *Fabric reinforced plastics*. Cleaver – Hume Press Ltd, London (U.K.).
- Bitton Ronit, Elinor Josef, Irena Shim Shelashvili, Keren Shapira, Dror Seliktar, Havazelet Bianco – Peled, (2009). Phloroglucinal – based biomimetic adhesives for medical applications. *Acta Biomaterialia*, Volume 5, Issue 5, 1582-1587.
- Cabeza Luisa F., Camila Barreneche, Laira Mirò, Joseph M. Morera, Esther Bartoli, A. Inès Fernandez, (2013). Low carbon and low embodied energy materials in buildings: a review. *Renewable and Sustainable Energy Reviews*, Volume 23, 536-542.
- Celli J., (2012). Process modelling of biomimetic mineralised natural fibre reinforced composites. *Master's Thesis*, Laboratory of Paper Coating and Converting, Faculty of Technology, Åbo Akademi University, Turku (FIN).
- Chawla K.K., (1993). *Ceramic matrix composites*. Chapman and Hall, London (U.K.).
- Chawla Krishan K., (2012). *Composite materials: Science and Engineering* (3rd ed.). Springer, Birmingham (U.S.A.).
- Clegg S.L., Whitfield M., (1991). *Activity coefficients in electrolyte solutions* (2nd ed.). CRC Press, Boca Raton (U.S.A.).
- Conte L., (2014). *Personal communication*.
- Cristaldi G., (2011). Sviluppo di materiali composite rinforzati con fibre naturali per l'ingegneria civile. Ph.D in Materials and technological innovation for engineering and architecture. *Ph.D Thesis*, Università degli Studi di Catania (IT).
- Cristaldi G., Latteri A., Recca G. and Cicala G., (2010). Composites based on natural fibers fabrics. Università degli Studi di Catania – Department of physical and chemical methodologies for engineering (IT).
- De Yoreo J.J., Vekilov P.G., (2003). Principles of crystal nucleation and growth. *Mineralogical Society of America - Geochemical Society*, Volume 54, Issue 1, 57-93.
- Dittenber D.B., H.V.S. GangaRao, (2012). Critical review of recent publications on use of natural composites in infrastructure. *Composites Part A: Applied Science and Manufacturing*, Volume 43, Issue 8, 1419-1429.
- Drzal L.M., Rich M.J., Camping J.D., Park W.J., (1980). Interfacial shear strength and failure mechanism in graphite fiber composite. *Proceedings of the 35th Annual Technical Conference*, Reinforced Plastics/Composite Institute, 20-C, pp. 1-7.

- Fagerlund Pi, Hägerstrand Piotr, Töyrylä Jim, (2013). Coral-mimetic superfibres. *Research work*. Katedralskolan, Turku (FIN).
- Fancey Kevin S. (2010). Viscoelastically prestressed polymeric matrix composites – Potential for useful life and impact protection. *Composites Part B: Engineering*, Volume **41**, Issue 6, 454-461.
- Faruk Omar, Andrzej K. Bledzki, Hans-Peter Fink, Mohini Sain (2012). Biocomposites reinforced with natural fibers: 2000-2010. *Progress in Polymer Science*, Volume **37**, 1552-1596.
- Feng Q.L., Pu G., Pei Y., Cui F.Z., Li H.D., Kim T.N., (2000). Polymorph and morphology of calcium carbonate crystals induced by proteins extracted from mollusc shell. *Journal of Crystal Growth*, Volume **216**, Issue 1-4, 459-465.
- Fratzl P., (2007). Biomimetic materials research: what can we really learn from nature's structural materials?. *Journal of the Royal Society Interface*, Volume **4**, Issue 15, 637-642.
- Gauthier R., Joly C., Coupas A.C., Gauthier H., Escoubes M., (1998). Interfaces in polyolefin/cellulosic fiber composites: chemical coupling, morphology, correlation with adhesion and aging in moisture. *Polymer Composites*, Volume **19**, Issue 3, 287-300.
- Goud Govardhan, Rao R.N., (2011). Effect on fibre content and alkali treatment on mechanical properties of Roystonea regia-reinforced epoxy partially biodegradable composites. *Bulletin of Material Science*, Volume **34**, Issue 7, 1575-1581.
- Griskey Richard G. (1995). *Polymer Process Engineering*. Chapman and Hall, London (U.K.).
- Herrera-Franco P.J., Drzal L.T., (1992). Comparison of methods for the measurement of fibre/matrix adhesion in composites. *Composites*, Volume **23**, Issue 1, 2-27.
- Heuer A.H., Fink D.J., Laraia V.J., Arias J.L., Calvert P.D., Kendall K., Messing G.L., Blackwell J., Rieke P.C., Thompson D.H., Wheeler A.P., Veis A., Caplan A.I., (1992). Innovative materials processing strategies: a biomimetic approach. *Science Magazine*, Volume **255**, 1098-1105.
- Hilt J.Z., (2004). Nanotechnology and biomimetic methods in therapeutics: molecular scale control with some help from nature. *Advanced Dry Delivery Reviews*, Volume **56**, Issue 11, 1533-1536.
- Hochart Fabienne, Joëlle Levalois-Mitjaville, Roger De Jaeger, Léon Gengembre, Jean Grimblot, (1999). Plasma surface treatment of poly(acrylonitrile) films by fluorocarbon compounds. *Applied Surface Science*, Volume **142**, Issues 1-4, 574-578.

- Hull D., Clyne T.W., (1996). *An introduction to composite materials* (2nd ed.). Cambridge University Press, Cambridge (U.K.).
- Islam M.R., Beg M.D.H., Mina M.F., (2013). Fibre surface modifications through different treatments with the help of design expert software for natural fibre-based biocomposites. *Journal of Composite Materials*, Volume **0**, 1-13.
- Jayamol George, Sreekala M.S., Sabu Thomas, (2001). A Review on interface modification and characterization of natural fiber reinforced plastic composites. *Polymer Engineering and Science*, Volume **41**, Issue 9, 1471-1485.
- John M.J. and Anandjiwala R.D., (2008). Recent developments in chemical modification and characterization of natural fiber-reinforced composites. *Polymer Composites*, Volume **29**, Issue 2, 187-207.
- Joshi S.V., Drzal L.T., Mohanty A.K., Arora S., (2004). Are natural fiber composites environmentally superior to glass fiber reinforced composites?. *Composites Part A: Applied Science and Manufacturing*, Volume **35**, Issue 3, 371-376.
- Kashchiev D., (2000). *Nucleation: basic theory with applications*. Butterworth-Heinemann, Oxford (U.K.).
- Kelly A., Tyson W.R., (1965). Tensile properties of fibre-reinforced metals: copper/tungsten and copper/molybdenum. *Journal of the Mechanics and Physics of Solids*, Volume **13**, Issue 6, 329-350.
- Khalil A., Rozman H.D., Ahamd N.N., Ismail H., (2000). Acetylated plant-fibre-reinforced polyester composites: a study of mechanical, hydrothermal and ageing characteristics. *Polym. Plast. Technol. Eng.*, Volume **39**, Issue 4, 757-781.
- Kim J.K. And Mai Y.W. (1999). Engineered Interfaces in Fiber Reinforced Composites. *Composites Part A: Applied Science and Manufacturing*, Volume **30**, Issue 8, 1035-1036.
- Kokubo T., Kim H.M., Miyaji F., Takadama H., Miyazaki T., (1999). Ceramic-metal and ceramic-polymer composites prepared by a biomimetic process. *Composites Part A: Applied Science and Manufacturing*, Volume **30**, Issue 4, 405-409.
- Koronis Georgios, Arlindo Silva, Mihail Fontul, (2013). Green composites: A review of adequate materials for automotive applications. *Composites Part B: Engineering*, Volume **44**, Issue 1, 120-127.
- Lee Stuart M. (1992). *Handbook of composite reinforcements*. John Wiley & Sons, New York (U.S.A.).
- Lewin M., Pearce E.M., (1998). *Handbook of fibre science and technology*. Marcel Dekker, New York (U.S.A.).

- Li Chunmei, David L. Kaplan, (2003). Biomimetic composites via molecular scale self-assembly and biomineralization. *Current Opinion in Solid State and Materials Science*, Volume 7, Issues 4-5, 265-271.
- Lilholt H., Toftegaard H., Thomsen A.B., Schmidt A.S., (1999). Natural composites based on cellulosic fibres and polypropylene matrix – Their processing and characterization. *Proceedings of ICCM 12*, p.9.
- Lowenstam H.A., Margulis L., (1980). *The mechanism of biomineralization in animals and plants*, Calcium regulation and the appearance of calcareous skeletons in the fossil record. Edited by: Omori M., Watabe N., Tokai University Press, Tokyo (J).
- Lowenstam H.A., Weiner S., (1989). *On biomineralization*. Oxford University Press, New York (U.S.A.).
- Lu Yen-Pei, Chih-Hui Yang, Andrew Yeh J., Fu Han Ho, Yu-Cheng Ou, Chieh Hsiao Chen, Ming-Yu Lin, Keng-Shiang Huang, (2013). Guidance of neural regeneration on the biomimetic nanostructured matrix. *International Journal of Pharmaceutics*, In Press.
- Ma Peter X., (2008). Biomimetic materials for tissue engineering. *Advanced Drug Delivery Reviews*, Volume 60, Issue 2, 184-198.
- Mahieux Cèline A. (2005). *Environmental Degradation of Industrial Composites* (1st ed.). 2 – Effect of temperature on polymer matrix composites., 17-83. Elsevier Science (NL).
- Mann S., (1996). *Biomimetic materials chemistry*. John Wiley & Sons, Bath (U.K.).
- Mann S., (2001). *Biomineralization: Principles and concepts in bioinorganic materials chemistry*. Oxford University Press, Oxford (U.K.).
- Massimino F., (2010). α -alanina e carbonate di calico: interazioni per la biomineralizzazione. *Master's Thesis*, Università degli Studi di Torino, (IT).
- Materials, (2010). Ford turns to soy to improve automotive rubber parts. *Additives for Polymers*, Volume 2010, Issue 9, 4-5.
- Matthews F.L. and Rawlings R.D. (2000). *Composite materials: Engineering and science*. CRC Press, London (U.K.).
- Maya Jacob John, Rajesh D. Anandjiwala, (2008). Recent developments in chemical modification and characterization of natural fiber-reinforced composites. *Polymer Composites*, Volume 29, Issue 2, 187-207.
- McMullen P., (1984). Fibre/resin composites for aircraft primary structures: a short history. *Composites*, Volume 15, Issue 3, 222-230.

- Modesti M. (2012). Processi di trasformazione e riciclo delle materie plastiche. Dipartimento di Ingegneria Industriale, Polymer Engineering Lab, Università degli Studi di Padova, (IT).
- Mohanty Amar K., Manjusri Misra, Lawrence T. Drzal (2005). *Natural Fibers, Biopolymers, and Biocomposites*. Taylor & Francis, London (U.K.).
- Morse John W., Arvidson Rolf S., Lüttge Andreas, (2007). Calcium carbonate formation and dissolution. *Chemical Reviews*, Volume **107**, Issue 2, 342-381.
- Mukhopadhyay S., Figueiro R., (2009). Physical modification of natural fibers and thermoplastic films for composites – A review. *Journal of Thermoplastic Composite Materials*, Volume **22**, Issue 2, 135-162.
- Mullin J.W., (1992). *Crystallization*, (3rd ed). Butterworth-Heinemann, Oxford (U.K.).
- Müssig Jörg (2010). *Industrial Applications of Natural Fibres: Structure, Properties and Technical Applications*. John Wiley & Sons, New York (U.S.A.).
- Narkis M., Chen E. J. H., Pipes R. B., (1988). Review of methods for characterization of interfacial fiber-matrix interaction. *Polymer Composites*, Volume **9**, Issue 4, 245-251.
- National Research Council, (1976). *Fibers as Renewable Resources for Industrial Materials*. Washington DC (U.S.A.).
- National Research Council of the National Academies, (2005). *Committee on High Performance Structural Fibers for Advanced Polymer Matrix Composites*. The National Academies Press, Washington DC (U.S.A.).
- Neilsen A.E., (1964). *Kinetics of precipitation*. Pergamon, Oxford (U.K.).
- Nelson D.L. and Cox M.M. (2000). *Lehninger Principles of Biochemistry* (3rd ed). Worth Publishers, New York (U.S.A.).
- Orme C.A., Noy A., Wierzbicki A., McBride M.T., Grantham M., Teng H.H., Dove P.M., De Yoreo J.J., (2001). Formation of chiral morphologies through selective binding of amino acids to calcite surface steps. *Nature*, Volume **411**, 775-779.
- Outwater J.O., Murphy M.C. (1970). The influences of environment and glass finishes on the fracture energy of glass-epoxy joints. *The Journal of Adhesion*, Volume **2**, Issue 4, 242-253.
- Peppas N.A., (2004). Intelligent therapeutics: biomimetic systems and nanotechnology in drug delivery. *Advanced Drug Delivery Reviews*, Volume **56**, Issue 11, 1529-1531.
- Petrini M., Ferrante M., Su B., (2013). Fabrication and characterization of biomimetic ceramic/polymer composite materials for dental restoration. *Dental Materials*, Volume **29**, Issue 4, 375-381.

- Pickering K.L., Ji C., (2004). The effects of Poly[methylene(polyphenyl isocyanate)] and Maleated Polypropylene coupling agents on New Zealand radiate pine fiber – Polypropylene composites. *Journal of Reinforced plastics and Composites*, Volume **23**, Issue 18, 2011-2024.
- Portela T.G.R., da Costa L.L., Santos N.S.S., Lopes F.P.D., Monteiro S.N., (2010). Tensile behaviour of lignocellulosic fiber reinforced polymer composites: Part II buriti petiole/polyester. *Màteria*, Volume **15**, Issue 2 (Rio de Janeiro).
- Praustnitz John M., Lichtenthaler Rudiger N., de Azevedo Edmundo Gomes, (1999). *Molecular thermodynamic of fluid-phase equilibria* (3rd ed.). Prentice Hall Inc., New Jersey (U.S.A.).
- Reuter M.A., van Schaik A., Ignatenko O., de Haan G.J., (2006). Fundamental limits for the recycling of end-of-life vehicles. *Mineral Engineering*, Volume **19**, Issue 5, 433-449.
- Romano F., (2012). Biomimetic catalyst for oxygen transfer reactions. *Ph.D. Thesis*, Università degli Studi di Padova (IT).
- Sarikaya Mehmet, Ilhan A.Aksay, (1995). *Biomimetics: Design and Processing of Materials*. American Institute of Physics, New York (U.S.A.).
- Scheifele G., B. Sc., M. Sc., (2001). An overview of the present hemp and flax/linen production and processing industry in China. *Bast Fibrous Plants on the Turn of Second and Third Millennium-International Conference*, Shenyang City (R.C.).
- Shahinpoor M., (2003). Ionic polymer-conductor composites as biomimetic sensors, robotic actuators and artificial muscles – A review. *Electrochimica Acta*, Volume **48**, Issue 14-16, 2343-2353.
- Simkiss K., Wilbur K., (1989). *Biomimetalization cell biology and mineral deposition*. Academic Press, Inc., San Diego (U.S.A.).
- Stamboulis A., Baillie C.A., Peijs T., (2001). Effects of environmental conditions on mechanical and physical properties of flax fibers. *Composites Part A: Applied Science and Manufacturing*, Volume **32**, Issue 8, 1105-1115.
- Stillfried D.G., (2012). Biomimetic mineralisation of organic fibres for enhanced composite mechanical properties. *Master's Thesis*, Laboratory of Paper Coating and Converting, Faculty of Technology, Abo Akademi University, Turku (FI).
- Stillfried D.G., Toivakka M., Alam P., (2013). Crispatotrochus-mimicking coatings improve the flexural properties of organic fibres. *Journal of Materials Science*, Volume **48**, Issue 24, 8449-8453.

- Sreekala M.S., Kumaran M.G., Seena Joseph, Maya Jacob, Sabu Thomas, (2000). Oil palm fibre reinforced phenol formaldehyde composites: influence of fibre surface modifications on the mechanical performance. *Applied Composite Materials*, Volume **7**, 295-329.
- Srogi Krystyna, (2008). An overview of current processes for thermo-chemical treatment of automobile shredder residue. *Clean Technologies and Environmental Policy*, Volume **10**, Issue 3, 235-244.
- Susheel Kalia, Kaith B.S., Inderjeet Kaur, (2009). Pretreatments of natural fibers and their application as reinforcing material in polymer composites - A review. *Polymer Engineering and Science*, Volume **49**, Issue 7, 1252-1272.
- Teir S, Sanni Eloneva, Carl-Johan Fogelholm, Ron Zevenhoven, (2007). Dissolution of steelmaking slags in acetic acid for precipitated calcium carbonate production. *Energy*, Volume **32**, Issue 4, 528-539.
- Thummalapalli Vimal Kumar, Steven L. Donaldson, (2012). Biomimetic composite structural T-joints. *Journal of Bionic Engineering*, Volume **9**, Issue 3, 377-384.
- Troger F., Wegener G., Seemann C., (1998). Miscanthus and flax as raw material for reinforced particleboards. *Industrial Crops and Products*, Volume **8**, Issue 2, 113-121.
- Vautrin-UI C., Boisse-Laporte C., Benissad N., Chausse A., Leprince P., Messina R., (2000). Plasma-polymerized coatings using HMDSO precursor for iron protection. *Progress in Organic Coatings*, Volume **38**, Issue 1, 9-15.
- Vincent Julian F.V., (2006). Applications-Influence of biology on engineering. *Journal of Bionic Engineering*, Volume **3**, 161-177.
- Wang J., Becker U., (2009). Structure and orientation of vaterite (CaCO₃). *American Mineralogist*, Volume **94**, 380-386.
- Wang T., Wen L., Liang J., Wu G., (2010). Fuzzy vorticity control of a biomimetic robotic fish using a flapping lunata tail. *Journal of Bionic Engineering*, Volume **7**, Issue 1, 56-65.
- Weiner S., Dove P.M., (2003). An overview of biomineralization process and the problem of the vital effect. *Mineralogical Society of America - Geochemical Society*, Volume **54**, Issue 1, 1-29.
- Wu W.L., (1989). Thermal technique for determining the interface and/or interply strength in polymeric composites. *National Institute of Standards and Technology*, Polymers Division.
- Xie Yanjun, Callum A.S. Hill, Zefang Xiao, Holger Militz, Carsten Mai, (2010). Silane coupling agents used for natural fiber/polymer composites: A review. *Composites Part A: Applied Science and Manufacturing*, Volume **41**, Issue 7, 806-819.

- Xuan-Hui QU, Lin ZHANG, Mao WU, Shu-bin REN, (2011). Review of metal matrix composites with high thermal conductivity for thermal management applications. *Progress in Natural Science:Materials International*, Volume **21**, Issue 3, 189-197.
- Yan Libo, Nawawi Chouw, Krishnan Jayaraman, (2013). Flax fibre and its composites - A review. *Composites: Part B*, Volume **56**, 296-317.
- Zafeiropoulos N.E, Baillie C.A, Matthews F.L, (2001). A study of transcrystallinity and its effect on the interface in flax fibre reinforced composite materials. *Composites Part A: Applied Science and Manufacturing*, Volume **32**, Issue 3-4, 525-543.
- Zhang Xiuli, Zhihai Fan, Qiang Lu, Yongli Huang, David L. Kaplan, Hesun Zhu, (2013). Hierarchical biomineralization of calcium carbonate regulated by silk microspheres. *Acta Biomaterialia*, Volume **9**, Issue 6, 6974-6980.
- Zhou Zhou, Xingchen Liu, Benting Hu, Jilong Wang, Danwei Xin, Zhengjia Wang, Yiping Qiu, (2011). Hydrophobic surface modification of ramie fibers with ethanol pretreatment and atmospheric pressure plasma treatment. *Surface and Coating Technologies*, Volume **205**, Issues 17-18, 4205-4210.

Siti web:

www.sigmaaldrich.com (24/01/2014)

Acknowledgements

I would like to thank Prof. Martti Toivakka for giving me the availability to develop this work in the Laboratory of Paper Coating and Converting at the Åbo Akademi University. I wish to thank my supervisor, Prof. (adj.) Parvez Alam, for following me during the period of work and his wide availability in helping me to carry out the thesis work. I would like also to acknowledge the support of Vinay Kumar during the experimental part. I would like to thank Prof. (asst.) Ali Miserez at Nanyang Technological University for facilitating the nanoindentation and XRD research.

Finally, I want to thank all the staff from the laboratory (Mari Nurmi, Pauliina Saloranta, Björg Friberg, Dimitar Valtakari, Jani Kniivilä) for having always provided me an adequate solution to all my problems regarding the project assigned.

